FLOW PATTERNS AND SPATIAL DISTRIBUTION OF ATHEROSCLEROTIC LESIONS IN HUMAN CORONARY ARTERIES

（ヒト冠動脈の血流動態からみた粥状硬化の局在と成因に関する考察）

1988

筑波大学大学院博士課程医学研究科

朝 倉 利 久

FLOW PATTERNS AND SPATIAL DISTRIBUTION OF ATHEROSCLEROTIC LESIONS IN HUMAN CORONARY ARTERIES

by

TOSHIHISA ASAKURA

A thesis submitted to Doctoral Program in Medical Sciences
University of Tsukuba Graduate School
in partial fulfillment of the requirements
for the degree of Ph.D. in
Medical Sciences

University of Tsukuba
Ibaraki, Japan

November, 1988

FOREWORD

This thesis work was carried out under the supervision of Dr. Takeshi Karino at the McGill University Medical Clinic, Montreal General Hospital, Montreal, Quebec, Canada during my one and a half years' research training in his laboratory as a special student from the University of Tsukuba Graduate School to the Department of Medicine, Division of Experimental Medicine, McGill University from June 1986 to December 1987.

This thesis was written based on two original papers which have been submitted to "Circulation Research" in August 1988, under the titles of "Flow Patterns and Spatial Distribution of Atherosclerotic Lesions in Human Coronary Arteries: I. Left coronary artery, and II. Right coronary artery", with little further modification. Thus, some details of basic fluid mechanical concepts and experimental apparatus are omitted from the main part of the thesis. These can be found in Appendices.

The results of this thesis work have so far been presented at seven meetings and used as a part of three book chapters which are to be published as proceedings of three international symposia.

ABSTRACT

To investigate the potential role of fluid mechanical factors in the localized genesis and development of atherosclerotic lesions in man, the exact anatomical locations of atherosclerotic lesions and the flow patterns at such sites in the human coronary artery were studied in detail by means of flow visualization and high speed cinemicrographic techniques using isolated transparent coronary arterial trees prepared from human postmortem. It was found that atherosclerotic plaques and wall thickenings were localized on the upper (pericardial side) wall and lower right lateral wall of the very entrance region of the left main coronary artery, the outer (hips) and lower (myocardial side) walls of the branching site of the left anterior descending (LAD) and left circumflex (LCx) branches. The lower right lateral and lower walls of the proximal portion of the LAD which corresponded to the inner wall of a gentle curved segment, and the outer wall (hip) of one or both daughter vessels at major bifurcations and T-junctions of the LAD and LCx were also the preferred sites for atherosclerotic lesions. Atherosclerotic wall thickenings were also found in an alternating pattern along the inner wall of each of the curved segments and at the outer walls of bifurcations and T-junctions of the right coronary artery (RCA). The results from fluid mechanical investigations revealed that these sites were the very places where flow was either slow or disturbed with the formation of slow recirculation and secondary flows and where wall shear stress was low. In no

instance were atherosclerotic lesions found at and around the flow divider where wall shear stress was high and where the formation of early atherosclerotic lesions has been observed in experimental animals fed high-cholesterol diets.

TABLE OF CONTENTS

LIST OF FIGURES

Fig. No. Page

Fig. No. Page

Chapter I

INTRODUCTION

Atherosclerosis is a degenerative disease which affects relatively large arteries by the progressive thickening and eventual hardening of the vessel wall through the formation of atheromatous plaques rich in cholesterol. During the past three decades, this disease has gained great attention and much work has been done to understand its pathogenesis, as well as to find ways to detect, prevent and cure the disease. However, despite recent advances in cardiovascular and pharmacological research, atherosclerosis and thrombosis still remain as major causes of mortality in our modern western society. Many questions concerning the factors which underlie the genesis and development of these diseases are yet unanswered.

1.1 The Risk Factors for Atherosclerosis

Atherosclerosis is rare in the undeveloped countries and in some with advanced socio-economic development (e.g. Japan) where the disease is much less important clinically. It has been repeatedly observed that people moving from a geographic area of low incidence to an area of high incidence gradually tend to exhibit the higher rates of the disease observed in the country of adoption. The best example is a study of the incidence of the disease in the native Japanese population when they migrate to

Hawaii and then to the United States mainland.[1] Such studies indicate that environmental factors are very important, while this does not excluding genetic factors. Certain lifestyles are associated with risk factors for atherosclerosis and for its clinical form of coronary artery disease and stroke. Various factors, among them heredity, dietary fat content, smoking, hypertension, diabetes mellitus, lack of exercise, personality and stress, are believed to affect the progress of the disease.

1.2 The Morphology of Atherosclerotic Lesions

Ultimately it leads to the development of lesions which typically have been classified as one of three types --- "the fatty streak", "the fibrous plaque", and the so called "complicated lesion". Histologically the focal lesions of atherosclerosis are characterized by three fundamental phenomena: proliferation of smooth muscle cells, deposition of intracellular and extracellular lipid, and accumulation of extracellular matrix components including collagen, elastic fibers and proteoglycans.[2]

In man the disease first becomes apparent as fatty dots or fatty streaks on the intima of the arteries. There is an unresolved question as to whether these lesions progress to the next phase of the disease, the fibrous plaque. The best answer from currently available information is that some do[3-5] and some do not.[6-9] In population with a low incidence of clinical manifestations of atherosclerosis lesion, progression usually does not evolve beyond the fatty streak stage. Progression of lesions involves extension to the media and the development of ulcer-

ation, accompanied by thrombosis, calcification hardening, hemorrhage and rupture. These lesions are dangerous because they lead to clinical events such as thrombosis and embolism, narrowing of the lumen of the arteries, stenosis, or destruction of the arterial wall locally, leading to dilatation (aneurysm formation).

1.3 The Lipid Hypothesis of Atherogenesis

Much attention has been focused on the possible correlations between diet and the occurrence of atheroma since the plaques are rich in lipid and can be produced experimentally in animals by feeding them with a diet containing a high cholesterol level.[10,11] It is further sustained by the close association between clinical disease and the presence of hypercholesterolemia, elevation of low density lipoproteins (LDL) and a decrease in high density lipoproteins (HDL) relative to LDL. The blood cholesterol may be normal in some individuals who show an increase in the ratio of LDL/HDL, considered to be atherogenic. Undoubtedly, anomalies in plasma lipid concentration and lipid metabolism by vascular endothelial cells, as hypercholesterolemia, exert a prominent influence on the genesis and progression of atherosclerosis. Thus, many researchers believe atherosclerotic lesions are derived from the insudation of plasma into the arterial wall.[12-14]

This lipid theory proposes that atherosclerotic lesions arise from altered endothelial permeability allowing plasma protein (lipoprotein and fibrinogen) to permeate the endothelium and react with the constituents of the arterial wall. LDL or other

lipoproteins can enter into the arterial wall and into and through endothelium by endocytosis or through gap junctions. The contraction and relaxation of the arterial wall produces a milking or sponge-like effect and this plus the intra-luminal blood pressure speeds up the passage of the lipoprotein so that they can either go right through to the vasa vasorum or be trapped somewhere in the intima or media. In the wall the lipoprotein may be altered by interaction and become chemotactic to blood born monocytes or chemotactic to fixed tissue histocytes or tissue macrophages in contrast the lipoprotein of plasma is not chemotactic. If the amount of lipoprotein trapped and taken up is substantial, a large number of macrophages will appear and this forms an early type of atherosclerotic lesion called "the fatty streak". These macrophages loaded with lipid are called macrophage type foam cells and the lesion is a macrophage type fatty streak atherosclerosis. However, some fatty streak show mainly smooth muscle cell loaded with lipid are called myogenic type foam cells and this lesions is a myogenic type fatty streak atherosclerosis.

Although that lipids and lipoproteins have a role in atherogenesis has been recognized for many years, until recently, very little attention has been paid to the mechanisms by which lipids and plasma lipoproteins alter the behavior of arterial cells. The rates of LDL degradation in tissues throughout the body are relevant to the problem of atherosclerosis in the sense that the metabolism in each of those tissues helps determine the steady state plasma LDL levels to which the artery wall is

exposed. The pioneering work of Brown and Goldstein[15,16] on human fibroblasts has dramatically changed this situation. These investigators have provided evidence that the cell surfaces of normal skin fibroblasts contain a receptor for plasma LDL, and that this receptor is absent from fibroblasts of patients with familial hypercholesterolemia.[17] This proposal suggests that a generalized absence of the receptor from cells, including fibroblasts, may contribute to the hypercholesterolemia seen in this disease. Thus, total body LDL degradation can be considered in two major categories: that dependent on the Brown-Goldstein LDL receptor, and that occurring via alternative mechanisms.[18] Various mechanisms available for LDL uptake are proposed and remains to be determined.[19]

1.4 The Thrombogenic Hypothesis of Atherogenesis

Much of the comparatively recent interest in a putative role for mural thrombosis as a contributor to plaque growth stems, in morphological terms at least, from the studies of Duguid.[20,21] Duguid put forward the view that "many of the lesions we now classify as atherosclerosis are altered thrombi which, by the ordinary process of organization, have been transformed into fibrous thickenings". This, as Duguid himself pointed out, represents a partial return to the "encrustation hypothesis" enunciated by Rokitansky a century before.[22] Rokitansky ascribed all the features of atherosclerosis to "recurrent deposition of elements derived from the blood mass".

Such a possible liaison is re-emphasized by the experimental

evidence of incorporation of mural thrombi (thrombi formed at one side of the vessel wall) into the arterial wall with the resultant thickening of the vessel wall.[23,24] It was suggested that since fibrin and platelets[25] have been found in atherosclerotic plaques, lesions may arise from thrombi deposited on the intimal surface and these would later be incorporated into the arterial wall by an overgrowth of the endothelium. The lipid content of the plaque would the be derived from the breakdown of leukocytes and platelets in the thrombi. While the latter part of this theory has not gained universal support,[26] it is true that there is a striking similarity between the sites for deposition of platelet aggregates and the development of atheromatous plaques.

There is a question as to whether plaques can arise as a result of platelet-vessel wall interaction in a previously le sion-free area of the arterial intima. The currently available observations show that small mural thrombi occur in macroscopically normal portions of the intima.[27,28] But these results can not tell us little or nothing about the fate of such microthrombi. If we are to form any valid assessment of the contribution mural thrombosis makes to plaque growth in human atherosclerosis, it is clear that we must be able to recognize accurately the presence of thrombus or its residua within the lesions.

1.5 The Response to Injury Hypothesis of Atherogenesis

In the last decade, the demonstration that intimal thicken-

ings could be induced by repeatedly injuring the intima in normal-fed animals or by a single removal of only the endothelial layer, have led to renewed interest in the response to injury hypothesis of atherosclerosis. This concept, originally proposed by Virchow,[29] suggested that injury to the artery wall somehow led to a series of tissue responses that culminated in the lipid-filled lesions of atherosclerosis, originally considered to be largely a degenerative process. The response to injury hypothesis of atherosclerosis[30-33] postulates that injury occurs specifically to the lining endothelial cells of the artery.

The injury may result from a number of different types of insult, on an interrupted or chronic basis, and may modify the critical balance between cell proliferation and cell destruction that determines whether lesions progress, remain relatively constant, or regress. When cholesterol deposition exceeds removal, lesion formation may progress toward irreversibility and clinical disease may develop.

The important discovery that serum but not plasma has led to the discovery of a platelet factor released from the alpha-granules a substance (platelet-derived growth factor) which in combination with other substances in the serum stimulate the proliferation of smooth muscle cells.[34,35] There is inhibition of the development of injury induced lesions in animals, lacking platelets (thrombocytopenic). Platelets also release a substance which stimulates the migration of smooth muscle cells. Thrombosis leads to the development of raised thromboatherosclerotic lipid containing lesions. While simple removal of the endothe-

lial layer, is characterized by the deposition of a transient monolayer of platelets followed by migration of smooth muscle cells from the media and their proliferation in the intima and this develops into an intimal thickening or lesion of injury.[36-41]

There is now a concept that other forms of injury particularly immunological injury in the presence of dietarily induced hypercholesterolemia produces lesions that closely resemble those of the disease in man.[42-46] There are a number of examples in clinical medicine of atherosclerosis resulting from injury to vessel walls. Homocystinemia which may damage endothelium, as incidated by decreased platelet survival, is associated with the precocious onset of atherosclerosis and thromboembolic disease.[47,48] Late rejection of transplanted organs is associated with arterial intimal thickenings, rich in foam cells.[45]

There are probably many factors in smoke from tobacco that might be responsible for causing endothelial injury in man, of sufficient severity to promote or intensify atherosclerosis. Small areas of endothelial cell denudation repair quickly by spreading and replication of neighboring endothelial cells. If this happens before there is time for smooth muscle cells to migrate and proliferate, no thickening will result. If a single endothelial cell dies endothelium migrates from the slides and replaces it from beneath. There is no evidence that hyperlipidemia itself causes endothelial denudation. Agents which may cause endothelial damage may include mechanical forces,[36-41]

immunologic injury,[42-46] various toxins,[47-49] viruses,[50] and chemical agents such as lipoproteins.[33,51-54]

1.6 The Hemodynamic Hypotheses of Atherogenesis

Both clinical and post-mortem studies indicate that, in humans, atherosclerotic lesions on the vessel wall develop not randomly, and not everywhere in the circulation, but localize at certain selected sites in the arterial tree such as the branching sites and curved segments of large arteries where the blood flow is disturbed and separation of streamlines from the vessel wall and formation of eddies are likely to occur.[6,14, 55-62] Thus, it is strongly suspected that arterial hemodynamics plays important roles both in the genesis and progression and in the regression of atherosclerosis.[63-66]

Various hemodynamic hypotheses have been proposed to correlate atherosclerotic lesions with local flow conditions in the arterial system. The relative merits of each hypothesis can best be examined by first defining certain relevant fluid dynamic terms (shown in Appendix A).

The present knowledge on flow behavior in the major central arteries is by no means well developed,[67,68] and further research is necessary to determine the extent of local flow phenomena in the arteries of man. This lack of knowledge inhibits, to a certain degree, the drawing of definitive conclusions about the validity of each hemodynamic model of atherogenesis which has been proposed. It is still possible, however, to examine each model on the basis of its relative merits.

(a) Pressure-Related Hypotheses

Based on the observed high incidence of atheromatous plaques in persons with high blood pressure, one school of researchers believed that local variations in pressure or vascular tensions in the arterial tree were responsible. By applying Laplace law for calculation of tension in curved vessels, Willis[69] concluded that high hydraulic pressure and luminal curvature induce increases in local tensions and therefore local atheroma formation. However, Oka[70] has shown that the simple Laplace law cannot be applied to elastic thick-walled blood vessels. Texon et al.[71] hypothesized that Bernoulli-type suction forces, acting in regions of locally increased blood velocity, exert a lift force on the endothelial lining (the protective surface coat of the vessels) and thereby produce damage to, and subsequent thickening of the layer of intimal cells beneath the surface leading to eventual formation of atheromatous plaques. The use of Bernoulli's equation for a viscous fluid, even in flow at high Reynolds number, is of course open to criticism,[72] and even when the suction force is calculated, it turns out[14,73] to be negligible under physiological conditions.

(b) Turbulence-Related Hypotheses

A model proposed by Wesolowski et al.[74,75] suggests that atherosclerotic lesions are formed in regions of turbulence as a result of (i) induced vibration of the arterial wall which may lead to the eventual injury of the intima, or (ii) local

increases in lateral (static) wall pressure which may injure the intima, suppression of lipid secretion from the interior of the arterial wall, or both. Whether this is true or not depends on the magnitude of the fluctuations under physiological conditions.[73]

(c) Wall Shear Stress Hypotheses

Finally, there are two well debated hypotheses for the genesis and localization of atherosclerosis: Fry[76] studied the effect of wall shear stress on mass transport at the endothelial surface of dog aortas and showed that endothelial cells were damaged, or torn away, when wall shear stresses exceeded 40 Nm^{-2}. Later,[77] observed that at low shear stresses, the transport of Evans blue dye from blood to aortic wall was increased with increasing wall shear stress. Fry concluded that mass transport to the wall is shear rate dependent, and suggested that wall permeability increases with increasing shear stress. Based on these findings, he postulated that atherogenesis occurs preferentially at arterial wall experiencing high shear stress, because of the resulting mechanical damage, and because of an enhanced flux of lipid, including cholesterol, from blood to endothelium.

In this connection, doubt has been expressed as to the existence of shear stresses as high as 30-44 Nm^{-2} in the actual circulation. Thus, Ling et al.[78] measured peak wall shear stress in the thoracic aorta between 8 and 16 Nm^{-2} over a cardiac cycle. In a later study Ling et al.[79] measured peak wall shear stresses in a distensible model of the renal artery branch under simulated

in vivo conditions. Here, a value of 26 Nm^{-2} was found on the inner walls of the renal bifurcation, which is only just below the lower limit of the acute yield stress measured by Fry(29.5 Nm^{-2}).[76] Therefore, high shear stresses may indeed contribute to the occurrence of lesions in channels of certain geometry.

In contrast to this, Caro et al.[14] found that early atheromatous lesions in human post-mortem artery specimens occur preferentially in regions, such as the inner walls of curved vessels and at the hips bifurcations, where the wall shear rate is expected to be low. Therefore, they suggested that the local wall shear rate exercises a control on atheroma formation through flow-dependent diffusion of lipid away from the vessel wall, leading to an accumulation in areas of low wall shear rate. They have pointed out that the concentration gradient for lipid transport at the vascular interface will depend on the associated blood velocity gradient. In general, the steeper the concentration gradient (a thinner momentum boundary layer), the steeper the concentration gradient (a thinner chemical boundary layer). Thus, transport across the interface will be facililated in a high shear field and inhibited in a low shear field. These workers suggested that the high shear on flow dividers maintains a high flux into and out of these regions, depending on the direction of the concentration gradient. They speculate, therefore, that spared regions are areas in which previously deposited or intrinsically generated lipid have been transported away by the shear-enhanced concentration gradient. Subsequent experiments on the transport of C^{14}-cholesterol between serum and

vessel wall in a perfused segment of the artery showed that while the process is shear dependent, it is the blood-wall interface which is the rate limiting step in the total transport of lipid.[80]

Since it is unlikely that the thickness of the momentum boundary layer ever exceeds one in any mammalian arterial tree, the thickness of the momentum boundary layer will always be very small compared to 200 for the case of albumin and also small compared to 130 for the case of VLDL. We conclude from this that a shear-enhanced concentration gradient at the vascular interface is one of the less important forces for transendothelial transport of proteins.

1.7 The Purpose of This Study

Since the causative effects of high and low wall shear stresses, originally claimed by Fry[76] and Caro et al.,[14] respectively, more than a decade ago, a considerable amount of work, both theoretical[81-85] and experimental (*in vivo*,[78,86-96] *in vitro*[97-102]), has been carried out by many investigators. The integrated results from animal studies show that, in cholesterol-fed rabbits and swine, early atherosclerotic changes to vessel walls occur preferentially at the flow divider (high shear region) of branching arteries,[103,104] giving support to the high shear hypothesis of atherogenesis. On the other hand, recent pathological investigations on humans post-mortem indicate that preferred sites for naturally formed atherosclerotic lesions in humans lie in regions of low shear stress.[5,105-112] Furthermore,

there have been several interesting but scattered reports on the effects of shear stress on the biological functions of endothelial cells which indicate that exposure of endothelial cells to moderate to high shear stresses prevents atherogenesis in cholesterol-fed monkeys,[113] and enhances the synthesis of prostacyclin[114] and Histamine[115] and uptake of low density lipoproteins[116] by endothelial cells in culture.

Therefore, despite the effort of many investigators, the effects of shear stress on vascular endothelium and the pathogenesis of atherosclerosis still remain unclear. Further detailed and systematic studies are required to understand the exact role of hemodynamic factors in the localization of the sites of atherosclerotic lesions in the human arterial tree.

As described earlier, though there is a distinct difference in the preferred sites of atherosclerotic lesions between humans and experimental animals, in both cases, the initial atherosclerotic changes are localized around the orifice of branching arteries where the flow is likely to be disturbed. Hence, the study in this laboratory has been focused on the characterization of the flow and microrheological investigation of the flow behavior and interactions of model particles and blood cells with each other and the vessel wall in regions of disturbed flow in order to relate the results from these fluid mechanical investigations to the localized genesis and development of atherosclerosis, thrombosis and aneurysms. The experiments were first carried out using various glass models of stenoses[117,118] and branching vessels.[119,120] Similar flow studies have also

been carried out by many other investigators.[121-123]

Due to the difficulties in visualizing the detailed hemodynamic phenomena such as flow patterns and interactions of blood cells with the vessel walls in vivo even with the latest technology of subtraction angiography and ultrasound and laser Doppler flowmetry,[91,124-130] it was necessary to carry out most of the fluid mechanical studies in vitro using various models of arteries[107,131-133] and arterial molds.[134-136] However, even with the high quality casting and molding techniques available today, it is still not easy to precisely duplicate the complex geometry of the vessel lumen encountered in various regions of the arterial system such as the coronary and cerebral circulations.

To improve the situation, a novel method to prepare isolated transparent natural blood vessels from animals and humans post-mortem has been developed in our laboratory.[137] This has, for the first time, enabled one to simultaneously study the exact anatomical locations and sizes of atherosclerotic plaques and wall thickenings, and the detailed characteristics of the flow prevailing at such sites by directly observing and photographing the behavior of suspended tracer particles and hardened blood cells flowing in both steady and pulsatile fashions through the transparent segments of normal and diseased arteries and veins. Using the above method, Karino and his co-workers have previously studied the detailed flow patterns through venous valves in dog saphenous veins,[138] the aortic arch and descending aorta of the dog[139] and the carotid artery bifurcation in man[140] because of

the high incidence of thrombogenesis and atherogenesis at these respective sites.

The study has since been extended to the major arteries of the human cardio- and cerebrovascular systems.

The present thesis describes the detailed fluid mechanical characteristics of the flow and the exact anatomical locations of atherosclerotic plaques and wall thickenings observed in isolated transparent coronary arterial trees prepared from humans post-mortem. The study was motivated by the fact that despite the high incidence of narrowing and occlusion of vessel lumens through the development of atherosclerotic lesions and the deposition there of platelet thrombi, little information is available on both the spatial distribution of atherosclerotic lesions and fluid dynamics in human coronary arteries.

Chapter II

MATERIALS AND METHODS

2.1 Preparation of Transparent Coronary Arterial Trees

Isolated transparent coronary arterial trees containing the proximal portion of the ascending aorta and left and right coronary arteries with their major branches were prepared from humans post-mortem by a modification of the method described by Karino and Motomiya.[137] In this case, since it is known that, in coronary arteries, most flow occurs during diastole, which is longer in duration than systole,[141] we constructed coronary arterial trees so that they represent the vascular geometries in the diastolic period of the cardiac cycle.

Five fresh and intact human hearts with an 8-10 cm long segment of the ascending aorta were obtained at autopsy from four male subjects aged 18, 56, 61 and 75 years, and a 51-year old female subject in whom the primary cause of death was not cardiovascular disease. After thoroughly rinsing the heart and aorta with isotonic saline, the ascending aorta was excised at about 5-7 cm downstream from the aortic valve and cannulated with a 10 cm long rigid plastic cylinder having an outer diameter approximately equal to the inner diameter of the aorta to provide an inlet to the coronary arteries. The other end of the plastic cylinder was connected to an overflow head tank via flexible plastic tubing. The heart was placed in a dissecting pan and the

aorta and coronary arteries were continuously perfused with ice-cooled saline by establishing a recirculatory system between the dissecting pan and the overflow head tank using a roller pump. The left and right coronary arteries and their major branches having diameters greater than 1.5 mm were exposed and separated from the heart to the desired point of cannulation by carefully dissecting the heart muscles and removing the surrounding tissues using fine scissors and pincers. All the other smaller branches were ligated with 6-0 Prolene suturing thread at positions close to their branching sites while leaving them still attached to their parent vessels and the heart. Each of the major branches was then incised at a location at least 1.5 cm downstream from its branching site, cannulated with a 2-2.5 cm long square-cut, thin-walled stainless steel pipe (made of a hypodermic syringe needle whose outer diameter was approximately equal to the inner diameter of the vessel to be cannulated) and firmly tied in place. The other end of the cannula was capped with a tightly fitted short plastic tubing whose end had been sealed. All the cannulae were then fixed on the heart by suturing and tying them onto the heart muscles while maintaining the original configuration of each vessel under a physiological perfusion pressure of ~ 100 mmHg.

The root of the ascending aorta was separated from the heart by dissecting the tissue surrounding the aortic valve, and then sealed by inserting a tightly fitting plastic disk into the aorta proximal and adjacent to the valve cusps and tying the surrounding aortic tissues over it. To simulate a diastolic condition of

the heart and the arterial tree, both the right and left ventricles were inflated approximately equal to their normal diastolic volumes by filling them with small pieces of gauze. Furthermore, to maintain the geometrical integrity of the coronary arteries and their major branches even after removing all the heart muscles and tissues, the arteries and aorta were tied at each cannula with a thick suturing thread and firmly fixed on a 3-dimensional stainless steel frame especially constructed for this purpose by bending and stretching a 3 mm outer diameter stainless steel pipe around the surface of the heart and aorta so that it crossed and made good contact with all the cannulae of the branches of both the left and right coronary arteries as well as the thick plastic cylinder cannulated into the aorta by winding several times around it.

The coronary arterial tree, still attached to the heart, was connected via flexible plastic tubing to a head tank and a collecting reservoir and then fixed by perfusing it with a mixture of 2% glutaraldehyde and 4% formaldehyde in isotonic saline at the physiological mean perfusion pressure of ~100 mmHg, and at the same time, immersing it in the same fixing solution. The arterial tree, together with the aorta, was then isolated from the heart, dehydrated by perfusing with and immersing it in ethanol-saline mixtures of progressively increasing ethanol concentration under the same perfusion pressure, and finally suspending it in pure ethanol. Finally, the coronary arterial tree attached to the aorta was filled with, and immersed in methyl salicylate (oil of wintergreen), containing 5% ethanol, under the

physiological mean perfusion pressure to render the vessel transparent.

2.2 Experimental Procedure

The schematic diagram of the experimental system used in this study is shown in Figure B-1.

The isolated transparent coronary arterial tree, mounted on a supporting frame was suspended in oil of wintergreen containing 5% ethanol in a transparent glass chamber, and trans-illuminated with condensed parallel light from a 200 W a.c. tungsten filament white lamp through a pair of 16 cm diameter plano-convex lenses aligned in series. The whole arterial tree and segments of interest were observed from various different angles by changing the orientation of the arterial tree relative to the direction of the light beams, and photographed together with a ruler on 35 mm color or black & white films using a Nikon FE 35 mm camera with zoom and close-up lenses.

The arterial tree, together with the glass chamber, was then placed on a vertically movable horizontal stage located in front of the vertically mounted stage of a microscope. The areas of interest on the arterial tree were trans-illuminated with condensed parallel light provided by a Reichert Binolux twin-lamp assembly supplying either low intensity light from a tungsten filament lamp, or high intensity light from a 200 W d.c. mercury arc lamp with a filter to eliminate ultraviolet illumination (shown in Figure B-2).

The aorta and each of the cannulated branches of the left

and right coronary arteries were connected via an approximately 150 cm long flexible plastic tubing, whose inner diameter was about the same as the outer diameter of the cannula, to a head tank and a triangular flask used as a collecting reservoir, respectively. Steady and pulsatile flows were obtained using a head tank system in combination with a sinusoidal oscillatory flow pump (shown in Figure B-3).

A dilute suspension of a mixture of 50, 80, 115 and 165 μm diameter polystyrene microspheres (density ρ_s = 1.06 g/cm^3, Particle Information Services, Bremerton, Washington) in oil of wintergreen containing 5% ethanol (density ρ = 1.16 g/cm^3, viscosity μ = 0.026 g/cm sec) was used as a substitute for blood. This is based on our assumption that, since the estimated mean shear rates in human coronary arteries are greater than the critical values of $\sim$100 sec^{-1} above which the blood behaves as a Newtonian fluid, the non-Newtonian characteristics of the blood would have no effect on coronary blood flow, and thus blood can be substituted by any Newtonian fluid.

After filling the arterial tree and the whole flow system with the suspension, the desired flow rates in the main artery and its branches were established by adjusting the height of the head tank as well as each collecting reservoir.

The suspension was subjected to steady or pulsatile flow through the transparent arterial tree, and the behavior of individual suspended tracer microspheres flowing through various regions of the left and right coronary arteries was observed through a zoom lens (1x to 5x) attached to a cine camera, and

photographed on 16 mm cine films (Kodak double X-negative) using a Hycam 16 mm cine camera (Red Lake Labs, Santa Clara, California) at film speeds from 1200 to 1500 pictures per second (shown in Figure B-2).

With respect to the flow conditions in the human coronary arteries, it is known that in strenuous exercise, the heart increases its cardiac output as much as four to six fold.[141] At the same time, the coronary blood flow also increases four to five fold to supply the extra nutrients needed by the heart.[141] If we assume that the localization of atherosclerotic lesions on the vessel wall is related to some kind of abnormality or disturbance of the flow in that vessel, the effect will be more pronounced at high Reynolds numbers (hence high flow rates) since the formation of disturbed flows is favored at high Re. Hence, taking all these factors into consideration, we have carried out flow studies at flow rates about 2-3 times higher than the reported mean values for humans[141] and at a high oscillatory frequency of 2 Hz (120 beats per minute) so that the flow mimics the typical coronary blood flow under mild exercise. Flow studies were carried out by having flow through only one (either the left or right) coronary artery at a time. The outflow rates through each branch were obtained by measuring the volume of suspension expelled in a given time during which filming of the flow patterns was carried out. Furthermore, at each branching site under investigation, the flow rate in each daughter vessel was first adjusted to its geometrical flow ratio (the flow rate ratio calculated by assuming that the fluid in the parent vessel

is distributed into the daughter vessels in proportion to their cross-sectional areas assessed at the apex of the flow divider) and then shifted to above or below the control value. In the present study, most of the flow experiments were carried out in steady flow since it is not practical to express the detailed flow patterns observed in pulsatile flow in 2-dimensional figures. Only a few experiments were carried out in pulsatile flow (steady + oscillatory flow) with an oscillatory frequency of 2 Hz, and displacement volumes of 0.5 and 1.5 ml in order to compare the results obtained in steady flow to those in pulsatile flow, and to find out whether the phenomena observed in steady flow do also occur in pulsatile flow. Whenever it was possible, flow was observed and recorded along two different diametrical planes which were normal to each other in order to obtain a better grasp of the complete flow patterns in various regions of disturbed flow along the arterial tree.

2.3 Analysis

The developed 35 mm films were subsequently projected onto a glass screen using a slide projector and analyzed to obtain some geometrical data such as the diameter and length of each segment, the angle of branching, and the size and thickness of atherosclerotic plaques and wall thickenings located on the inner surface of vessel walls.

The 16 mm cine films were projected onto a drafting table and the movements of individual tracer particles were analyzed frame by frame with the aid of a stop-motion 16 mm movie analyzer

(Vanguard Instrument Corp. Melville, New York) to obtain the detailed flow patterns and distributions of fluid velocity and wall shear stress (shown in Figure B-4).

The representative geometrical and flow conditions such as the vessel diameter, D_o, mean volume flow rate, Q_o, mean fluid velocity, U_o, and the Reynolds number, Re ($=D_oU_o \rho/\mu$ where ρ and μ being the respective density and viscosity of the flowing fluid) were evaluated for each main vessel proximal to the site of branching and bending. The velocity distributions at various axial locations were obtained by plotting approximately 100 points of the axial components of particle translational velocities (calculated from the tracings of the paths of the tracer particles which were in good focus and appeared to be located in or close to the median plan of the vessel normal to the viewing axis) against the distance from the vessel wall. Wall shear stresses were determined by using the slope of the tangents drawn at the vessel wall on the best fit curves of velocity profiles at various axial locations and multiplying them by the viscosity of the fluid. The locations of separation and stagnation points were determined from the movements of the smallest (50 μm diameter) tracer microspheres which were too small to be traced to obtain the detailed flow patterns but appeared like dust in the picture. Throughout the entire analysis, special attention was paid to the phenomena occurring near the vessel wall by finding and tracing the behavior of the smallest microspheres located as closer as possible to the vessel wall.

Chapter III

RESULTS

As described in detail in the previous section, five isolated transparent coronary arterial trees were prepared from humans post-mortem by cannulating the aorta and the major branches of the left and right coronary arteries, fixing them under physiological pressure, dehydrating with ethanol and finally suspending in oil of wintergreen containing 5% ethanol. Figure 1 shows the typical anatomical structure of the human left coronary artery (A) and right coronary artery (B) with its major branches and bends encountered in the present investigation. The detailed anatomy of the arterial tree is also shown in Figure 2, 3 and 4 by some photographs taken during and at the end of the long process of preparation.

The transparent arterial trees prepared by the above method lost the elasticity of living natural artery during the process of fixing, dehydrating and rendering them transparent.

However, the method assured us of preserving the complex 3-dimensional configuration of the natural coronary arteries. Moreover, since the vessel walls were well soaked in oil of wintergreen, they became transparent without any optical distortion even in the presence of atherosclerotic thickening of the vessel wall, although the areas of calcification remained as non-transparent dark spots as shown in Figure 2D, 3(C,E) and 4D.

FIGURE 1. Schematic representation of the human left coronary artery (A) and the human right coronary artery (B) with its major branches. The circles indicate the preferred sites for atherosclerotic lesions and the regions of interest for the present anatomical and fluid mechanical investigation. The arrows with figure numbers indicate the directions in which observations, photographing and filming of the flow were carried out to produce the particular figures.

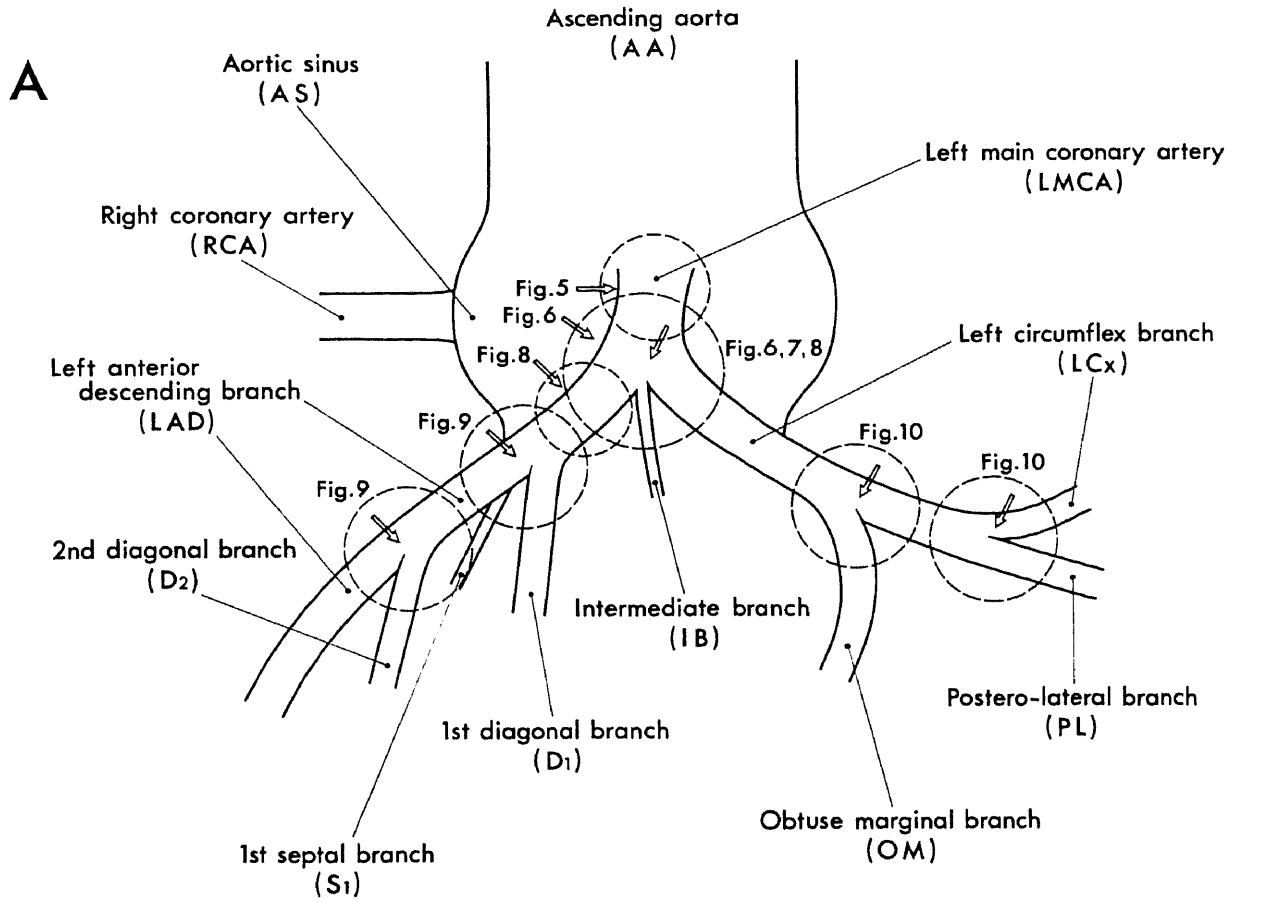
A
Ascending aorta
(AA)
Aortic sinus
(AS)
Left main coronary artery
(LMCA)
Right coronary artery
(RCA)
Fig.5
Fig.6
Fig.8
Fig.6,7,8
Left circumflex branch
(LCx)
Left anterior
descending branch
(LAD)
Fig.9
Fig.10
Fig.10
Fig.9
2nd diagonal branch
(D2)
Intermediate branch
(IB)
Postero-lateral branch
(PL)
1st diagonal branch
(D1)
Obtuse marginal branch
(OM)
1st septal branch
(S1)

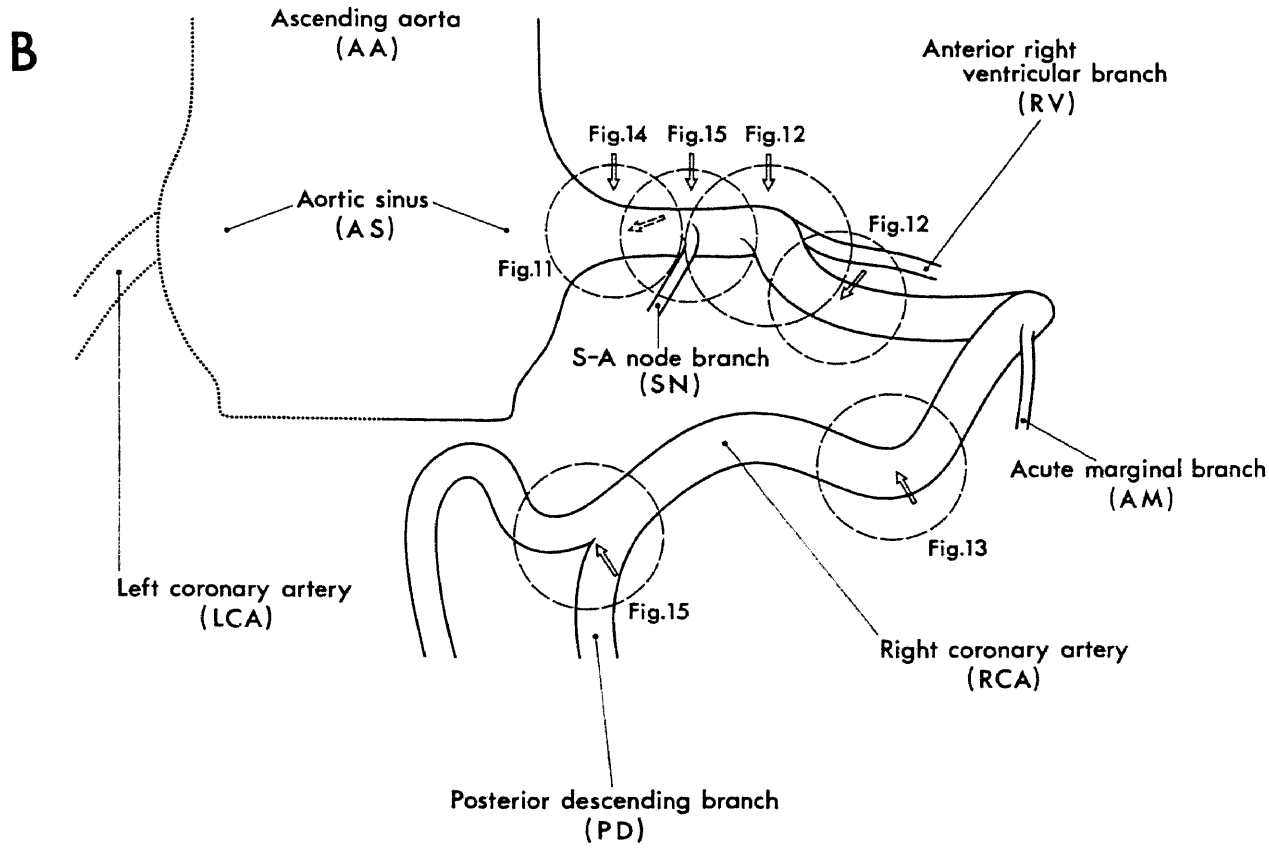
B
Ascending aorta
(AA)
Anterior right
ventricular branch
(RV)
Fig.14
Fig.15
Fig.12
Aortic sinus
(AS)
Fig.12
Fig.11
S-A node branch
(SN)
Acute marginal branch
(AM)
Fig.13
Left coronary artery
(LCA)
Fig.15
Right coronary artery
(RCA)
Posterior descending branch
(PD)

FIGURE 2. Photographs taken during and at the end of the long process of preparing the isolated transparent coronary arterial trees, showing A: a human coronary arterial tree exposed, cannulated and firmly fixed on a solid 3-dimensional stainless steel frame, but still attached to the heart (the picture was taken just before fixation while the arterial tree was perfused with isotonic saline under physiological pressure); B: an isolated human coronary arterial tree after fixation with a mixture of 2% glutaraldehyde and 4% formaldehyde in isotonic saline under the physiological mean pressure of ~100 mmHg; C: an isolated transparent human coronary arterial tree prepared from a young, 18-year old male subject (the arterial tree was suspended in a glass chamber filled with oil of wintergreen containing 5% ethanol); and D: an isolated transparent human coronary arterial tree prepared from a 75-year old male subject with severe atherosclerotic lesions.

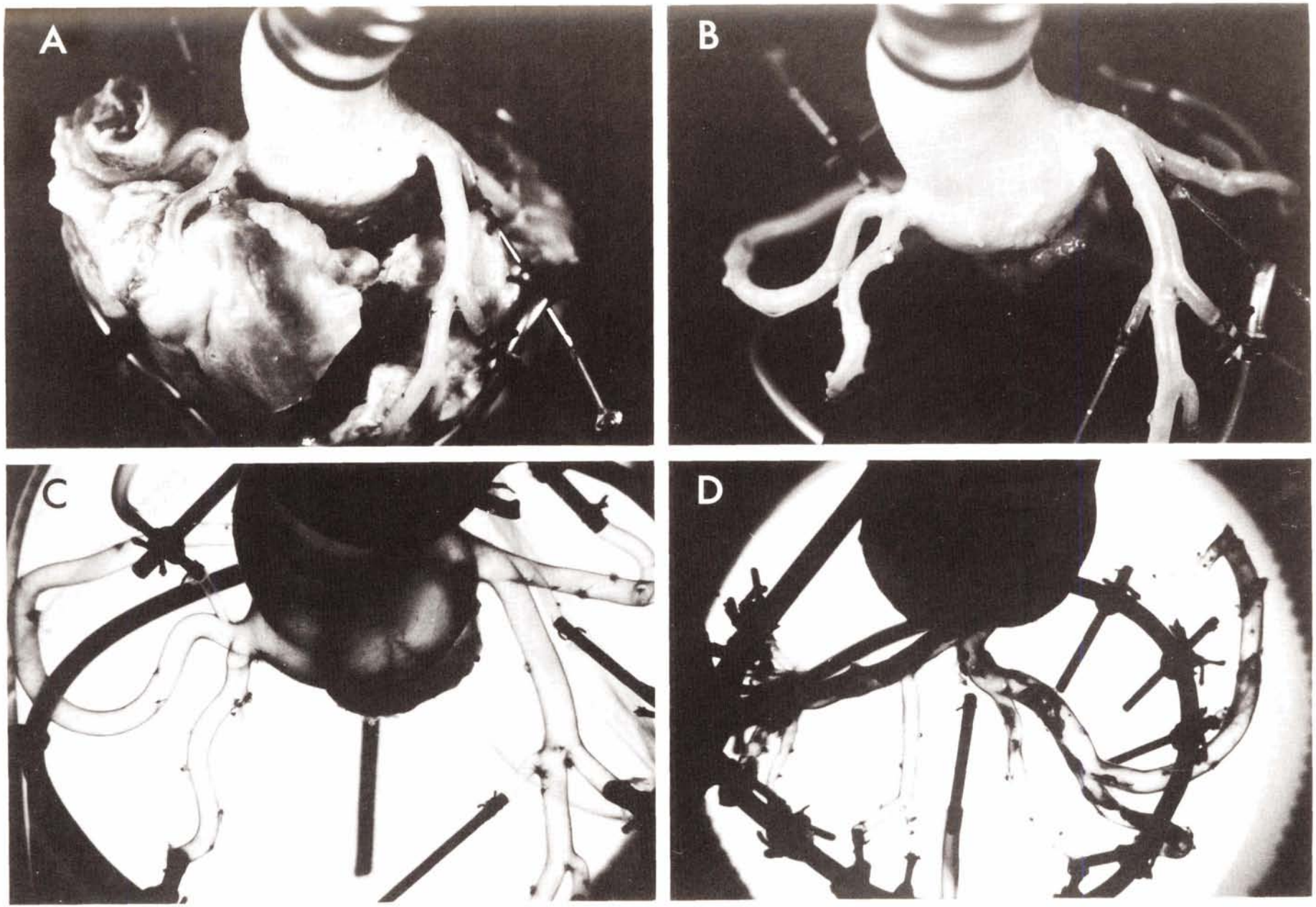
A
B
C
D

FIGURE 3. Photographs of various segments of transparent human left coronary arteries showing the exact anatomical location of atherosclerotic wall thickenings and calcified plaques at A: the hips of a trifurcation of the LMCA in an arterial tree prepared from a 61-year old male subject (top view); B: the lower wall of the LAD (right lateral view of the artery shown in A); C: the lower right lateral wall of the LAD (right lateral view) in an arterial tree prepared from a 75-year old male subject; D: the outer walls (hips) of branching sites and the inner wall of curved segments in the middle portion of the LAD containing the branches of the D_2 and S_2 in the same arterial tree as in A (top view); E: the curved segments of the LCx containing the branches of the OM and PL in the same arterial tree as in C (top view); and F: the inner wall of a curved segment of the LCx and the sharp bend at the branching site of the OM in the same arterial tree as in A (top view).

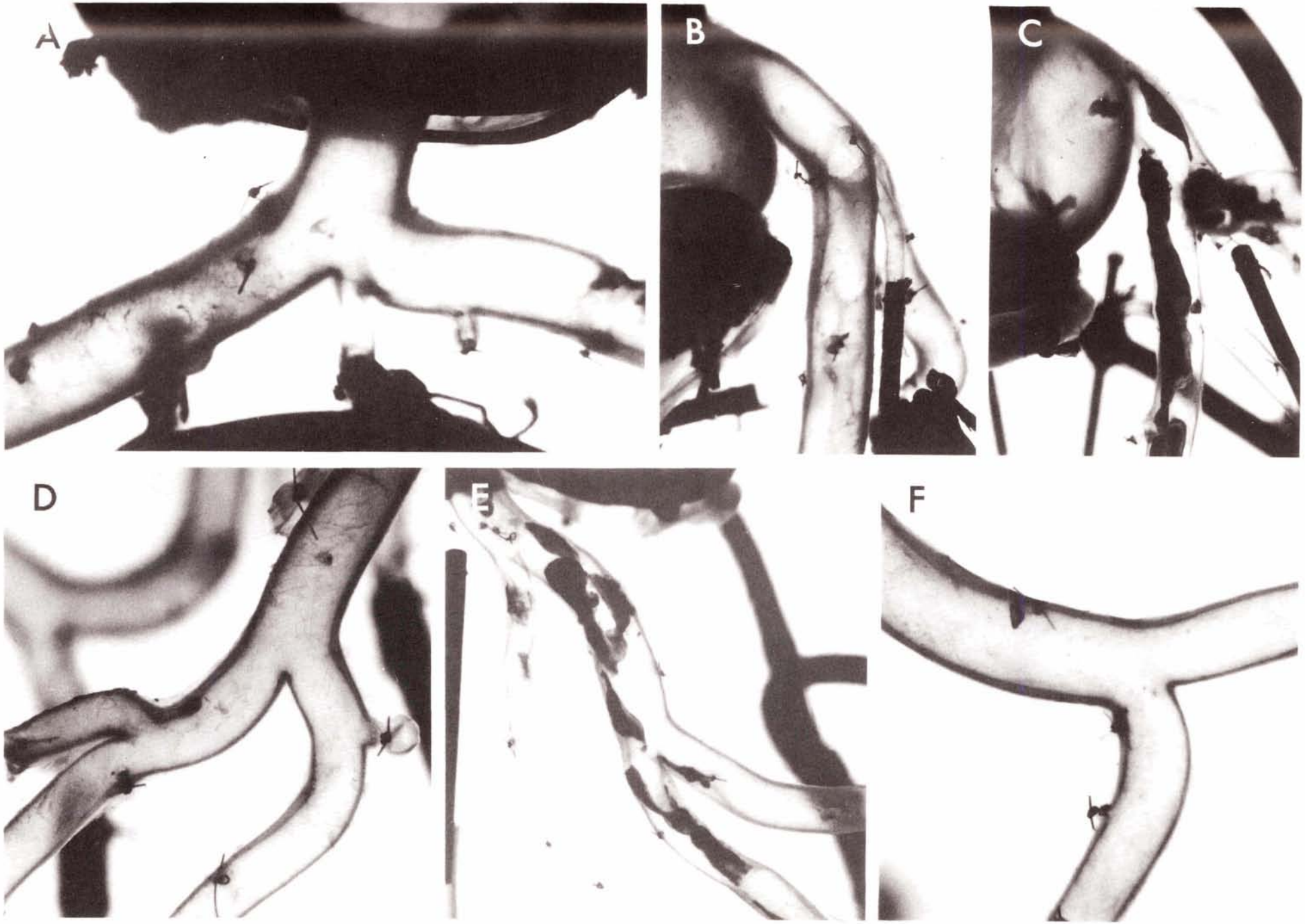
A
B
C
D
E
F

FIGURE 4. Photographs of isolated transparent human right coronary arteries showing the exact anatomical locations of early and advanced atherosclerotic wall thickenings and calcified plaques along the coronary arterial tree prepared from A: a 61-year old male subject with mild atherosclerotic lesions (right lateral view); B: the same subject as in A (top view); C: an 18-year old male subject with minimal degree of intimal thickening (top view); and D: a 75-year old male subject with severe atherosclerotic lesions (top view).

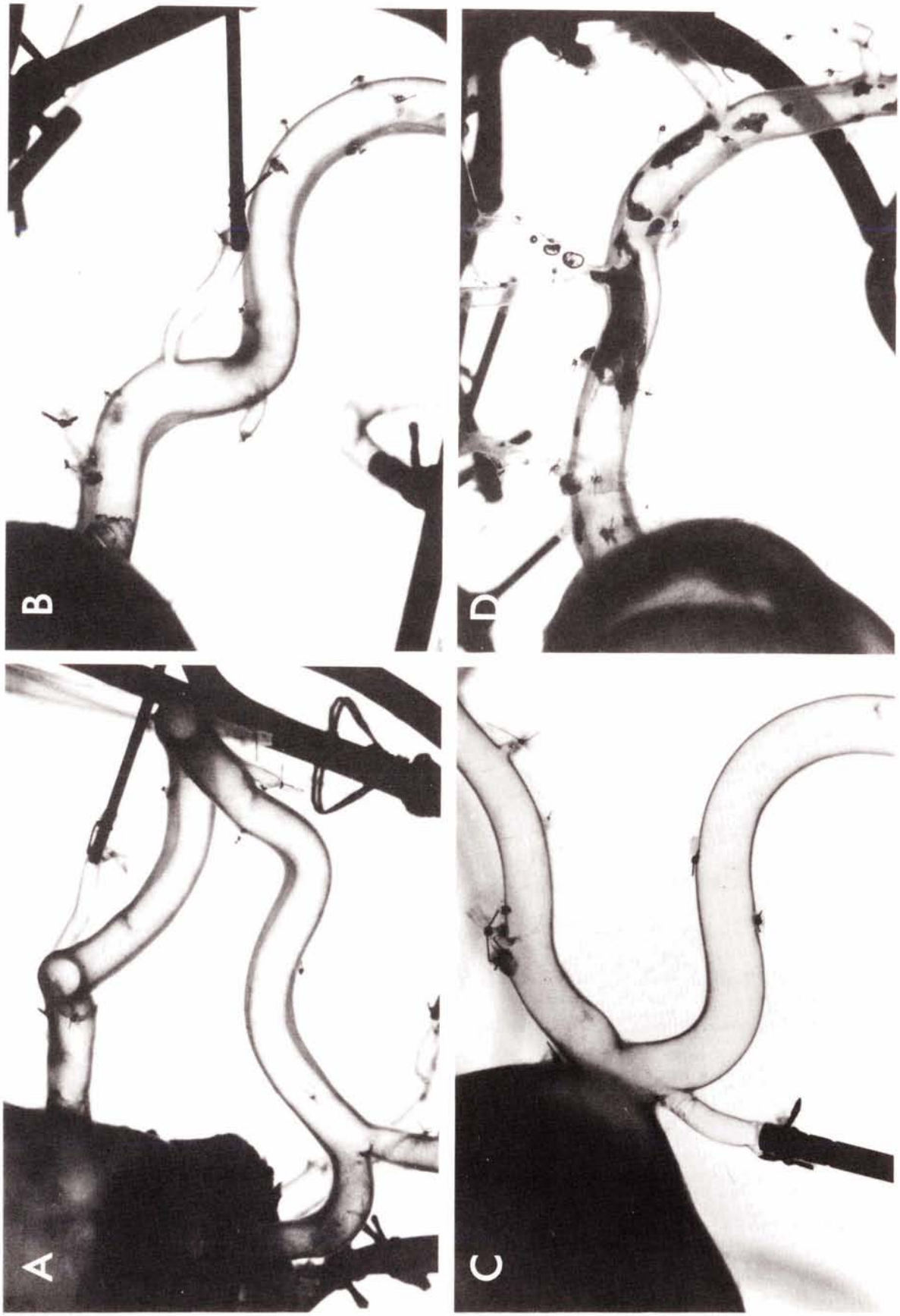
B
D
A
C

Thus, it was possible to make observations and measurements of the exact locations of atherosclerotic lesions and the flow in both normal and diseased vessels, and from any desired direction without the errors arising from optical distortions (due to the difference in the refractive index between the vessel wall and the flowing liquid) which are inevitable when glass models and plastic casts are used. The transparent arterial trees were used to first study the exact anatomical locations of atherosclerotic lesions and then to study the detailed fluid mechanical characteristics of the flow at such sites. The results obtained from these anatomical and fluid mechanical investigations are described in detail for each location along the arterial tree in the following sections.

3.1 The Left Coronary Artery

(a) The Left Main Coronary Artery

As shown in Figures 2(A,B) and 3(B,C), the relatively straight left main coronary artery (LMCA) arose with a bell-shaped entrance from the distal end of the aortic sinus. Close observation of the anatomical structure of the entrance region revealed that curvatures of the vessel wall were very gentle on the upper (pericardial side) wall, but rather sharp like the flow divider at branching sites on the lower (myocardial side) wall. The measured angles (acute towards the heart) between the axes of the LMCA and the ascending aorta, when viewed laterally, were between 25° and 60° in four aged subjects (51-75 years old) and 70° in a young, 18-year old subject. Moreover, when observations

were made along the axis of the ascending aorta, the axis of the LMCA was skewed towards the right coronary artery with angles of deviation from the diametrical plane of the ascending aorta which passed through the center of the orifice of the LMCA between 50° and 70°. The internal diameter of the LMCA, measured at the mid portion of its entire length was between 3.8 mm and 4.1 mm in the four aged subjects and 5.3 mm in the young subject.

Atherosclerotic lesions were found in three regions. In 4 cases out of 5, atherosclerotic wall thickening was observed on the right upper wall opposite to the sharp leading edge of the lower wall as can be seen in Figure 3C. In the above 4 cases, 2 cases were calcified plaques. The second preferred site was located on the lower right lateral wall just downstream of the lower leading edge of the LMCA. In 3 cases, mild wall thickening was found at this site. The third preferred site was the distal portion of the LMCA along the lower wall. In 3 cases, a wide and long atherosclerotic wall thickening which extended into the two daughter vessels of the LMCA after branching off, was found at this site as can be seen in Figure 3B. In no case, were atherosclerotic lesions found on the lateral wall of the LMCA.

The results from fluid mechanical investigation revealed some interesting relationships between flow patterns, the levels of wall shear stress and the preferred sites for atherosclerotic wall thickening. Figure 5 illustrates the detailed flow patterns and distributions of fluid velocity in the median plain (right lateral view) of the entrance region of the LMCA observed in steady flow in one of the transparent coronary arterial trees

FIGURE 5. Detailed flow patterns (A) and distributions of fluid axial velocity and wall shear stress (B) observed in steady flow in a median plane (normal to the pericardium) of the entrance region of the LMCA in an arterial tree prepared from a 51-year old female subject. The figures show the formation of a recirculation zone along the lower right lateral wall distal to the sharp-angled leading edge of the lower wall of the LMCA, and changes in velocity distribution with distance from the entrance. In Figure 5A, the solid lines represent the paths of particles located in, or close to the median plane, the short dashed lines paths far out of the median plane, and the long dashed lines those located between the above two types of paths. The arrows at S and P indicate the respective locations of separation and stagnation points. The numbers along the particle paths indicate particle translational velocities in mm/sec at the positions shown. The numbers at the outside and inside of the vessel indicate the inner diameter of the vessel and wall shear stress measured at each location, respectively. The maximum velocity at each of measurement is also shown on the curve of velocity distribution.

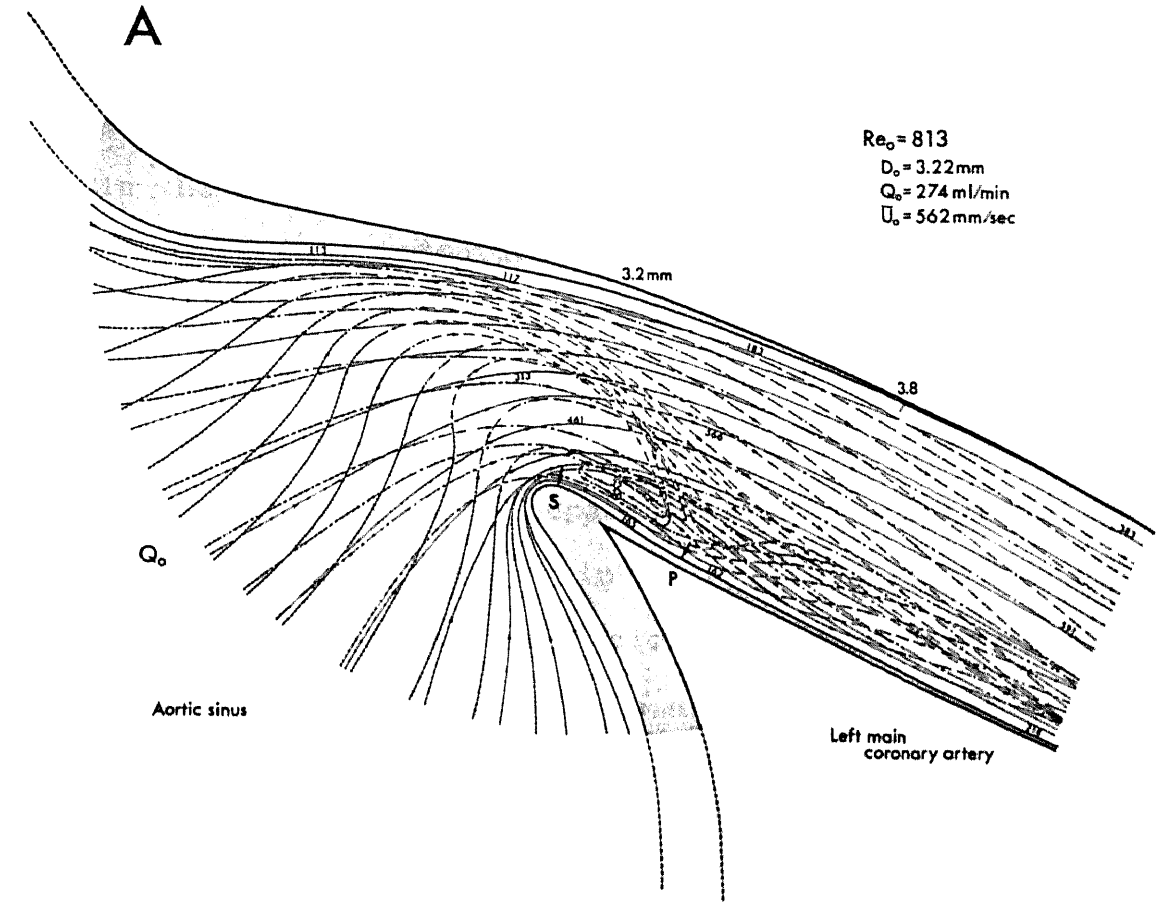
A
Re_o = 813
D_o = 3.22mm
Q_o = 274 ml/min
$\bar{U}_o$ = 562mm/sec
3.2mm
3.8
S
P
Q_o
Aortic sinus
Left main
coronary artery

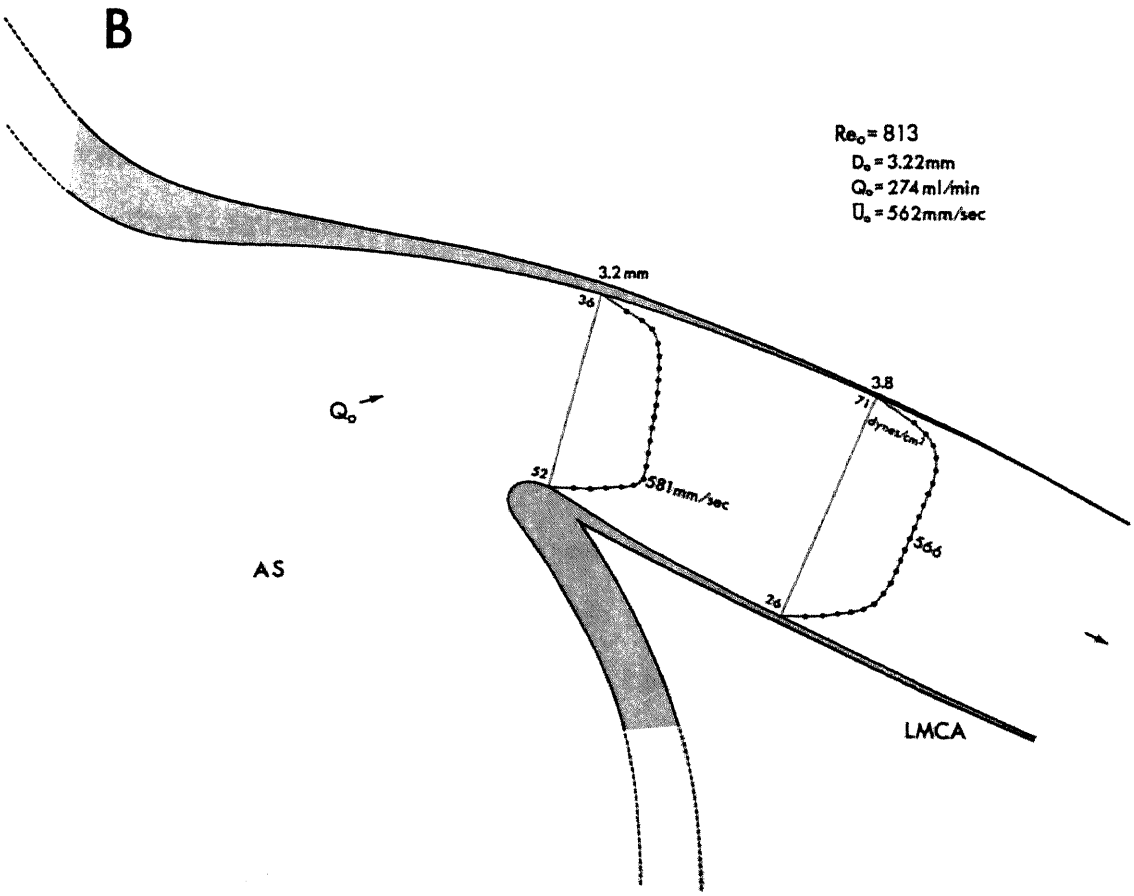
B
Re_o = 813
D_o = 3.22mm
Q_o = 274 ml/min
$\bar{U}_o$ = 562mm/sec
3.2mm
36
3.8
71
dynes/cm²
Q_o
52
581mm/sec
566
26
AS
LMCA

prepared in the present investigation. As show in Figure 5A (as well as in Figure 6A), formation of a recirculation zone was observed in 3 vessels out of 5, right at the entrance of the artery. Due to the rather sharp angulation of the lower leading edge of the LMCA which stemmed off the aortic sinus, flow separation occurred. The region of separated flow was filled up by a band of slow peripheral flow which originated from the right upper wall and traveled laterally along the dashed streamlines, eventually resulting in the formation of a backflow region along the lower right lateral (myocardial side) wall where a small calcified plaque was found in three vessels as described earlier. This was the only region where disturbed flow was observed in the LMCA. Another characteristic of the flow in the LMCA was the large variation in fluid velocity. It was noticed that in the entrance region, particles located near the gently curved upper wall traveled more slowly than those located near the lower wall. Thus, to identify the regions of fast and slow flow along the vessel wall, hence the regions of high and low wall shear stresses in the LMCA, distributions of fluid velocity were calculated from the velocity of tracer particles. As is evident from Figure 5B, (as well as Figure 6C), velocity distribution in the LMCA was skewed toward the lower wall at the entrance, but quickly reversed within a short distance (less than one diameter) from the lower leading edge, and skewed towards the upper wall, thus creating a low wall shear stress region along the upper wall right at the entrance and at the lower wall further downstream. Comparison of these results with the anatomical study of the

sites of atherosclerotic lesions indicates that preferred sites for the formation of a atherosclerotic plaques and wall thickenings are located in regions of slow flow and low wall shear stress.

(b) The LAD-LCx Junction and the Proximal Portions of the LAD and LCx

As shown in Figures 2 and 3(A,B), within 2-3 diameter distance after stemming off the aortic sinus, the LMCA divided into two major branches having approximately equal diameter, i.e., the left anterior descending branch (LAD) and the left circumflex branch (LCx), and not uncommonly into three, with a third, intermediate branch (IB). In the present investigation, 3 vessels out of 5 had the intermediate branch. After branching off the LMCA, the proximal portion of the LAD gently curved towards the lower wall along the curved surface of the myocardium. The measured branching angle between the axes of the LAD and LCx ranged from about 70° in 2 subjects including the youngest 18-year old one to 105° in the other 3 subjects.

Atherosclerotic lesions were found at two distinct locations at the branching site as shown in Figure 3A by a photograph of the artery prepared from a 61-year old man. In all the 5 transparent arterial trees prepared and studied, atherosclerotic wall thickenings were located almost exclusively along the outer wall (hip) of the bifurcation or trifurcation. To be more specific, they were formed along the lower lateral walls of the bifurcation and extended further distally and to the lower

(myocardial side) walls of the LAD and LCx. Calcified plaques were also found at these sites as a part of the wall thickening (3 cases on the LAD side and 1 case on the LCx side). As an extension of these two lesions, the lower wall of the distal LMCA was also thickened. In no case, were the flow divider and upper (pericardial side) walls affected by atherosclerotic lesions.

In the proximal portion of the LAD, atherosclerotic plaques and wall thickenings were found along the right lateral and lower walls (inner wall of the curved segment). In two cases, atherosclerotic wall thickening was also found along the inner wall of the trifurcation or the lower left lateral wall of the LAD as shown later in Figure 7. However, it was discovered that this was formed as a continuation of the first wall thickening. In these vessels, atherosclerotic wall thickening extended laterally and diagonally along the circumference of the lower half of the LAD all the way from the lower right lateral wall of the trifurcation to the left lateral wall of the LAD. It was also noted that atherosclerotic lesions in the LAD were confined within the initial few centimeters from the junction of the LAD and LCx. No atherosclerotic plaque or wall thickening was found on the upper (pericardial side) wall as shown in Figure 3C even in the most severe case encountered in the present investigation.

In the proximal LCx, atherosclerotic wall thickenings were found in the 4 aged subjects along the lower lateral wall as an extension of the one formed at the hip of the LAD-LCx junction. No atherosclerotic change was found along the inner (right lateral) wall of the bifurcation or trifurcation. Except for one

severely calcified case, no atherosclerotic plaque or wall thickening was found on the upper wall. In the one severely calcified case mentioned above, several small calcified plaques were found in an area where the LCx curved towards the upper wall (inner wall of a gently curved segment).

It was also noted that the frequency and degree of severity of the atherosclerotic lesions decreased with increasing distance from the origin of the artery from the aortic sinus.

Flow studies were carried out on 4 transparent arterial trees. The remaining one, prepared from a 75-year old male subject, was not usable because of the presence of non-transparent severely calcified plaques all over the LAD and LCx as shown in Figure 2D and 3(C,E). In 3 vessels prepared from aged subjects (51, 56 and 61 years old), formation of spiral secondary flows and recirculation zones was observed in one or both daughter vessels of the LMCA near the outer walls (hips) of the bifurcation or trifurcation at the very sites where atherosclerotic plaques and wall thickenings were located. Figure 6 illustrates the detailed flow patterns, traced out from the movements of tracer microspheres, and distributions of fluid axial velocity and wall shear stress observed in steady flow at the trifurcation of the LMCA prepared from a 61-year old male subject. As shown in Figure 6(A,B), flow separation occurred at the outer walls (hips) of the bifurcation, creating wide regions of separated flow. The regions of separated flow were then filled with the spiral and recirculation flows formed as a result of a strong deflection of the flow from the LMCA at the obtuse-angled flow

FIGURE 6. Detailed flow patterns (A,B) and the distributions of fluid axial velocity and wall shear stress (C) in steady flow as in Figure 5 at the trifurcation of the LMCA in an arterial tree shown in Figure 3A as observed normal (A) and parallel (B,C) to the common median plane of the LMCA and its two major branches. The figures show the formation of recirculation zones and complex secondary flows at the branching site of the LAD and LCx from the LMCA. Atherosclerotic wall thickenings were found at the hips of the trifurcation adjacent to regions of disturbed flow. Figures 6B and 6C are the right lateral views of the flow shown in Figure A. As shown in Figure 6C, atherosclerotic wall thickening was formed along the lower (myocardial side) wall of the distal LMCA and proximal LAD where both the fluid velocity and wall shear stress were low.

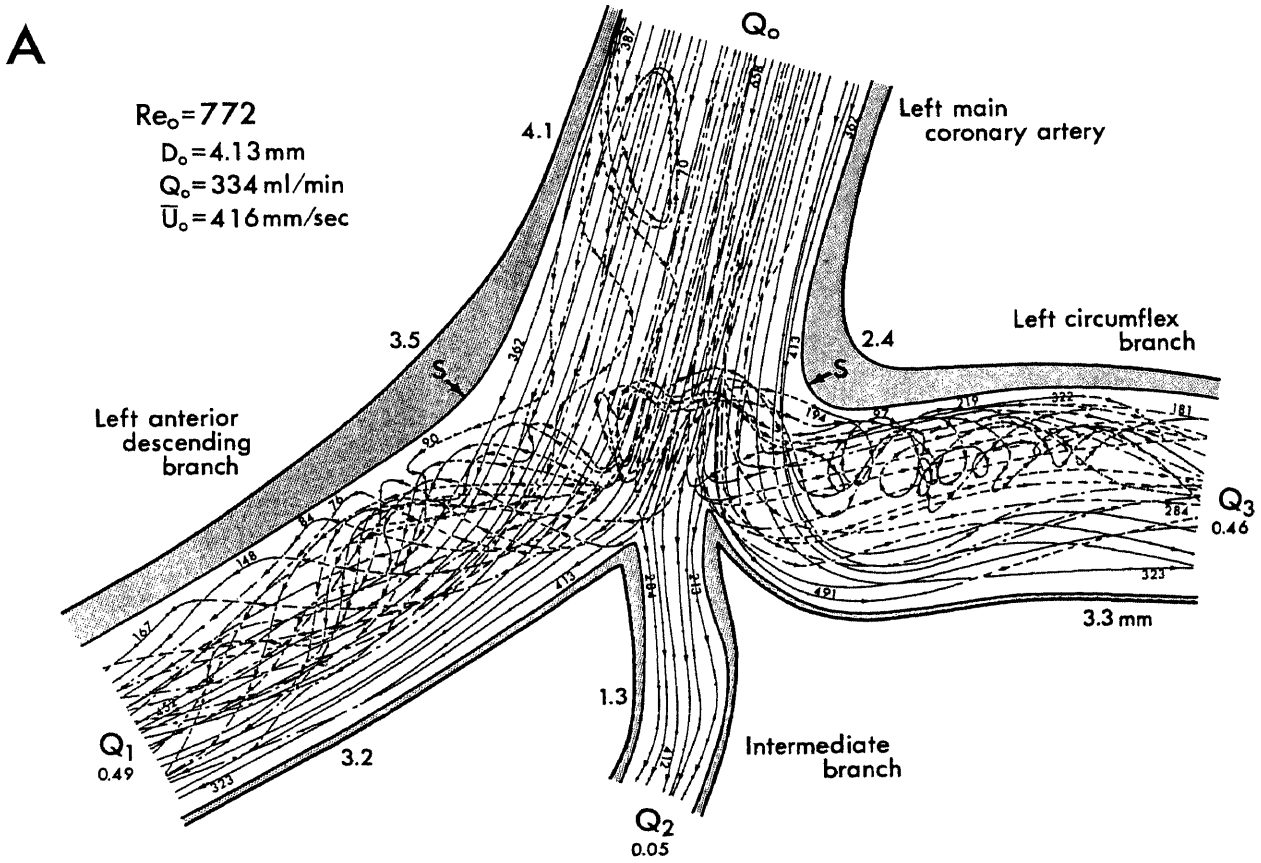
A
Re_o=772
D_o=4.13mm
Q_o=334 ml/min
$\bar{U}_o$=416mm/sec
Q_o
Left main coronary artery
Left circumflex branch
Left anterior descending branch
Intermediate branch
Q_1 0.49
Q_2 0.05
Q_3 0.46
4.1
3.5
2.4
3.2
1.3
3.3 mm
S

B

$Re_o = 831$
$D_o = 3.91$ mm
$Q_o = 340$ ml/min
$\bar{U}_o = 472$ mm/sec

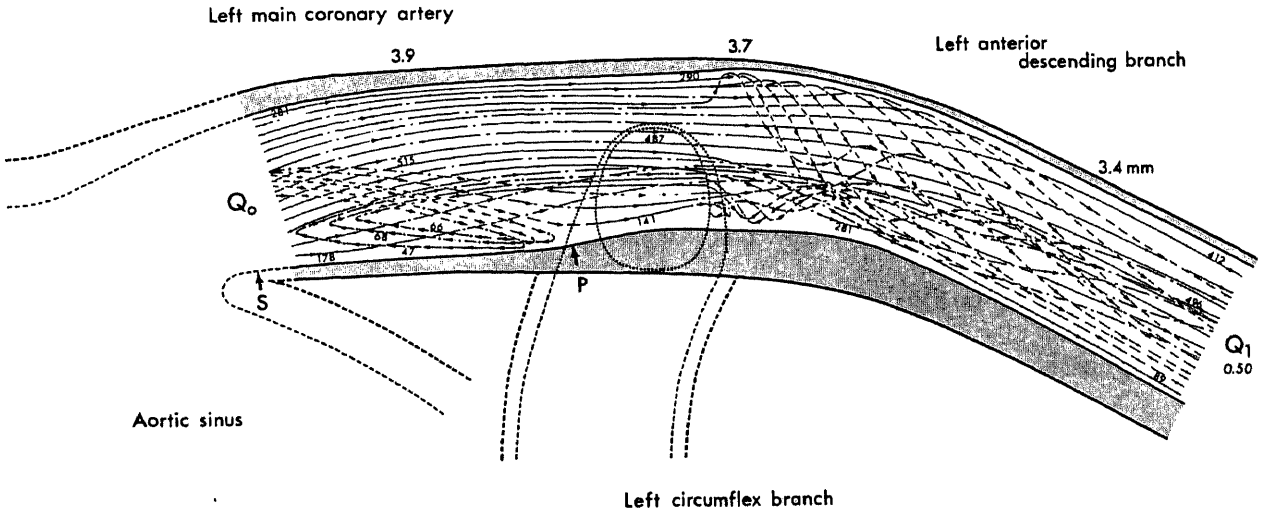

C

$Re_o = 831$
$D_o = 3.91$ mm
$Q_o = 340$ ml/min
$\bar{U}_o = 472$ mm/sec

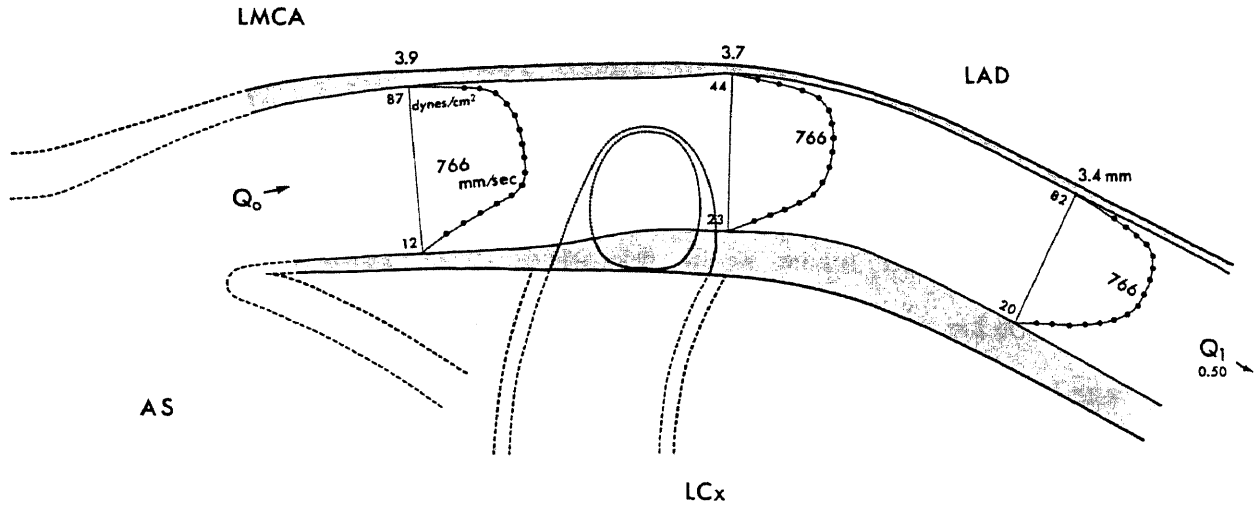

FIGURE 6. (continued)

divider. Due to the particular anatomical structure of the trifurcation, e.g., slight bending of the LAD and LCx towards the lower walls at the branching site, as well as the skewing of the approaching velocity (higher along the upper wall) in the distal LMCA, the deflection of flow at the flow divider was not symmetric about the common median plane (a curved plane parallel to the pericardium) of the LMCA and its two major daughter vessels. The deflection of flow was much stronger in the lower half of the common median plane in both the LAD and LCx, resulting in the formation of a spiral secondary and recirculation flows along the lower lateral walls of the trifurcation. To confirm this, observations were also made laterally. Figure 6B illustrates the flow patterns observed when the viewing axis was aligned with the common median plane of the LMCA and LAD which was parallel to the pericardium (right lateral view of the flow shown in Figure 6A). As shown in the figure, a long, thin-layered recirculation zone was formed adjacent to the lower right lateral wall of the LMCA just downstream of the lower leading edge where a mild wall thickening was found. Going further down, flow was deflected at the flow divider on both sides of the common median plane, but the movements of tracer microspheres were more complicated near the lower wall, where atherosclerotic lesion was also severe, than near the upper wall. The axial velocity distributions in the median plane of both the LMCA and LAD, normal to the pericardium, were calculated from the paths of tracer particles located close to each diametrical plane. The results are shown in Figure 6C. As evident from this figure, the velocity

distributions skewed towards the upper wall in both the distal LMCA and proximal LAD. The long and wide atherosclerotic wall thickening was located along the lower wall where both fluid velocity and wall shear stress were much lower.

Two other examples of flow patterns at this branching site are given in Figures 7 and 8. Figure 7 shows the detailed flow patterns and distributions of fluid axial velocity and wall shear stress in the common median plain (parallel to the pericardium) of the LMCA, LAD and LCx obtained in steady flow in the arterial tree prepared from a 51-year old female subject. As illustrated in Figure 7A, particles traveling on streamlines very close to the lateral walls of the LMCA were separated from the vessel walls at the hips of the trifurcation and were pushed towards the inner walls downstream of the flow divider, resulting in the formation of a long, wide region of separated flow in each major daughter vessel. Particles located close to the center on both sides of the common median plane were deflected sideways at the flow divider. They then traveled laterally and slowly along the upper and lower walls of the LAD and LCx, finally entering the regions of separated flow. In the LCx, this resulted in the formation of weak spiral flows along the lower left lateral wall of the LCx. In the LAD, some of the slowly traveling deflected particles suddenly changed directions upon reaching the right lateral wall, and then moved backward and laterally along the lower wall of the LAD, resulting in the formation of a wide, thin-layered recirculation zone which encompassed the wide area between the two distinct regions of atherosclerotic wall thick-

FIGURE 7. Detailed flow patterns (A) and the distributions of fluid axial velocity and wall shear stress (B) in steady flow as in Figure 5, at the trifurcation of the LMCA in an arterial tree prepared from a 51-year old female subject. As shown in Figure 7A, a wide, thin-layered recirculation zone was formed along the lateral and lower walls of the LAD between the two distinct regions of atherosclerotic wall thickening. As in the previous case, atherosclerotic lesions were localized at the hips of the trifurcation where wall shear stress was low.

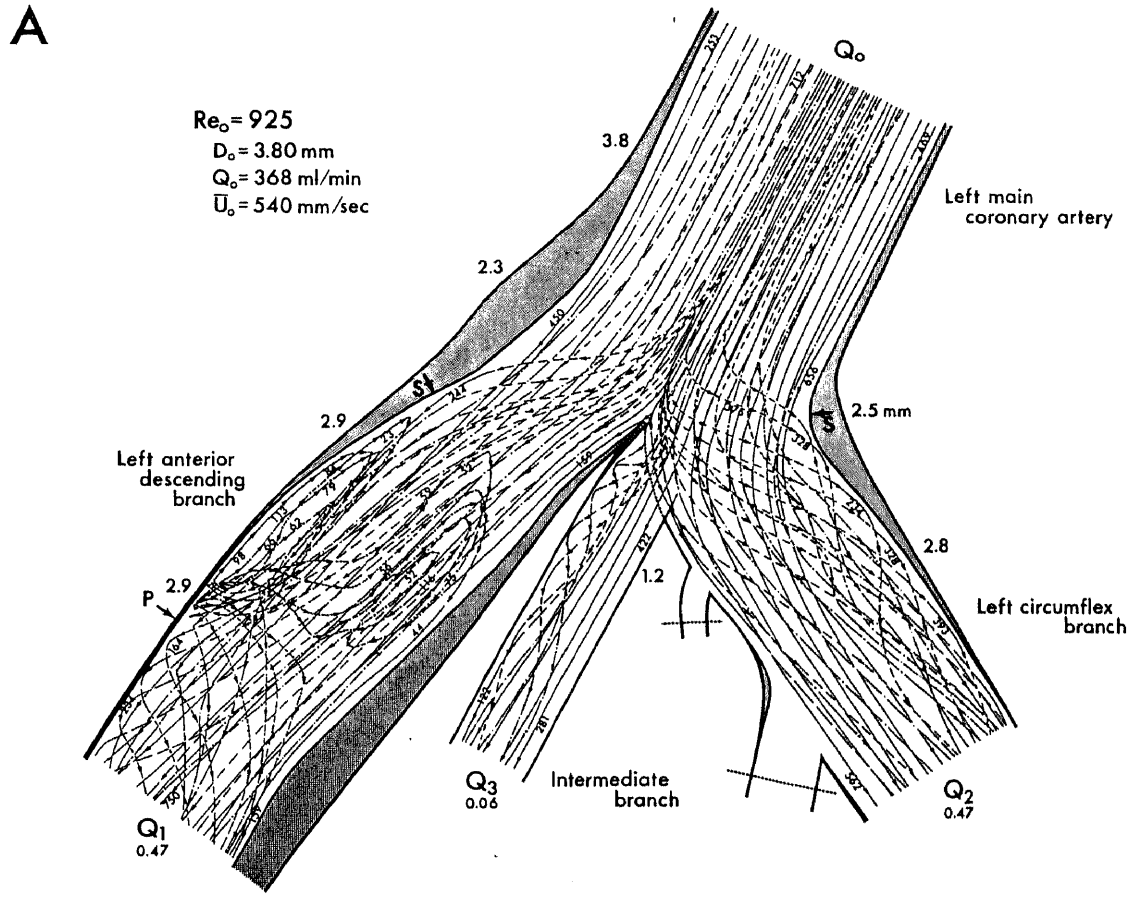
A
Re_o = 925
D_o = 3.80 mm
Q_o = 368 ml/min
$\bar{U}_o$ = 540 mm/sec
Q_o
3.8
2.3
2.9
2.9
P
Left main coronary artery
2.5 mm
2.8
1.2
Left anterior descending branch
Left circumflex branch
Q_3 0.06
Intermediate branch
Q_2 0.47
Q_1 0.47

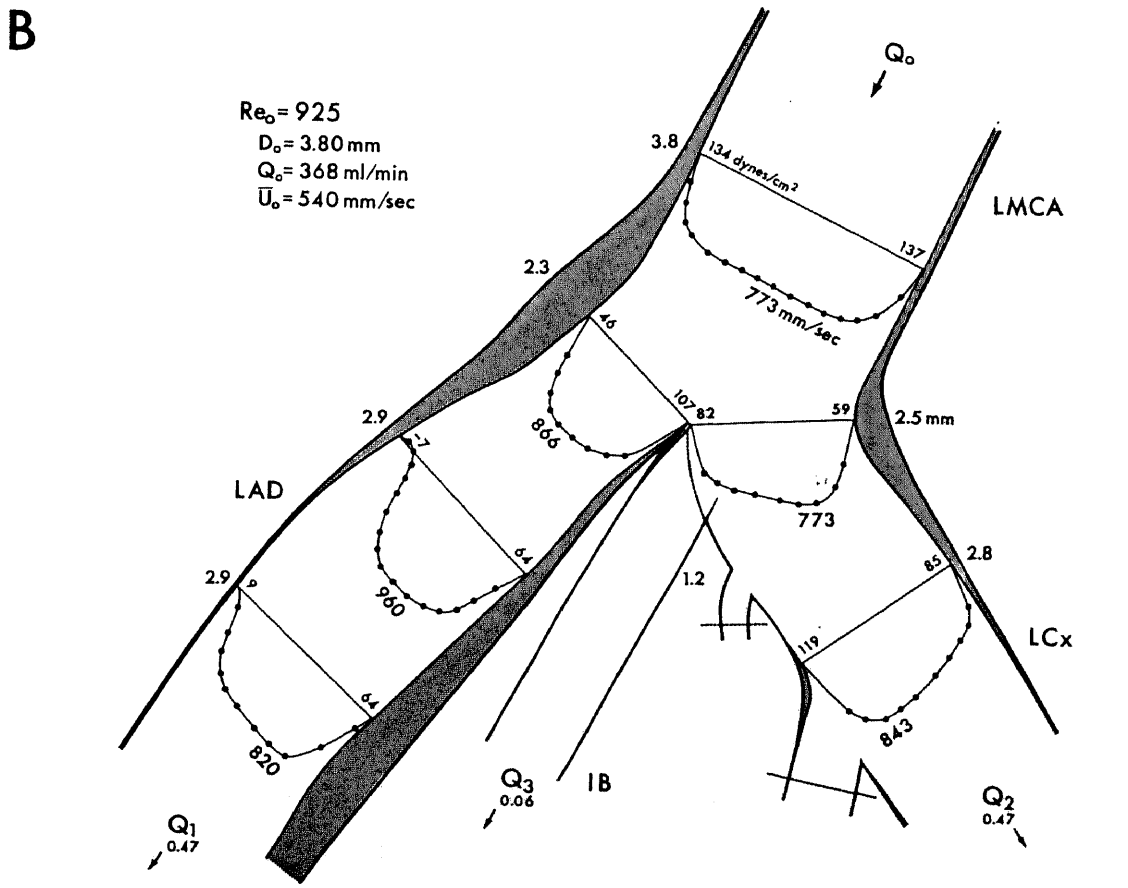
B
Re_o = 925
D_o = 3.80 mm
Q_o = 368 ml/min
$\bar{U}_o$ = 540 mm/sec
Q_o
3.8
134 dynes/cm²
137
LMCA
773 mm/sec
2.3
46
2.9
866
107
82
59
2.5 mm
LAD
773
2.9
960
64
2.8
85
1.2
LCx
119
843
64
820
Q_3 0.06
IB
Q_2 0.47
Q_1 0.47

ening as shown in the figure. When observations were made laterally along the common median plane of the trifurcation, it was found that the region of the lower wall, where the thin-layered, slowly moving backflow was formed, was also covered by a thick layer of atherosclerotic lesion which extended from the right lateral wall (hip of the trifurcation) to the left lateral (inner wall of the trifurcation) wall of the LAD downstream of the bifurcation. The distributions of fluid axial velocity and wall shear stress in the common median plain were calculated for the main and daughter vessels. The results are presented in Figure 7B. As shown in this figure, the approaching velocity profile on this plane was flattened. Thus, even at the flow divider, the velocity distribution in each daughter vessel was not skewed towards the inner walls of the trifurcation, although wall shear stresses were higher on the inner walls. As in the first case shown in Figure 6, the sites of atherosclerotic wall thickenings located at the hips of the trifurcation correspond to the regions of low wall shear stress. In the LAD further downstream of the flow divider, the site of atherosclerotic wall thickening was not the region of low shear. In actual fact, however, although it was not clear from the movements of tracer particles in the present investigation, it is very likely that the thin-layered, slowly moving backflow, formed along the lower wall of the LAD (c.f. Figure 7A), had reached the inner wall, thus creating a very wide region of low wall shear stress which extended spirally from the hip of the trifurcation to the inner wall of the trifurcation (left lateral wall of the LAD). The above results were compared

with those obtained in another, third arterial tree which was prepared from a young, healthy, 18-year old male subject who died in a car accident. It was found that the pathological and fluid mechanical phenomena occurring at the junction were basically the same as those observed in the previous two cases. As shown in Figure 8(A,C), the separation of streamlines from the vessel wall at the hip of the trifurcation, deflection of flow at the flow divider, and formation of helicoidal flows in regions of separated flow along the distal portion of the outer walls did occur even in this young vessel. However, it was evident that the flow patterns were much simpler than those observed in aged subjects (c.f. Figures 6 and 7), and no recirculation zone was formed in this trifurcation. Distributions of fluid axial velocity and wall shear stress were calculated along two diametrical planes parallel and normal to the pericardium. The results are shown in Figure 8(B,D). As evident from Figure 8B, in the common median plane, both the distributions of fluid axial velocity and wall shear stress in the young subject were almost the same as those obtained in the aged subject shown in Figure 7B. The velocity distribution was flattened proximal to the flow divider, slightly skewed towards the outer walls at the flow divider, and then gradually shifted towards the inner walls with increasing distance from the flow divider. The calculated wall shear stresses were higher along the inner walls than the outer walls of the trifurcation. The outer walls (hips), where a slight thickening of the vessel wall was found, were the regions of low wall shear stress. Another characteristic of the flow in the LAD was that,

FIGURE 8. Detailed flow patterns (A,C) and distributions of fluid axial velocity and wall shear stress (B,D) in steady flow as in Figure 5, at the trifurcation of the LMCA and proximal LAD in an arterial tree prepared from a young, 18-year old male subject in which wall thickening was minimal. Figures C and D are the right lateral views of the flow shown in Figures 8A and 8B. Figure 8 (A,C) shows the formation of double helicoidal flows in each major daughter vessel along the outer walls (hips) of the trifurcation where slight wall thickening was found. Wall shear stress was lower along the outer walls even in this young vessel as has been found in the previous two aged cases.

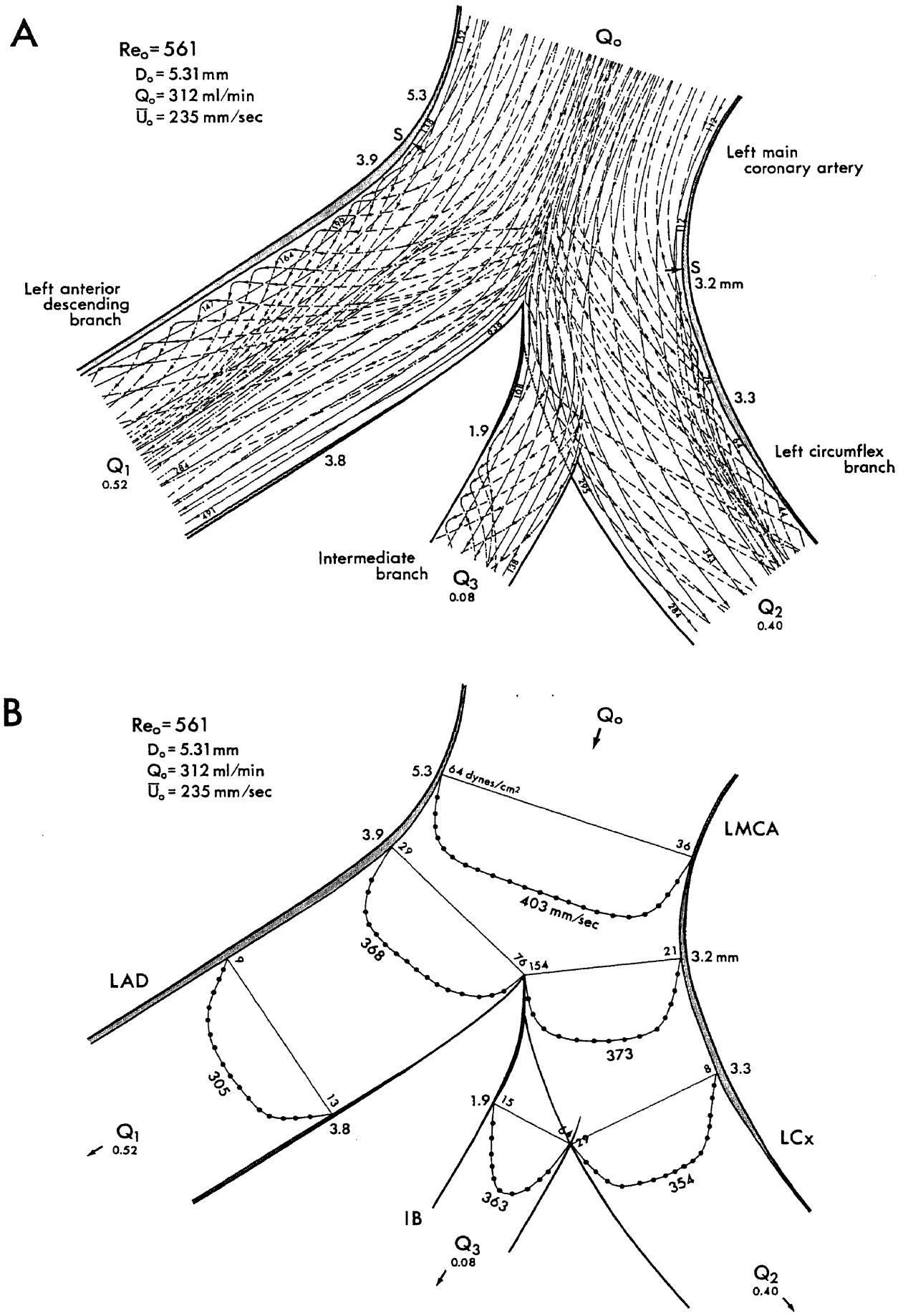
A
Re$_o$ = 561
D$_o$ = 5.31 mm
Q$_o$ = 312 ml/min
$\bar{U}_o$ = 235 mm/sec
Q$_o$
5.3
S
3.9
Left main coronary artery
S
3.2 mm
Left anterior descending branch
3.3
1.9
Left circumflex branch
Q$_1$
0.52
3.8
Intermediate branch
Q$_3$
0.08
Q$_2$
0.40
B
Re$_o$ = 561
D$_o$ = 5.31 mm
Q$_o$ = 312 ml/min
$\bar{U}_o$ = 235 mm/sec
Q$_o$
5.3
64 dynes/cm^2
LMCA
3.9
29
36
403 mm/sec
368
76
154
21
3.2 mm
LAD
9
373
305
13
3.3
1.9
15
64
29
LCx
Q$_1$
0.52
3.8
363
354
IB
Q$_3$
0.08
Q$_2$
0.40

C

$Re_o = 462$
$D_o = 3.72$ mm
$Q_o = 180$ ml/min
$\bar{U}_o = 276$ mm/sec

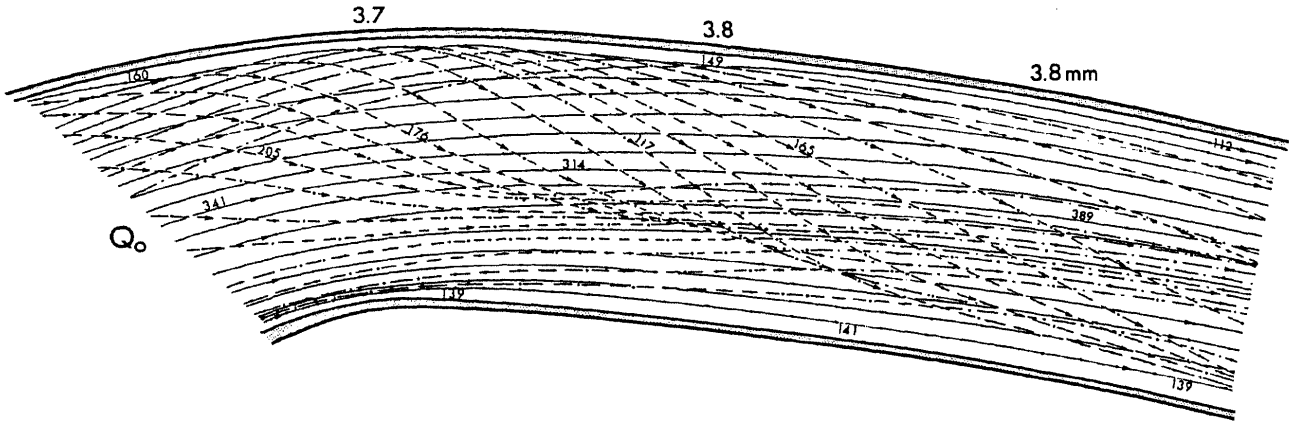

Left anterior descending branch

D

$Re_o = 462$
$D_o = 3.72$ mm
$Q_o = 180$ ml/min
$\bar{U}_o = 276$ mm/sec

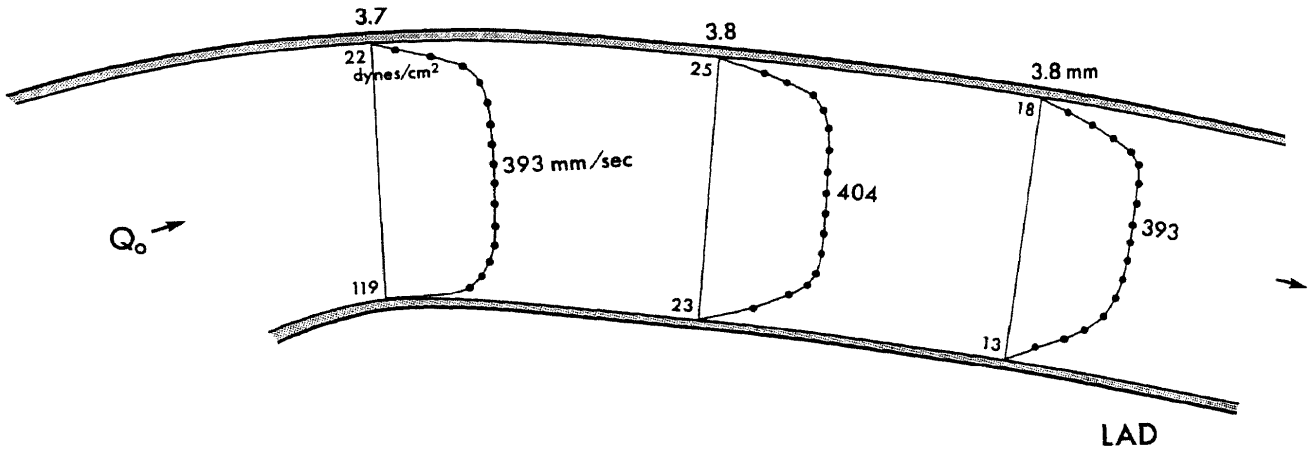

Figure 8. (continued)

as shown in Figure 8D, in the diametrical plane normal to the pericardium, velocity distribution was flattened over a long distance from the flow divider. Due to a short length of the LMCA, the wall shear stress at the proximal LAD was higher on the lower wall near the flow divider as was observed previously in Figure 5B, but gradually reversed with increasing distance from the flow divider, eventually becoming higher on the upper wall. The velocity profile also changed from a flat to a more parabolic shape with distance.

(c) The Middle & Distal LAD and its Major Branching Sites

In the middle and distal portions of the LAD, the degree of severity of atherosclerotic lesions was much reduced. Except for one severely calcified case shown in Figures 2D and 3C, most atherosclerotic lesions were confined to branching sites. As shown in Figure 3D as an example, atherosclerotic plaques and wall thickenings on the middle and distal LAD were found along the outer walls (hips) of one or both daughter vessels of bifurcations, and along the inner wall of curved segments. It was also noticed that the stem of the LAD was more tortuous in aged subjects than in the young one shown in Figure 2C. In such tortuous vessels, atherosclerotic wall thickenings were found very regularly along the inner wall of the curved segments.

Flow studies were carried out at some major branching sites of the LAD. It was found that the flow patterns at each branching site in steady flow were greatly affected by the nature of the flow proximal to the branching site, e.g., whether the ap-

proaching flow was laminar or already disturbed. In general, flow was disturbed to some extent at all the major bifurcations of the LAD. Much stronger and more pronounced disturbed flows were observed when two large diameter side branches came off the LAD at the same location as shown in Figure 9A. As illustrated in the figure, when the flow in the proximal LAD was distributed proportionally to the cross-sectional area of each daughter vessel evaluated at each flow divider (geometrical flow ratio), formation of a recirculation zone and complex secondary flows were observed in the LAD and the 1st diagonal branch, respectively. However, only a mild wall thickening was found in the vessel wall adjacent to the region of disturbed flow. A pronounced wall thickening was formed along the right lateral wall at the hip of the trifurcation opposite to the flow divider of the 1st septal branch. Flow patterns at branching sites are very sensitive to the flow ratios in daughter vessels. Thus, it is possible that if the flow rate in the LAD were higher than the geometrical value, the flow patterns at this trifurcation might be completely different from those shown in Figure 9A. It is likely that at the entrance of the 1st septal branch, the slowly moving fluid, deflected at the flow divider, may flow backwards along the outer wall of the trifurcation, thus forming a recirculation zone adjacent to the region of wall thickening. On the contrary, in the LAD, the recirculation zone may disappear with increasing the flow ratio in that branch.

Another example of the flow at a major bifurcation of the LAD is given in Figure 9B. The figure illustrates the detailed

FIGURE 9. Detailed flow patterns observed in steady flow as in Figure 5, at the major branching sites of the LAD showing the formation of disturbed flows with a recirculation zone and double helicoidal flows at A: the branching sites of the D_1 and S_1 from the LAD in an arterial tree prepared from an 18-year old male subject (c.f. Figure 2C) and B: the branching site of the D_2 in a vessel prepared from a 61-year old male subject (c.f. Figure 3D). As evident from the figures, atherosclerotic wall thickenings were localized at the hips of the trifurcation and bifurcation and along the inner wall of curved segments where fluid velocity and wall shear stress were low.

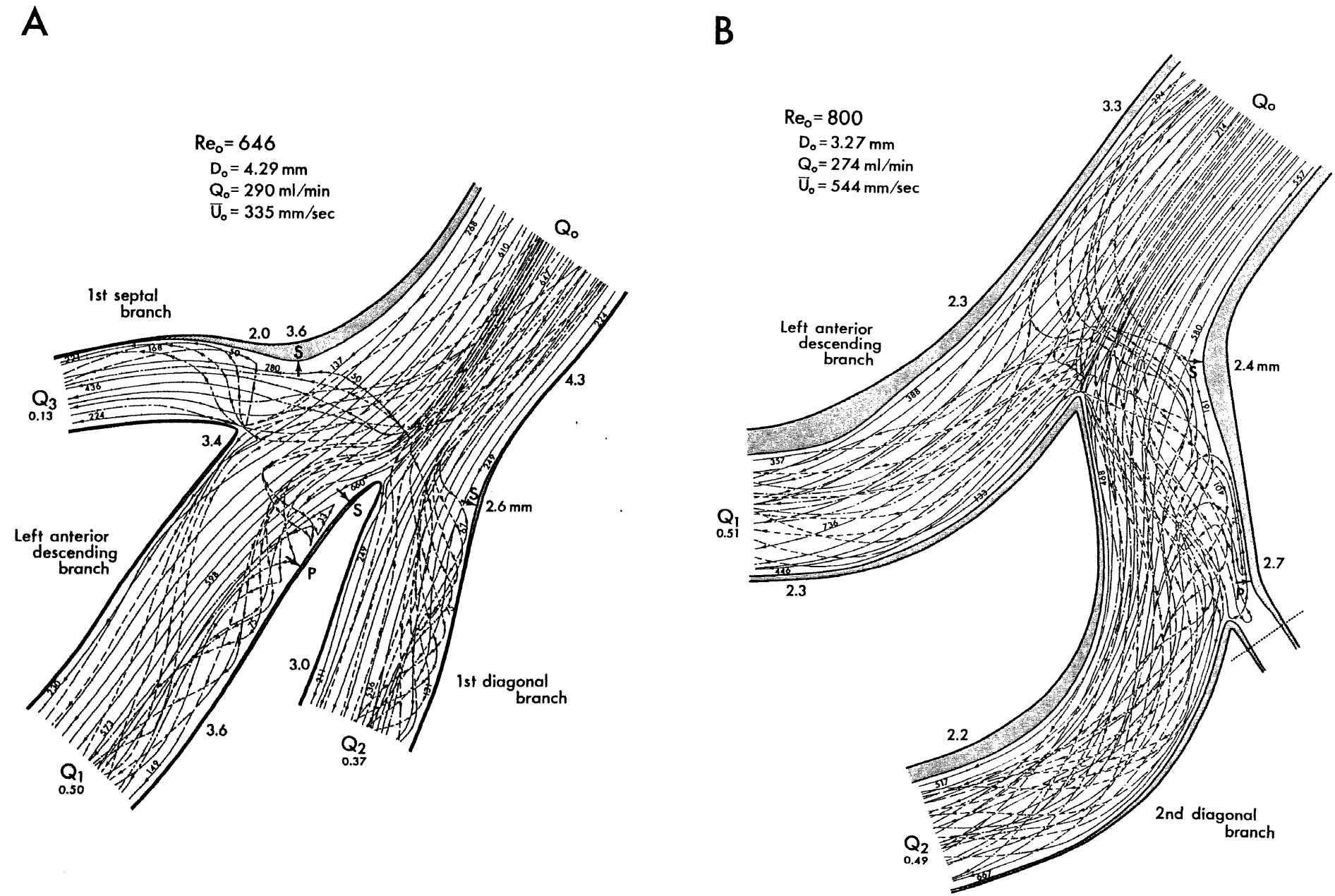
A
Re$_o$= 646
D$_o$= 4.29 mm
Q$_o$= 290 ml/min
Ū$_o$= 335 mm/sec
Q$_o$
1st septal branch
2.0
3.6
S
Q$_3$
0.13
3.4
4.3
2.6 mm
Left anterior descending branch
P
3.0
1st diagonal branch
3.6
Q$_2$
0.37
Q$_1$
0.50
B
Re$_o$= 800
D$_o$= 3.27 mm
Q$_o$= 274 ml/min
Ū$_o$= 544 mm/sec
Q$_o$
3.3
2.3
Left anterior descending branch
2.4 mm
Q$_1$
0.51
2.3
2.7
P
2.2
2nd diagonal branch
Q$_2$
0.49

flow patterns observed in steady flow at the branching site of the 2nd diagonal branch (D_2) in one of the arterial trees with a moderate degree of atherosclerotic wall thickening and tortuosity in the LAD. As evident from the figure, a recirculation zone was formed in the D_2 adjacent to the outer wall (hip) of the bifurcation at the very site where an atherosclerotic wall thickening was found. The inner wall of each curved segment was also a preferred site for atherosclerosis.

(c) The LCx and its Major Branching Sites

The anatomical structure of the left circumflex branch (LCx) was quite variable from subject to subject. The LCx was also tortuous in aged subjects. Thus, there was no particular region where atherosclerotic lesions were concentrated. In general, the lesion was more severe in the proximal portion than in the middle (the region of the branching site of the obtuse marginal branch) and distal portions. Atherosclerotic lesions were found at the inner wall of curved segments and along the outer walls (hips) of bifurcations as shown in Figure 3F by a photograph of the segment of LCx with obtuse marginal branch (OM) prepared from a 61 year old male subject. In vessels with severely calcified plaques, the atherosclerotic lesions were distributed in more complicated fashions as shown in Figure 3E. However, even in this case, in some regions, calcified plaques were distributed according to the above rule.

The results from fluid mechanical investigations are presented in Figure 10. As evident from Figure 10(A,C), at the

FIGURE 10. Detailed flow patterns as in Figure 5A at the major branching sites of the LCx in steady flow, showing the formation of disturbed flows with a re-circulation zone and complex spiral secondary flows at the branching site of A: the OM in an arterial tree prepared from a 61-year old male subject (c.f. Figure 3F); B: the PL in an 18-year old male subject; and C: the OM in a 51-year old female subject. Note that the formation of disturbed flows are affected by geometric factors such as the branching angle and the radius of curvature at the hips (outer walls) of a bifurcation, and the nature of the approaching flow proximal to the flow divider. In both vessels prepared from aged subjects (Figures 10A and 10C), atherosclerotic wall thickenings were localized at one or both outer walls of the bifurcation adjacent to the regions of disturbed flow.

A

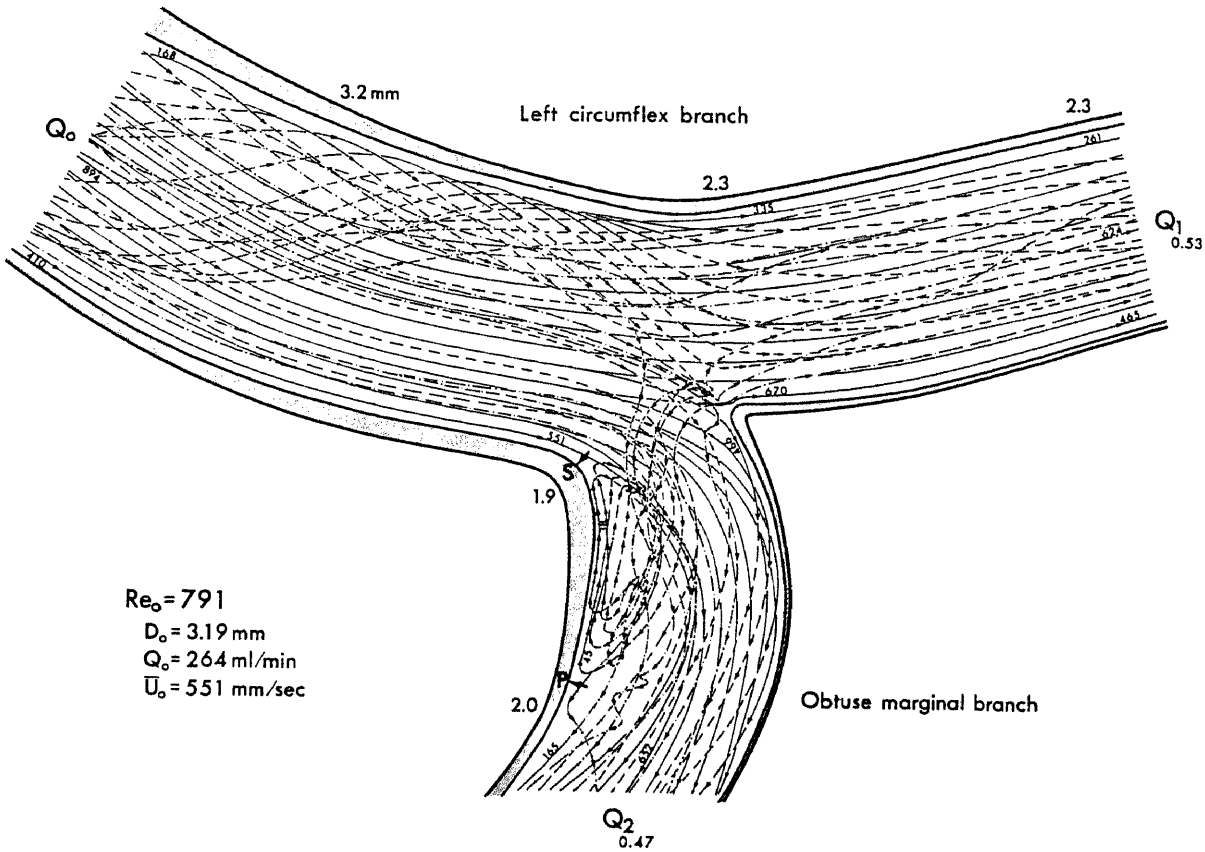
3.2 mm
Left circumflex branch
2.3
2.3
Q_o
Q_1 0.53
1.9
2.0
Re_o = 791
D_o = 3.19 mm
Q_o = 264 ml/min
$\bar{U}_o$ = 551 mm/sec
Obtuse marginal branch
Q_2 0.47

B

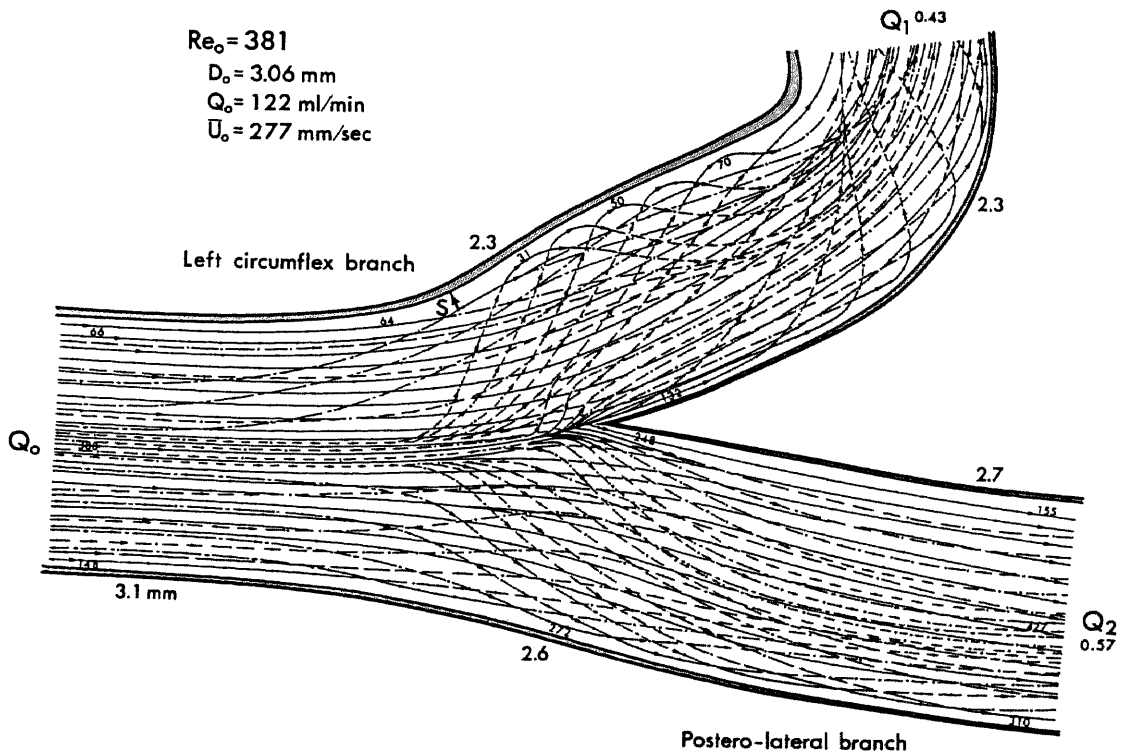
Re_o = 381
D_o = 3.06 mm
Q_o = 122 ml/min
$\bar{U}_o$ = 277 mm/sec
Q_1 0.43
2.3
Left circumflex branch
2.3
Q_o
2.7
3.1 mm
2.6
Q_2 0.57
Postero-lateral branch

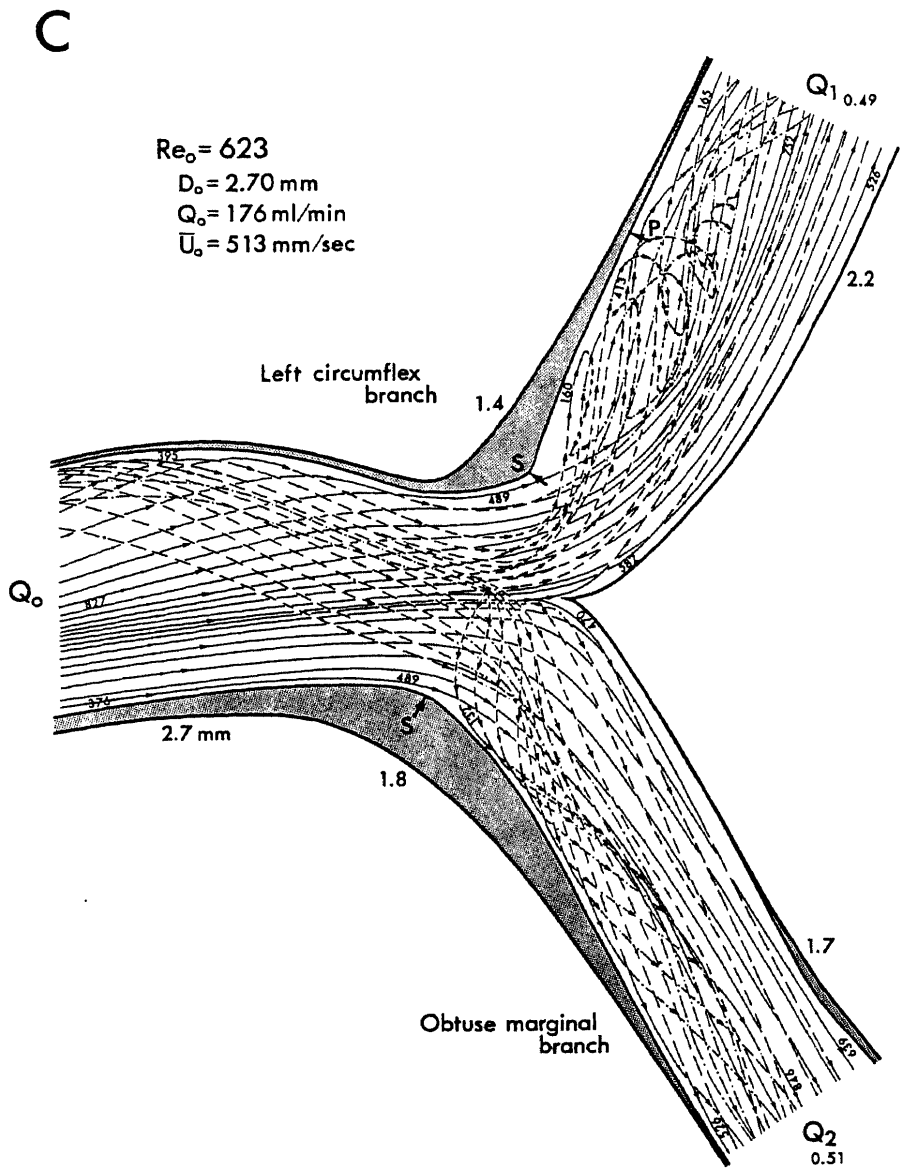

FIGURE 10. (continued)

branching site of the obtuse marginal branch (OM), the approaching flow in the LCx, proximal to the flow divider, was already disturbed due to the irregularly bending nature of the LCx. The approaching velocity distribution was skewed towards one side of the wall in both the common median plane (parallel to the pericardium) and the median plane normal to it (not slow in the figure). These factors appeared to determine the exact nature of the flow at this branching site. Due to the irregular bending of the LCx proximal to the branching site of the OM, flow patterns observed at this bifurcation were also quite complex. In both cases, the bifurcation was located just distal to a mild bend. Thus, in this particular vessel, shown in Figure 10A, the left lateral wall of the LCx corresponded to a region of separated flow. Particles in the slowly moving spiral flow (indicated by the dashed lines in the figure) located adjacent to the lower (myocardial side) wall passed through this region. They then traveled along the left lateral and upper walls of the LCx and approached the flow divider. After being deflected at the flow divider near the upper wall, they split into two groups, some entering the OM and others trailing down along the upper wall of the LCx. Flow separation occurred at the sharp bend of the OM opposite to the flow divider. The particles located near the lower wall close to the right lateral wall entered this region from the far end. They then moved backward along the outer wall of the bifurcation and suddenly changed their direction and were entrained by the rapid flow from the LCx. In this way, a recirculation zone was formed downstream of the sharp bend right at

the entrance of the OM. A pronounced atherosclerotic wall thickening was found at the sharp bend (hip of the bifurcation) where a triangular-shaped recirculation zone was formed. A similar type of disturbed flow was observed in another vessel as illustrated in Figure 10C. Here, complex spiral recirculation flows and helicoidal flows were formed along the outer walls adjacent to the pronounced atherosclerotic wall thickening.

Formation of disturbed flows was also observed at the branching site of the postero-lateral branches (PL). Figure 10B illustrates the detailed flow patterns observed in steady flow at the junction of the PL in an arterial tree prepared from a young, 18-year old male subject. In this particular case, both the LCx and PL slightly curved towards the pericardium. Thus, the flow at this bifurcation was also asymmetric about the common median plane of the parent and daughter vessels. Deflection of flow at the flow divider was much stronger on the side of the lower (myocardial side) wall than the upper wall. Strong double helicoidal flows were formed in the LCx. However, no significant wall thickening was associated with this flow disturbance in this particular vessel.

(e) Flow Patterns Observed in Pulsatile Flow

Observations of flow were carried out also in pulsatile flow by superimposing a sinusoidal oscillatory flow with a frequency of 2 Hz and displacement volumes of 0.5 and 1.5 ml on steady flow. Studies were focused on two locations along the left coronary artery: the branching site of the LAD and LCx in the

vessel shown in Figures 3A and 6A, and the branching site of the 2nd diagonal branch from the LAD in the vessel shown in Figures 3D and 9B. The cine films which recorded the behavior of tracer microspheres revealed that, in both vessels chosen for flow studies, the observed phenomena were qualitatively the same as those found in steady flow. At a small displacement volume of 0.5 ml, at which the flow field was still dominated by steady flow component, the secondary and recirculation flows observed in steady flow persisted throughout the entire cycle of pulsation. However, at a higher displacement volume of 1.5 ml, which created a condition nearing a temporal arrest of the mainflow at the end of the receding period of pulsation (which corresponded to the peak point of the systolic period in the cardiac cycle), both the secondary and recirculation flows vanished when the mainflow velocity attained a minimum in each cycle of pulsation. It was also found that the degree of flow disturbance judged from the size and the velocity of the formed recirculation flows was much higher in pulsatile than steady flow when compared at the same Reynolds numbers (hence flow rates), and it appeared to be the highest just after the mainflow velocity reached a maximum in each cycle of pulsation, though none of these variables were measurable with accuracy from the movie.

3.2 The Right Coronary Artery

(a) The Entrance Region of the RCA

As in the case of the left coronary artery, the right coronary artery (RCA) arose with a bell-shaped entrance from the

distal end of the aortic sinus. The measured angles (towards the heart) between the axes of the RCA and the ascending aorta, when viewed laterally, were between 75° and 95° with a mean value of 88°. The mean angle (away from the left main coronary artery) of deviation from the diametrical plane of the ascending aorta which passed through the center of the orifice of the RCA was about 2°, indicating that the RCA stemmed from the aorta almost symmetrically. The internal diameter of the RCA, measured in its entrance region, ranged from 3.3 to 3.8 mm in the 5 coronary arteries studied in the present investigation.

In all five right coronary arteries, atherosclerotic wall thickenings were found right at the entrance region within 1 cm from the route of the RCA. In most cases, the vessel wall was thickened not on one particular side but equally all around the intima. In only one case was the intimal thickening found at the left lateral wall as shown in Figure 4B and 12A. Figure 11 illustrates the detailed flow patterns (A), traced from the movements of tracer microspheres, and distributions of fluid velocity (B) in the median plane (normal to the pericardium) of the entrance region of the RCA observed in steady flow in one of the transparent coronary arterial trees used in the present investigation. As shown in this figure (as well as in Figure 14A), the flow in the entrance region of the RCA was laminar in all cases. As shown in Figure 11B, the velocity distribution in the median plane normal to the pericardium was flattened at the entrance and then gradually shifted to a more parabolic profile. Due to the more gentle curvature of the wall at the lower leading edge of

FIGURE 11. Detailed flow patterns (A) and distributions of fluid axial velocity (B) observed in steady flow in a median plane (normal to the pericardium) of the entrance region of the RCA prepared from a 51-year old female subject. Figure 11A shows that the flow field consists of parallel streamlined undisturbed mainflow (solid lines) and counterclockwise peripheral secondary flow (dashed lines) locates adjacent to the left lateral wall (due to the intake of the flow by a side branch located just distal to this relatively straight segment). Figure 11B shows the gradual changes in velocity distribution with distance from the entrance. The numbers along the particle paths indicate particle translational velocities in mm/sec at the positions shown. The numbers at the outside and inside of the vessel indicate the inner diameter of the vessel and wall shear stress measured at each location, respectively. The maximum velocity at each of measurement is also shown on the curve of velocity distribution.

A

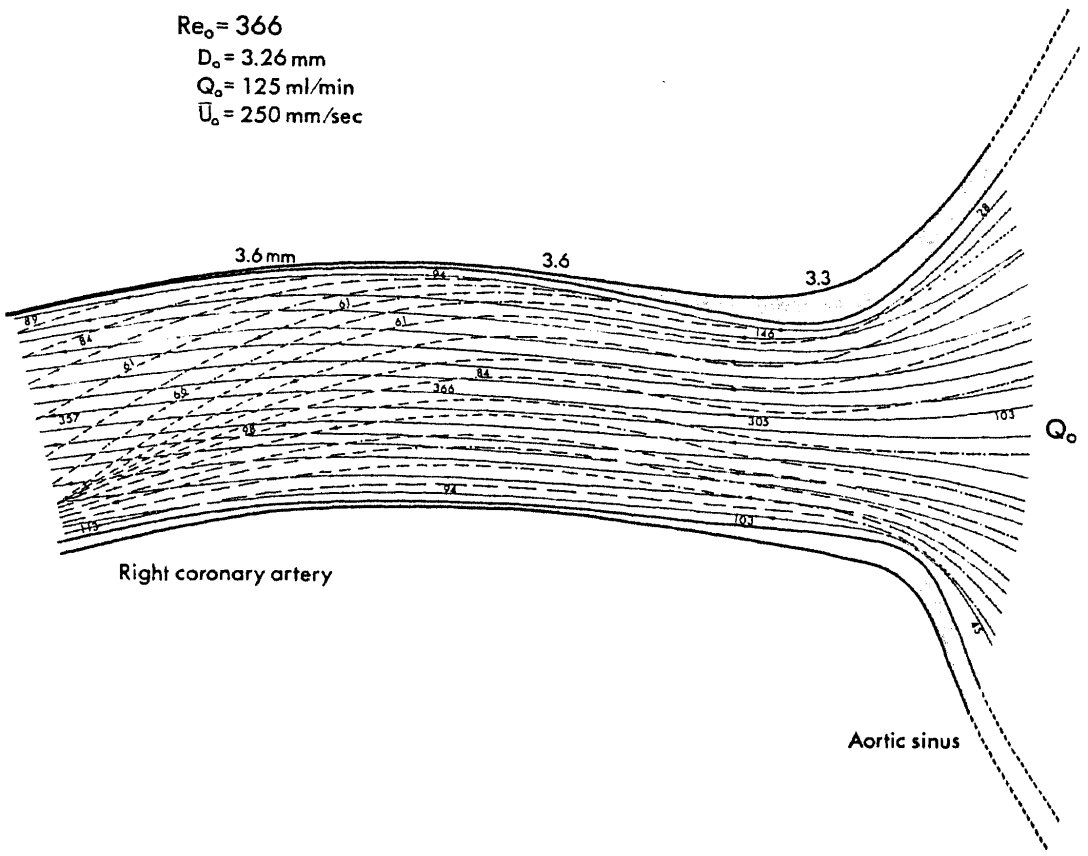
Re_o = 366
D_o = 3.26 mm
Q_o = 125 ml/min
$\bar{U}_o$ = 250 mm/sec
3.6 mm
3.6
3.3
Q_o
Right coronary artery
Aortic sinus

B

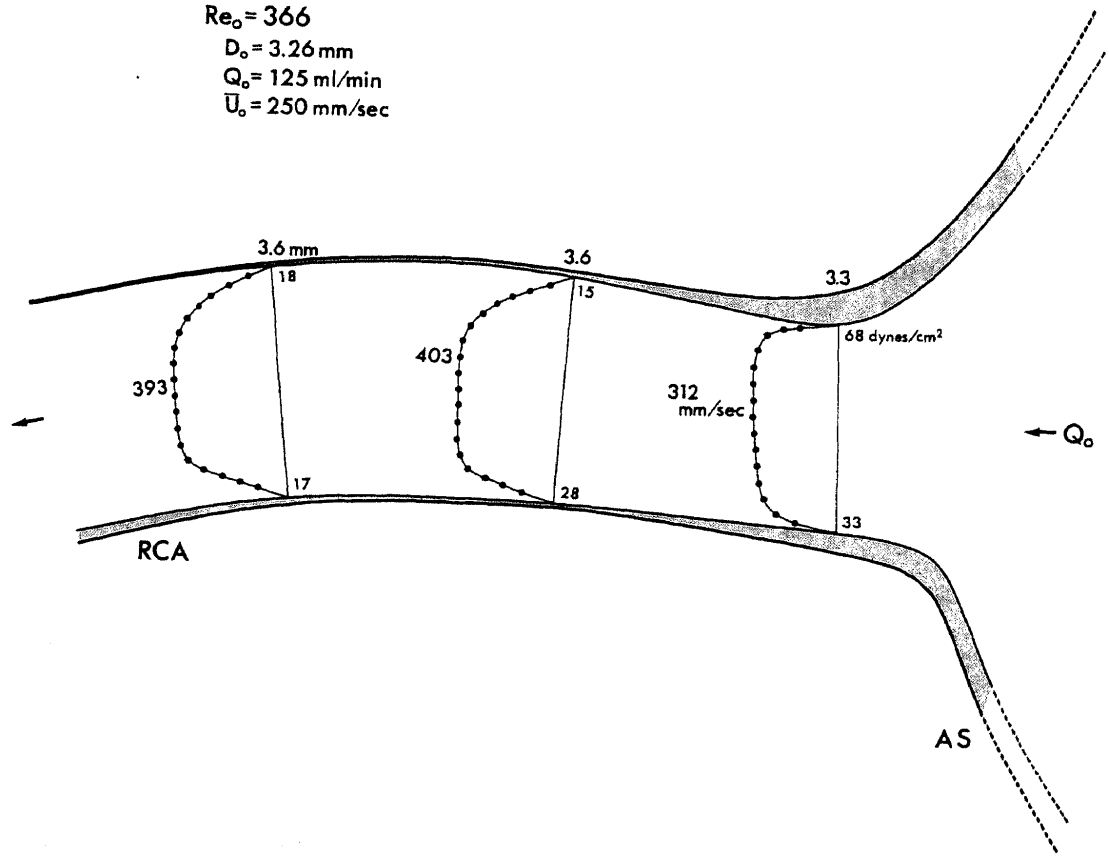
Re_o = 366
D_o = 3.26 mm
Q_o = 125 ml/min
$\bar{U}_o$ = 250 mm/sec
3.6 mm
3.6
3.3
18
15
68 dynes/cm²
393
403
312
mm/sec
Q_o
17
28
33
RCA
AS

the RCA compared to the left main coronary artery (LMCA), skewing of the velocity distribution was not as pronounced as in the case of the LMCA. The wall shear stress calculated from the velocity distribution was a little higher on the upper leading edge than the lower one, but gradually decreased and evened out with increasing distance from the origin of the RCA.

(b) The Major Bends of the RCA

In the proximal and middle portion of the RCA, from the origin of the artery to the branching site of the posterior descending branch (PD), the vessel diameter remained almost constant as can be seen in the photographs of the RCA in Figure 4. Except for one particular case in which the conus branch was unusually large as shown in Figure 4C, the diameters of the side branches in the proximal and middle portions of the RCA were quite small. The artery was tortuous with a series of asymmetrically arrayed sharp and gentle bends. Atherosclerotic wall thickenings were found at the inner wall of the curved segments in an alternating fashion, and at the outer walls (hips) of the major bifurcations and T-junctions of the RCA. In two vessels with severe atherosclerotic lesions, calcified plaques were found scattered all over the proximal and middle portions of the RCA as shown in Figure 4D. However, even in such severe cases, the frequency and degree of severity of atherosclerotic lesions tended to decrease with increasing distance from the origin of the artery.

Flow studies were carried out on 4 transparent coronary

arterial trees. The remaining one was not usable because of the presence of non-transparent calcified plaques all over the proximal and middle portions of the RCA as shown in Figure 4D. It was found that even though there are fewer bifurcations and T-junctions in the RCA than the left coronary artery (LCA), due to the presence of sharp and gentle bends, the flow in the RCA was by no means simpler than that in the LCA. Formation of strong secondary flows and standing recirculation zones were observed in most of the bends as shown in the following three examples. Figure 12 illustrates the typical flow patterns observed in steady flow in the arterial bends in the proximal portion of the RCA prepared from an aged 61-year old (A) male subject and a young 18-year old (B) male subject. As shown in Figure 12A, flow separation occurred at the inner wall of the first bend. At the outer wall of the bend, the fluid elements in the mainstream, having high momentum, were strongly deflected sideways, resulting in the formation of thin layered spiral secondary flows adjacent to the vessel wall. The region of separated flow along the inner wall was filled by the peripheral secondary flows. A part of the secondary flows moved backward along the inner wall of the bend, then suddenly changed direction and rejoined the mainstream on the median plane of the bend after describing a single orbit. Thus, a very thin-layered region of slow reverse flows (recirculation zone) was formed along the inner wall of the curved segment at the very place where atherosclerotic wall thickening was found. Similar flow patterns were observed also on the second bend where a much wider area of the inner wall of the bend

FIGURE 12. Detailed flow patterns observed in steady flow at some bends of the proximal and middle portions of the RCA prepared from A: a 61-year old male subject (shown in Figure 4B), and B: an 18-year old male subject (shown in Figure 4C). The figures show the strong deflection of mainflow at sites of confrontation with the outer wall of the arterial bends, development of peripheral secondary flows and the formation of slow recirculation flows adjacent to the inner wall. The solid lines are the paths of particles in or close to, and the dashed lines paths which are far away from the common median plane of the bends (the projection of the particle paths on the common median plane). The arrows at S and P denote the respective locations of the separation and stagnation points. The numbers at the outside of the vessel wall and along the streamlines (particle paths) indicate the inner diameter of the vessel in mm and the particle translational velocities in mm/sec at the positions shown, respectively.

A

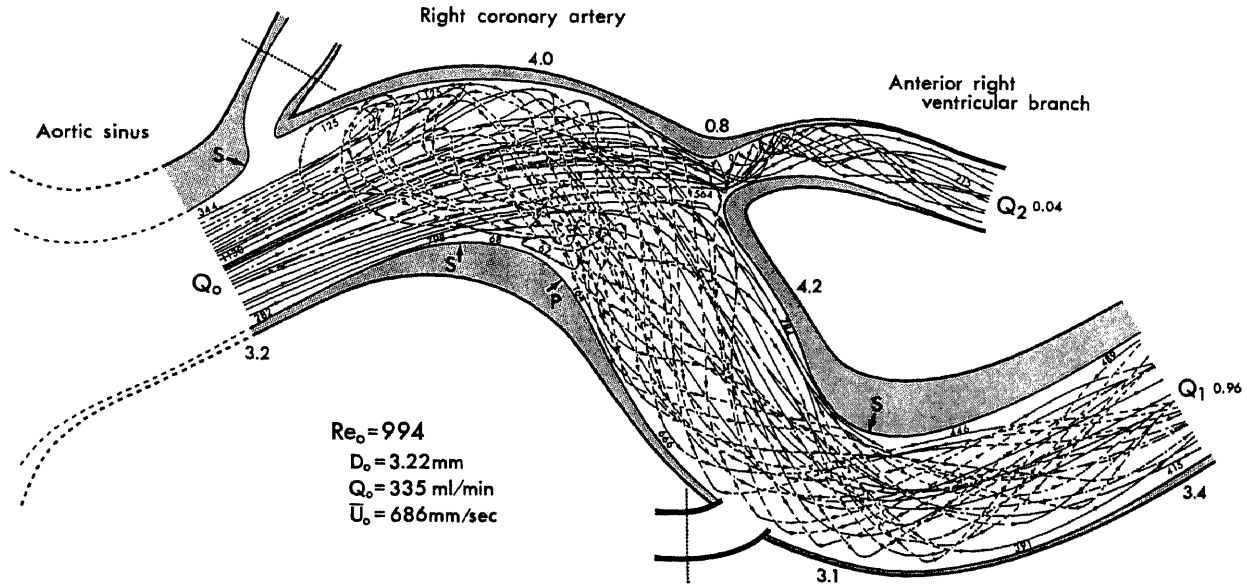
Right coronary artery
4.0
Anterior right ventricular branch
Aortic sinus
0.8
Q_2 0.04
Q_o
4.2
3.2
Q_1 0.96
Re_o=994
D_o=3.22mm
Q_o=335 ml/min
$\bar{U}_o$=686mm/sec
3.4
3.1

B

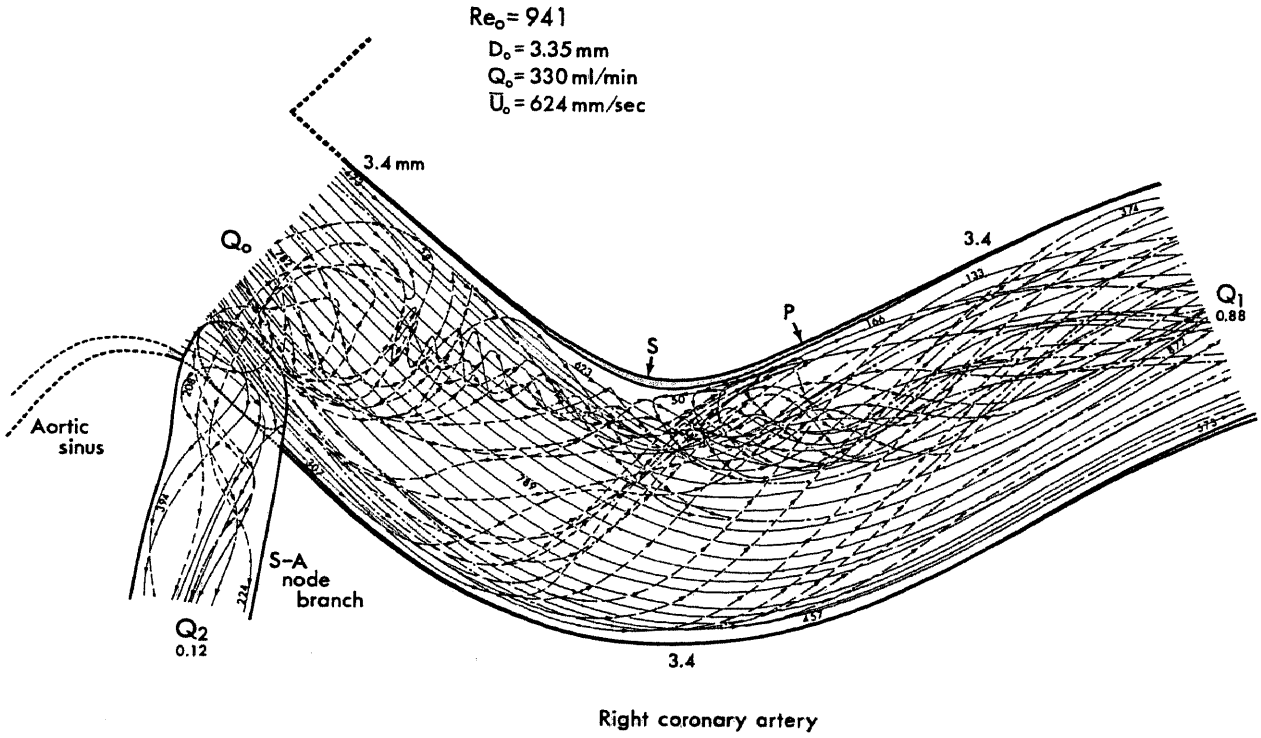
Re_o=941
D_o=3.35mm
Q_o=330 ml/min
$\bar{U}_o$=624 mm/sec
3.4 mm
Q_o
3.4
Q_1 0.88
P
S
Aortic sinus
S-A node branch
Q_2 0.12
3.4
Right coronary artery

was covered by a thick layer of atherosclerotic lesion. As occurred in the first bend, flow separation occurred at the inner wall of the second bend as well. The region of separated flow was then filled by the peripheral spiral secondary flows which were created as a result of a strong deflection of the flow at the outer wall of the bend. However, due to the technical difficulty in focusing on the smallest dust-like particles traveling along the vessel wall of the two connected bends which were not on the same plane, it was not possible to confirm the presence of a thin-layered reverse flow along the inner wall of the second bend.

The above finding raised a question whether the recirculation zone was created as a result of the formation of an atherosclerotic wall thickening or not. Thus, to clarify the doubt, studies were also carried out with a coronary arterial tree prepared from a young subject. Figure 12B illustrates the detailed flow patterns observed in an arterial bend found in the proximal portion of the transparent RCA prepared from an 18-year old male subject. As is evident from the figure, formation of a recirculation zone at the inner wall of an arterial bend was observed even in the artery from a young subject in which the degree of wall thickening was minimal. Flow separation occurred at the inner wall of the bend, and then the region on separated flow was filled with the fluid from the thin layered spiral secondary flows located near the upper (pericardial side) wall of the RCA. A part of the secondary flows slowly moved backward along the inner wall on the median plane of the bend, then

suddenly changed direction and was entrained by the rapid main-flow on the median plane. Flow disturbance was also created at the branching site of the S-A node branch. Here, the counter-clockwise helicoidal flow located near the upper wall distal to the branch joined the peripheral secondary flows near the inner wall, making the flow patterns in the arterial bend more complex. A slight but noticeable wall thickening was found at the inner wall of the bend right in the region where a standing re-circulation zone was located. The results clearly indicate that the exact location of atherosclerotic wall thickening is closely related to the regions of disturbed flow with flow separation and the formation of slow secondary and recirculation flows.

Figure 13A gives another example of flow patterns observed in an arterial segment with multiple bends located in the middle to distal portions of the RCA prepared from a 61-year old male subject. As shown in the figure, although there was no side branch, due to the presence of a series of sharp and gentle bends which were not located on one plane, flow patterns in this arterial segment were very complex. Flow separation occurred at the inner wall of the middle and distal bends. The regions of separated flow were filled with the fluid from the peripheral thin-layered secondary flows which traveled along the vessel wall all the way from the outer wall of each bend. In the middle bend where observations were focused, a thin-layered standing re-circulation zone was formed along the upper (pericardial side) inner wall just distal to the apex of the sharp bend where atherosclerotic wall thickening was localized. To identify the

FIGURE 13. Detailed flow patterns (A) and distributions of fluid axial velocity (B) as in Figure 11 and 12 observed in steady flow in the common median plane (parallel to the pericardium) of an arterial segment with multiple bends located in the middle to distal portions of the RCA prepared from a 61-year old male subject (shown in Figure 4A). Figure 13A shows the development of secondary flows and the formation of a recirculation zone adjacent to the inner wall of the middle bend. Figure 13B shows the changes in velocity distributions along the arterial segment. Note that the location of atherosclerotic wall thickenings was closely related to the region of recirculation flow where both the fluid velocity and wall shear stress were low.

A

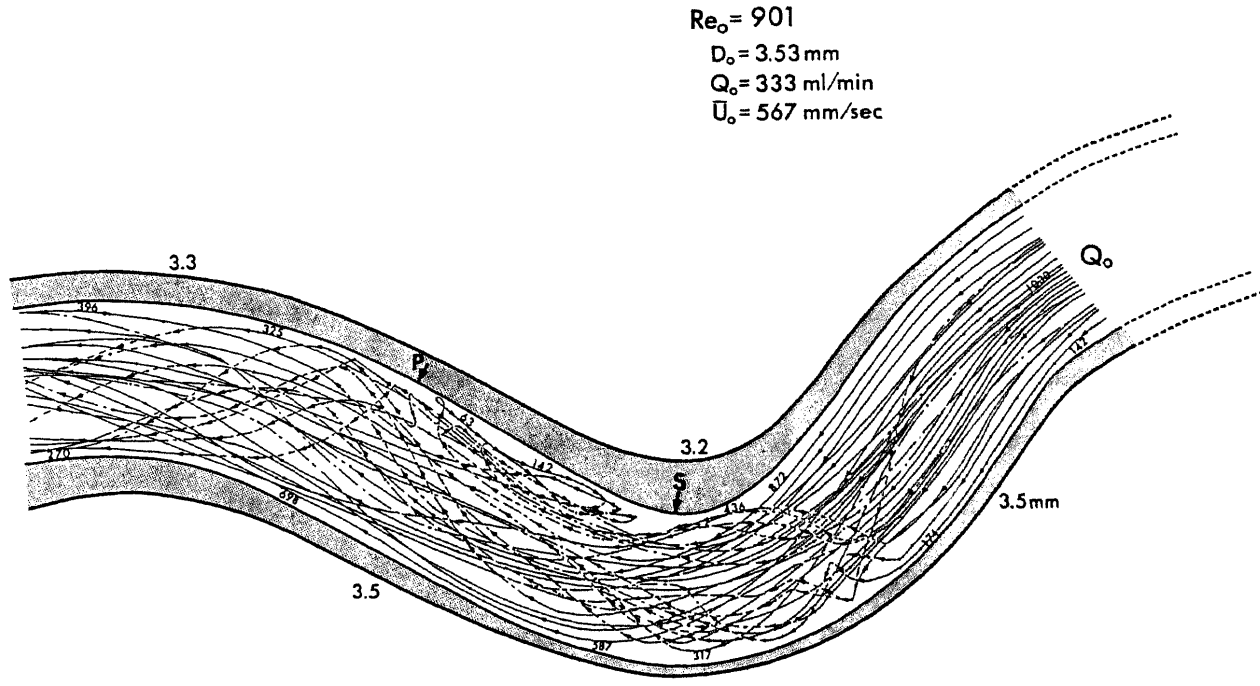

Right coronary artery

B

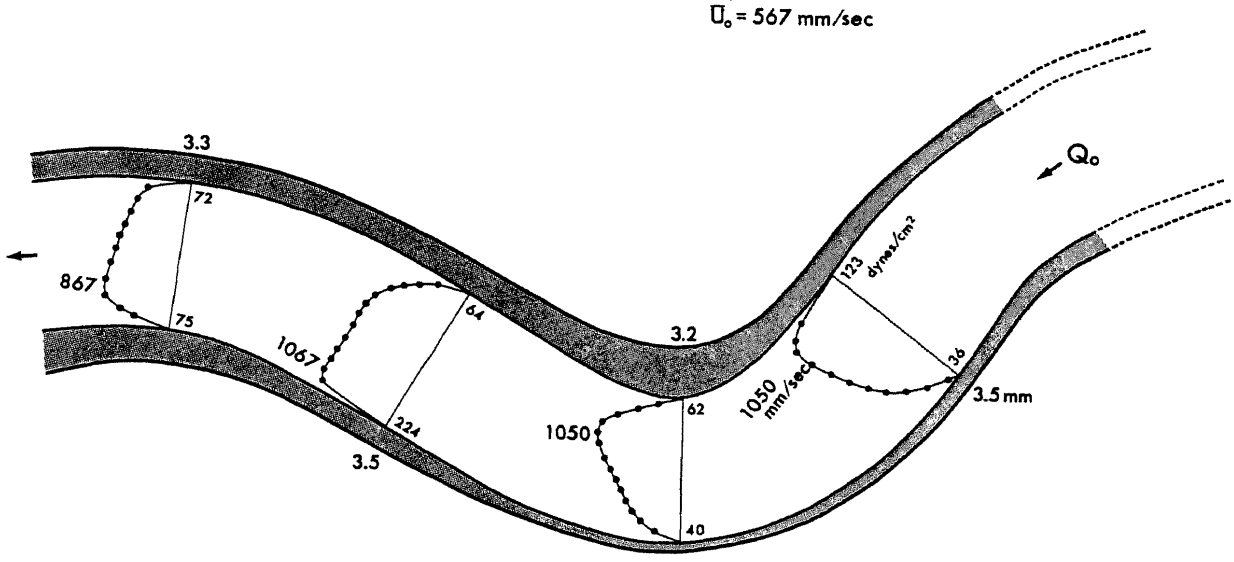

RCA

regions of high and low wall shear stress, attempts were made to obtain the distributions of fluid axial velocity (axial component of the fluid linear velocity) across the lumen of the arterial segment. The results are shown in Figure 13B. Due to the difficulty in focusing the zoom system, attached to a cine camera, on the median plane of the multiple bends which were not located on one common plane, as well as the complexity of the flow which did not allow tracer particles to stay in good focus because of the continuous change of distance from the median plane (focal plane), it was not possible to make accurate measurements from cine films. Thus, the results shown here are only a rough estimation of fluid velocity and wall shear stress in this arterial segments. Nevertheless, the results showed some interesting characteristics of the flow in arteries with multiple bends. As is evident from the figure, velocity distribution drastically changed within a few diameter distance between the locations proximal and distal to the apex of each bend. In the proximal portion of a bend, velocity distributions were skewed towards the inner wall, thus facilitating flow separation and formation of a recirculation zone along the inner wall distal to the apex of the bend. Just distal to the apex of the first bend, the peak in velocity distribution gradually shifted towards the outer wall of the first bend, hence towards the inner wall of the second bend, again favoring flow separation at the inner wall of the second bend. Atherosclerotic wall thickenings were localized in an alternating manner at the inner wall of each bend with a maximum thickenings occurring in regions of recirculation flows where

fluid velocity and wall shear stress were low.

(c) The Major Branching Sites of the RCA

At the major bifurcations and T-junctions of the RCA, atherosclerotic plaques and wall thickenings were found almost exclusively on the outer wall (hip) of one or both daughter vessels. In no case were flow dividers affected by atherosclerotic lesion.

Flow studies were carried out on four transparent coronary arterial trees. Figure 14A gives an example of flow patterns at the branching site of the conus (CB) and S-A node (SN) branches observed in a coronary arterial tree prepared from an 18-year old male subject. In this particular case, the diameter of the conus branch was unusually large, thus forming a major bifurcation similar to that at the branching site of the left anterior descending and the left circumflex branches in the left coronary artery. As shown in the figure, flow separation occurred at the hips of the bifurcation. In the conus branch, the region of separated flow was filled with the peripheral secondary flow which was formed as a result of the deflection of the mainflow at the flow divider. A slightly noticeable wall thickening was formed along the outer wall of the bifurcation just distal to the point of flow separation. In the RCA, a thin-layered spiral secondary flow was formed at the branching site of the S-A node branch adjacent to the upper (pericardial side) wall of the RCA. A part of it entered the S-A node branch at the proximal portion of the bend opposite to the flow divider, filling up the region

FIGURE 14. Detailed flow patterns (A) and distributions of fluid axial velocity (B) as in Figures 11 and 12 observed in steady flow at the branching site of the conus and S-A node branches at the proximal portion of the RCA prepared from an 18-year old male subject (shown in Figure 4C).

A

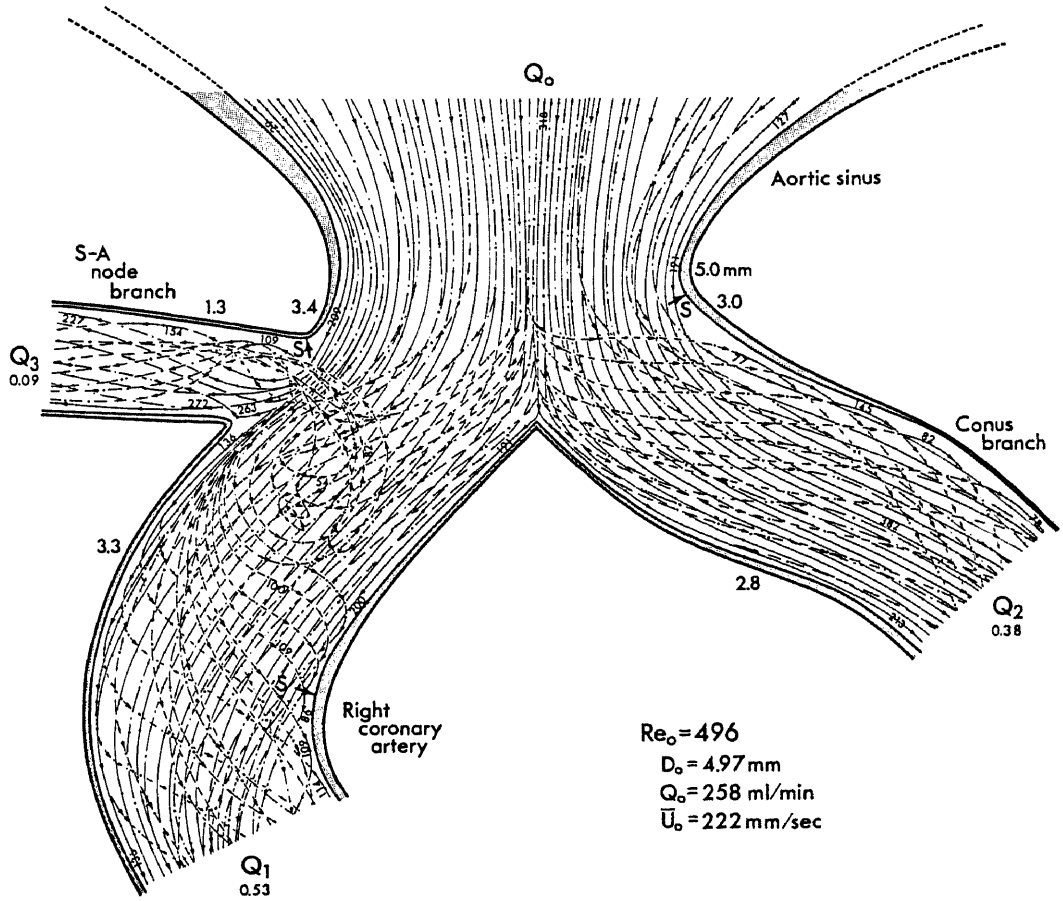
Q_o
Aortic sinus
S-A node branch
1.3
3.4
5.0 mm
3.0
S
St
Q_3 0.09
Conus branch
3.3
2.8
Q_2 0.38
Right coronary artery
$Re_o = 496$
$D_o = 4.97$ mm
$Q_o = 258$ ml/min
$\bar{U}_o = 222$ mm/sec
Q_1 0.53

B

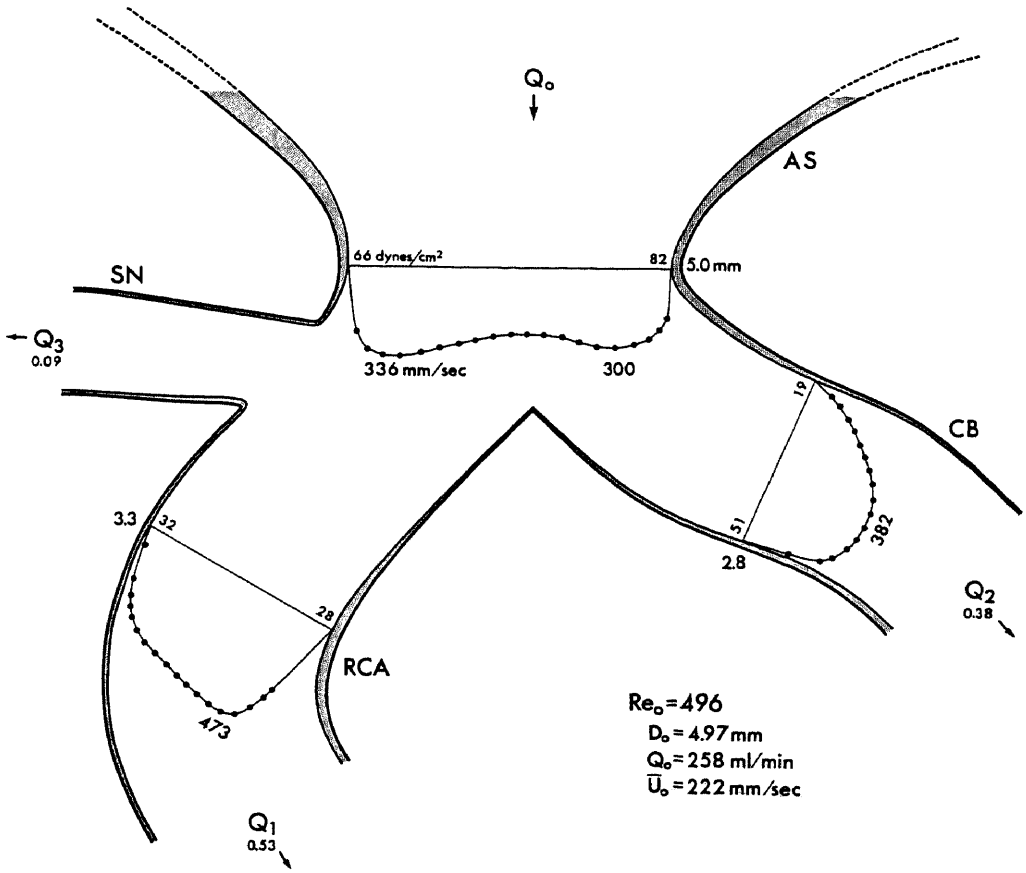
Q_o
AS
SN
66 dynes/cm²
82
5.0 mm
Q_3 0.09
336 mm/sec
300
CB
3.3
32
28
RCA
473
51
382
2.8
Q_2 0.38
$Re_o = 496$
$D_o = 4.97$ mm
$Q_o = 258$ ml/min
$\bar{U}_o = 222$ mm/sec
Q_1 0.53

of separated flow. The rest of the spiral secondary flow was entrained by the strong peripheral secondary flow which was formed to fill the region of separated flow located at inner wall of the sharp bend of the RCA where an initial wall thickening was found.

The velocity distributions in the diametrical planes parallel to the pericardium were obtained from the velocity of tracer particles. The results are shown in Figure 14B. As is evident from the figure, the velocity distribution at the throat of the bifurcation of the RCA and the conus branch was bipolar with two peaks slightly skewing toward the outer walls of the bifurcation. Due to this, the wall shear stresses calculated from the velocity distributions were much higher than anticipated. In the RCA and the conus branch about 1.5 diameters downstream of the flow divider, the velocity distributions was skewed toward the inner walls of the bifurcation, facilitating the onset of flow separation at the inner wall of the sharp bend of the RCA. The wall shear stress assessed at these locations ranged from about 20 to 50 dynes/cm^2.

Two other examples of flow patterns at the major branching sites of the right coronary artery are given in Figure 15. Figure 15A shows the detailed flow patterns observed in steady flow at the branching site of the S-A node branch in the arterial tree prepared from a 56-year old male subject when a viewing axis was aligned normal to the pericardium. In this particular case, the S-A node branch was located at the upper half of the RCA with slight bending toward the upper (pericardial side) wall. Due to

FIGURE 15. Detailed flow patterns as in Figure 12 observed in steady flow at the major branching sites of the RCA, showing A: the strong upward deflection of the mainflow around the flow divider of the S-A node branch which resulted in the formation of a rapid counterclockwise helical flow adjacent to the upper wall in a coronary arterial tree prepared from a 56-year old male subject, and B: the formation of secondary flows and a recirculation zone at the branching site of the posterior descending branch in a coronary arterial tree prepared from a 61-year old male subject. Observations were made along the axis normal to the pericardium.

A

$Re_o = 499$

$D_o = 3.80$ mm

$Q_o = 199$ ml/min

$\bar{U}_o = 291$ mm/sec

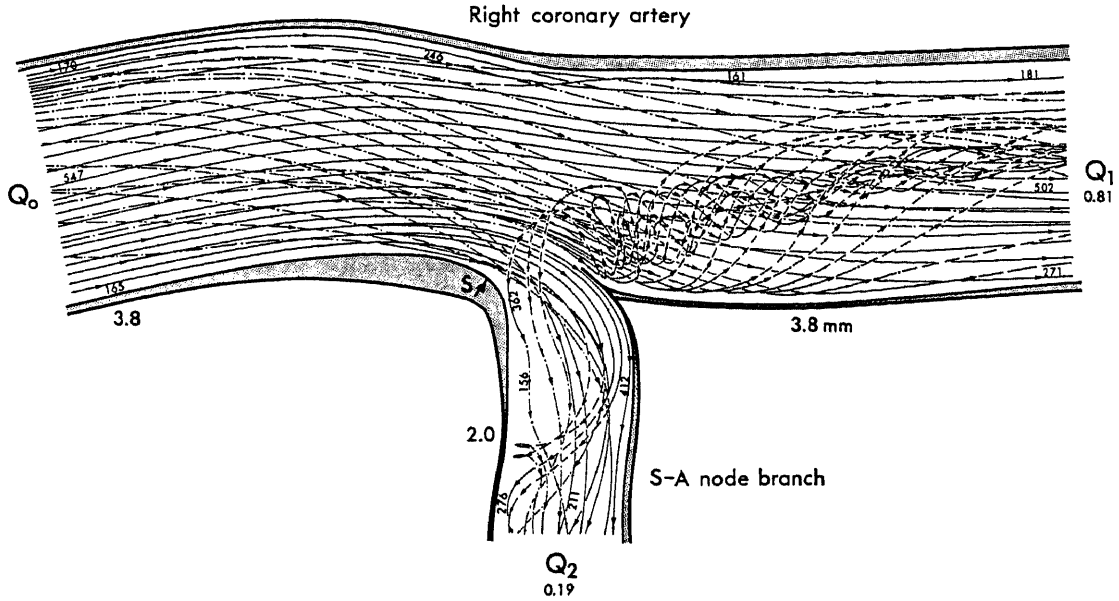

B

$Re_o = 797$

$D_o = 3.93$ mm

$Q_o = 328$ ml/min

$\bar{U}_o = 451$ mm/sec

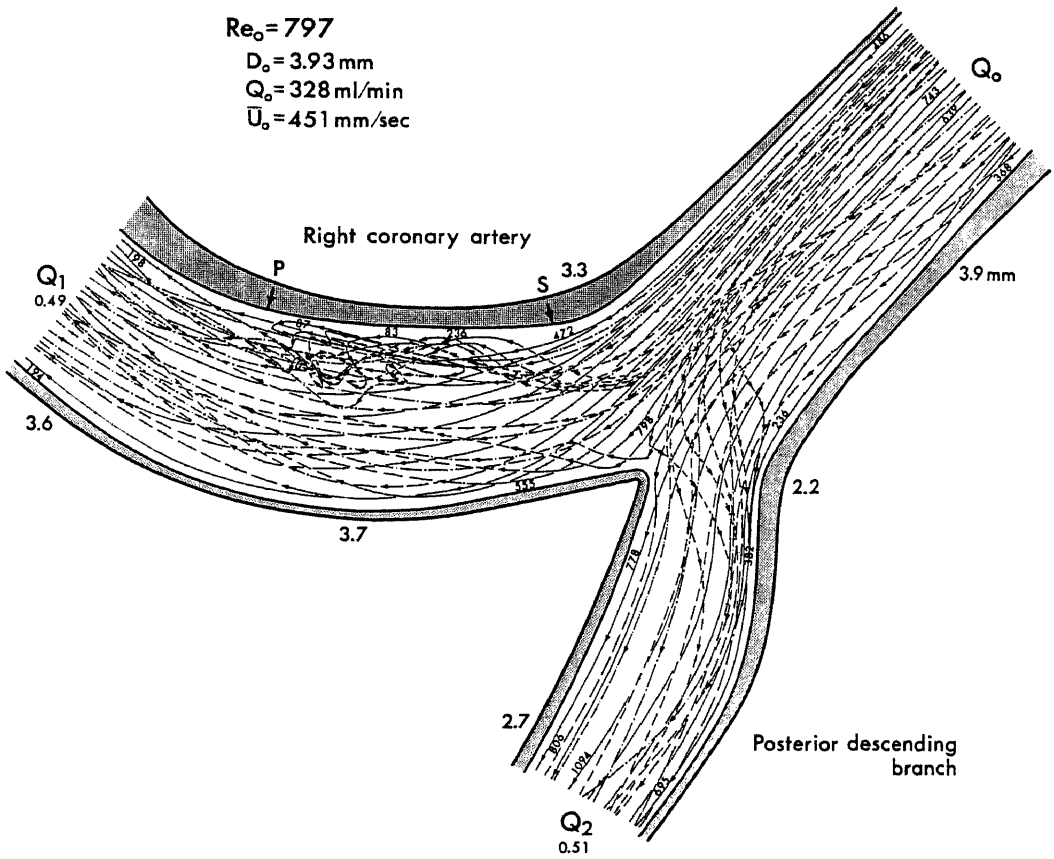

this, the flow patterns at this T-junction were highly asymmetric. As shown in the figure, the major part of the flow into the S-A node branch originated from the streamlines located near the right lateral and lower walls of the RCA. Flow separation occurred at the proximal leading edge of the sharp bend opposite to the flow divider, creating a region of separated flow distal to it. The strong upward deflection of the mainstream around the flow divider resulted in the formation of a rapid counterclockwise helicoidal flow (vortex cylinder) with a gradually decreasing diameter in the RCA adjacent to the upper (pericardial side) wall. This was accompanied by the formation of an induced counterclockwise swirling flow in the entire periphery of the RCA from the lower (myocardial side) to the right lateral and upper walls. In the region of separated flow in the S-A node branch, no recirculation flow was observed with tracer particles. Instead, the region was filled by the peripheral flow from the lower wall and part of the stray flows from the rapid helicoidal flow formed at the flow divider adjacent to the upper wall of the RCA. Atherosclerotic wall thickenings were found at the leading edge of the S-A node branch and the left lateral wall of the RCA just opposite to the flow divider.

Figure 15B shows the detailed flow patterns at the bifurcation of the posterior descending branch (PD) and the RCA observed in an arterial tree prepared from a 61-year old male subject (shown in Figure 4A). The bifurcation was located just distal to a bend, thus the RCA forming a S-shaped double bend. Due to this, the flow in the parent vessel was already disturbed

as evident from the figure by the formation of a clockwise peripheral secondary flow adjacent to the left lateral and upper (pericardial side) walls. Furthermore, the velocity distribution in the parent vessel, not shown in the figure, was skewed toward the right lateral wall which became a part of the inner wall of the distal bend of the RCA. Flow separation occurred in the RCA at the hip of the bifurcation. The region of separated flow was filled with slow peripheral flow from the lower (myocardial side) wall of the RCA. Particles which entered this region exhibited irregular movements, some of them moving backward, then suddenly changed direction and rejoined the rapidly passing mainstream. Thus, a thin layered recirculation zone was formed adjacent to the lower wall of the RCA just downstream of the separation point, though the exact size of the recirculation zone was not measurable. In the posterior descending branch, neither flow separation nor the formation of a recirculation zone occurred. However, there was a thin layered slow peripheral secondary flow from the lower wall of the RCA toward the hip and the outer wall of the bifurcation. Atherosclerotic wall thickenings were found at the hips of the bifurcation and along the inner wall of the distal bend of the RCA where both the fluid velocity and wall shear stress are expected to be low.

(d) Flow Patterns Observed in Pulsatile Flow

Flow studies were carried out also in pulsatile flow by superimposing a sinusoidal oscillatory flow with a frequency of 2 Hz and displacement volumes of 0.5 and 1.5 ml on steady flow.

Observations were focused on three locations along the right coronary artery: the double bend of the proximal and middle portions of the RCA in the vessel shown in Figure 4B and 12A, the multiple bends of the middle to distal portions of the RCA in the vessel shown in Figure 13, and the branching site of the posterior descending branch from the RCA in the vessel shown in Figure 15B. It was found that, in all vessels studied, the observed phenomena were qualitatively the same as those in steady flow described earlier. At a small displacement volume of 0.5 ml, the secondary and recirculation flows formed in steady flow were observed to persist throughout the entire cycle of pulsation. However, at a higher displacement volume of 1.5 ml, which created a condition nearing a temporal arrest of the mainflow at the end of the receding period of pulsation (corresponding to the peak point of the systolic period in the cardiac cycle), it was found that both the secondary and recirculation flows vanished when the mainflow velocity attained a minimum during the cycle of pulsation. The formation of disturbed flows was most evident just after the mainflow velocity reached a maximum in each cycle of pulsation.

Chapter IV

DISCUSSION

We have described the results on the spatial distribution of atherosclerotic lesions on the vessel wall and the detailed flow patterns and other characteristics of the flow existing at such sites in the human left and right coronary arteries in relation to the localization of atherosclerotic lesions in the human arterial tree.

The studies were carried out using isolated, pressure-fixed, transparent coronary arterial trees prepared from humans post-mortem. The transparent natural vessels are especially well suited to this kind of anatomical and fluid mechanical investigation of the cardiovascular system since they allow one to simultaneously study the exact anatomical structure of the vessels, the locations and sizes of diseased areas on the vessel wall, and the detailed flow patterns existing at such sites.

Unfortunately, it was not possible to render blood vessels transparent while maintaining the elasticity of normal living blood vessels. Thus, one may dispute the applicability of the results obtained in such rigid-walled vessels to the real situation where it is known that vessel walls are elastic and undergo a considerable degree of geometrical deformation during each cardiac cycle due to the contraction and relaxation of cardiac muscle. However, due to the following reasons, we have assumed

that the flow patterns in coronary arteries are not affected significantly by the elastic nature of the vessel wall. First of all, in coronary arteries, most blood flow occurs during the diastolic period of the cardiac cycle where the arteries are fairly well inflated and stretched close to their full lengths. Therefore, under such conditions, the changes in vessel diameter and length during the diastolic period alone will not be so large as to change the flow patterns. Secondly, the changes in the diameter of the coronary arteries are quite small even over the entire cardiac cycle. The results from in vivo measurements[142] show that, in humans, the changes in the cross-sectional area of arteries during a cardiac cycle are $\pm$ 6% in the largest diameter ascending aorta, and $\pm$ 1% in much smaller diameter vessels such as the common carotid and femoral arteries whose diameters range from 6 to 9 mm. In the latter cases, the changes in longitudinal length of the vessels were also found to be about $\pm$ 1%. For human coronary arteries, we were unable to find corresponding data. However, the results from some angiographic assessments [143,144] indicate that the changes in proximal coronary artery diameter are either undetectably small or within the range of measurement errors. Lastly, in most of the aged subjects, the walls of the coronary arteries were thickened and hardened to some extent through the development of atherosclerotic lesions. Thus, in such vessels, the elasticity of the vessel wall would be much reduced.

The results from the present investigation revealed several interesting and unique features of flow in the human coronary

arterial tree and the intimate relationship between the regions of disturbed flow and the preferred sites for atherogenesis on the vessel wall. It was demonstrated convincingly that complex secondary flows and standing recirculation zones form in many regions of human coronary arteries. In both steady and pulsatile flow, the general flow patterns observed at each branching site and bend of human coronary arteries were similar to those found in various glass models and plastic casts of arteries.[131-133,135] However, due to the asymmetric and complex structure of the bifurcations, T-junctions and bends in natural blood vessels, the exact flow patterns in these vessels were highly asymmetric and far more complex than those observed in model vessels. Furthermore, the flow patterns at each location of the arterial tree were dependent not only on the local anatomical structure of the vessel wall but also on the nature of the entering flow, i.e., whether the flow entering the region was laminar or already disturbed, and the velocity distribution was axisymmetric or skewed toward a particular side of the vessel wall due to the presence of side branches and bends immediately upstream of the region of interest. Thus, the observed flow patterns were highly specific to the particular anatomical structure of each coronary artery studied in the present investigation.

Due to the large variations in the anatomical structure of human coronary arteries, it is difficult to generalize our findings to all the cases encountered in the human coronary arterial tree and describe the detailed characteristics of the flow at each location of the arterial tree. However, if we focus our

attention only on the regions of disturbed flow in any arterial tree, we can find certain common characteristics of the flow at such sites. It was shown that disturbed flows were formed in many regions of the coronary arterial tree by at least one or a combination of the following three mechanisms: (i) through a flow separation caused by the irregularity of the vessel wall, (ii) through the development of strong secondary flows (as a result of flow deflection) caused by sudden changes in the direction of flow, and (iii) through mismatching of the flow rate entering each daughter vessel at the branching sites which forces the backflow of excess fluid entering a particular branch due to the inertia of the fluid. Thus, at bifurcations and T-junctions, complex spiral secondary flows and recirculation zones were formed in the junction region by a combination of the above three mechanisms. Formation of such disturbed flow was largely affected by the inflow Reynolds number (flow rate), the flow ratios in the daughter vessels, the curvature of the walls at the flow divider and the bend opposite to it, and the branching angle. Except for the branching vessels with very asymmetric structure relative to the common median plane of the main and side daughter vessels, disturbed flows were always formed in a paired structure, symmetrically about the common median plane. In sharp bends, strong secondary flows and a recirculation zone were formed along the vessel wall, in paired structures symmetrically about the median plane of the bend (respectively from the outer to the inner walls of the curved segment and just distal to the point of flow separation at the apex of the curva-

ture of the inner wall) by a combination of the first two mechanisms. However, in neither case was the recirculation zone in the form of a closed vortex. Thus, even in regions of recirculation flow, there was continuous inflow of fluid and particles from the mainstream, thereby assuring the exchange of material between the region of recirculation flow and the mainstream as it has been demonstrated previously in various models of arterial bifurcations[140,145] and T-junctions.[119,120]

It was also found that all the fluid mechanical phenomena, such as flow separation, flow deflection and formation of secondary and recirculation flows, observed in steady flow occurred in pulsatile flow during each cycle of pulsation. However, in pulsatile flow in a given vessel, the instantaneous Reynolds numbers at the maximum and minimum velocity points during a cycle of pulsation are respectively much higher and lower than the time-averaged Reynolds number which is equal to the Reynolds number in steady flow. Due to this fact, the sizes and intensity of the secondary and recirculation flows observed in pulsatile flow were much larger and stronger at the maximum velocity point (actually, it occurred slightly after the maximum point) and much smaller and weaker at the minimum velocity point than those observed in steady flow. In fact, when experiments were carried out with an oscillatory displacement volume of 1.5 ml, the instantaneous fluid velocity at the minimum velocity point was nearly zero and the instantaneous Reynolds number was probably well below the critical Reynolds number for the formation of recirculation flows. Thus, it was found that both the secondary and

recirculation flows vanished for a brief period between the end of the receding period and the beginning of the advancing period of the pulsatile flow. These findings are in good agreement with those obtained from various models studies.[107,132,133]

The significance of the present finding lies in the fact that there was a certain positive correlation between the sites of abnormal or disturbed flow and the preferred sites for atherogenesis in human coronary arteries. As it has already been shown by several investigators in human coronary arteries[5,106,108] and carotid artery bifurcations[107] using conventional pathological techniques, it was also shown convincingly in the present investigation that, in both left and right coronary arteries, atherosclerotic plaques and wall thickenings were formed almost exclusively on the outer wall (hip) of one or both daughter vessels at major bifurcations and T-junctions and along the inner wall of curved segments of the arteries. Furthermore, when the flow patterns were studied in detail in these vessels, it was found that these regions were the very places where flow was either slow (low shear region) or disturbed with formation of slow secondary and recirculation flows. In no instance were atherosclerotic lesions found at and around the flow divider of branching vessels where flow was fast and wall shear stress was high. These findings are quite different from those by Flaherty et al.[10], Roach et al.[103,146] and Cornhill et al.[147] who reported that in cholesterol-fed rabbits and swine, atherosclerotic (sudanophilic) lesions tend to develop along the distal leading edge (flow divider) of the branching site of intercostal arteries

and other major arteries of the descending aorta where wall shear stress is elevated. This suggests that initiating mechanisms for atherosclerosis differs between humans in which lesions were formed slowly and spontaneously over many years and experimental animals in which lesions were induced artificially and acutely by diets containing unusually high levels of cholesterol.

To pursue this apparent paradox, we try to speculate the responses of the artery wall to a number of physical factors. Our views are essentially that certain structural and functional changes in the arterial intima occur as a result of the mechanical stress exerted on the vessel lining by the adjacent blood flow. These responses are modulated by the magnitude and, no less important, the stability of the stress pattern as well as the duration of exposure to the stress.

In humans, intimal regions exposed to moderately elevated values of steady unidirectional stress over many years develop intimal fibrosis characterized by a dense, highly oriented, subendothelial collagenous sheet that is sparsely populated with smooth-muscle and other connective tissue cells. Such regions show decreased permeability to proteins and almost never contain stainable lipid. The flow divider of a branch point can be regarded as the paradigm of a region so exposed and the apparent paradox of a high shearing stress region being protected against atherogenesis can thus be explained. In contrast to this, intimal regions that appear to be exposed to an unstable stress pattern or one that varies throughout the day tend to show a greater degree of intimal thickening characterized by poorly

oriented collagen fibres and an increased population of smooth-muscle and other connective tissue cells. These areas show evidence of increased permeability and deposition of stainable lipid.

But at and around the flow divider in experimental animals fed high-cholesterol diets, acute exposure of the endothelial surface to mechanical stress (stretch rather than pressure) with the high concentration of cholesterol is associated with an increased transendothelial flux of protein by functional changes of endothelial cells.

The speculation has been advanced that these changes may play a role in local restructuring of the arterial conduit both to maintain stable flow configurations on the one hand and to correct unstable flow configurations on the other. The appearance of atherosclerosis would be viewed as a design error in this system of processes, perhaps as a result of too great an influx of lipoprotein in the proliferative or preproliferative phase.

It is clear at this point that hemodynamic factors are certainly involved in the pathogenesis, progression or prevention of atherosclerosis in the human arterial tree. What is not clear at present is what factor or factors are exercising control on this phenomenon.

As it has been described repeatedly, atherosclerotic plaques and wall thickenings were localized in most cases in regions of disturbed flow which contained both the points of flow separation and reattachment (stagnation). Thus, one may hypothesize that separation and reattachment points play a specific role in

atherogenesis as previously proposed by some investigators.[148-150] However, it is not likely that the presence of these two points is an absolute requirement for this phenomenon since atherosclerotic lesions were formed even in very gently curved branching arteries and arterial bends, as in the case of the LAD in the left coronary artery, where neither flow separation nor the formation of secondary and recirculation flows was observed under various flow conditions. In such regions, the only noticeable anomaly in hemodynamic factors was the skewing of the velocity distribution away from the vessel wall where atherosclerotic changes occurred. In other words, the only hemodynamic factor associated with this intimal thickening was the low fluid velocity in the vicinity of the suffering vessel wall and the resultant low shear stress on the vessel wall. This implies that in the arterial system, low fluid velocity (hence low wall shear stress) and high fluid velocity (hence high wall shear stress) respectively play pathogenic and preventive roles in atherosclerosis. This may explain the gradual decrease in frequency and degree of severity of atherosclerotic lesions with increasing distance from the origin of coronary arteries observed in the present investigation and also reported previously by several investigators.[57,59,106,151,152] Simple calculations carried out by applying the Poiseuille's law to the flow in transparent human coronary arterial trees show that both the fluid mean velocity and wall shear stress increase gradually up to about 1.5 fold in going from the proximal to the distal portions of the left and right coronary arteries as it has also been shown by Nerem and

Seed.[153]

It is also noteworthy that, as it has been shown by other investigators as well,[107,108,154-157] the intimal thickening at the hip of bifurcations and the inner wall of curved segments occurred not suddenly and irregularly, but very gradually and very smoothly in both longitudinal and circumferential directions, with the maximum thickening appearing around the point of flow separation if any existed. The cross-sections of the atherosclerotic wall thickenings appeared as eclipsed lunar shapes with their points of maximum thickness locating close to the bisector plane of the wall thickening which contained the points of flow separation and reattachment (stagnation) if there were any. Thus, the stereoscopic structure of the intimal thickening appeared as if it reflected the spatial distribution of some hemodynamic factors such as wall pressure, fluid velocity or wall shear stress. This suggests the possibility that redistribution of accumulated atherosclerotic materials takes place within the vessel wall and it is controlled by a hemodynamic factor which is characterized by a gradually and continuously varying nature such as wall pressure.

If we assume that local fluid velocity and high blood pressure prevailing in the arterial system play a key role in atherogenesis, the phenomena at the blood-endothelium boundary would be envisaged as follows. Due to the fact that every atherogenic lipoprotein particle (will be referred to as particles hereafter) have a certain finite size, their translational velocity will not be zero even when they are in contact with the endothelium.

Thus, their movements over the endothelium will be largely affected by the fluid velocity in the immediate vicinity of the endothelium. In regions of slow flow, since the vessel wall (hence the endothelium itself) is permeable to water, solute and macromolecules, the radial component of the fluid velocity in fluid layers adjacent to the endothelium may become about the same order or even greater than the longitudinal component, resulting in the arrest or permanent adhesion of the particles on the endothelium, even though both the particles and endothelium are charged negatively and their interaction is hampered by an electrostatic repulsive force. This may in turn result in the enhanced infiltration and uptake of the particles by endothelial cells. In this way, the accumulation of particles within the intima will continue. However, since their further penetration into the adventitia of the vessel wall is obstructed to some extent by the fine structure of the underlying media, especially the elastin layers, it is necessary for the particles to diffuse or migrate laterally within the intima. If there is any regional difference in pressure on the endothelium and within the intima, they will migrate toward the lower pressure region (which usually occurs at the point of flow separation), resulting in the highest accumulation, thus thickening, of the particles at such sites. In this way, the lumen becomes narrower and narrower at the point of minimum pressure on the endothelium, thereby further promoting flow separation and formation of recirculation flows. The slower the velocity, and the higher the blood pressure, the higher and faster the accumulation of the particles in the vessel wall.

This may explain our observation that the severest lesions were located in regions of separated flow where the particle velocity was the lowest. In such regions, it has been shown previously by Karino and Goldsmith[118,158] that the transport of cells and macromolecules to the vessel wall is enhanced by the radially directed flow along the curved streamlines existing in the vicinity of the reattachment (stagnation) point. It is possible that, in such regions, since the fluid velocity and wall shear stress are very low, and the endothelium is leaky as evidenced by the enhanced uptake of Evans blue dye by the endothelium in regions of atherosclerosis, platelets, monocytes and atherogenic lipoproteins may have a greater opportunity to interact for longer periods with the endothelial cells than elsewhere. This, in turn, may lead to and enhance the deposition of platelets and monocytes on the endothelium, the release of certain chemical agents such as the platelet-derived growth factor for smooth muscle cells, and the uptake and infiltration of atherogenic lipoproteins by the endothelial cells located in such regions, further worsening the disease. What is not clear at present is how much the infiltration and uptake of the atherogenic lipoproteins by endothelial cells are affected by the nature of the individual cells located in different regions of the vessel wall (shown in Figure 16).

It has been shown that vascular endothelial cells are susceptible to flow, and exhibit certain morphological changes corresponding to the direction and magnitude of the shear stress.[159-168] Thus, in arterial bifurcations, the endothelial

FIGURE 16. Schematic diagram of the involvement of fluid dynamics in the atherosclerotic process. It is possible that in regions of disturbed flow where the translational velocity and wall shear stress are very low, platelets and lipids may have a greater opportunity to interact for longer periods with the vessel wall than elsewhere. This, in turn, may lead to and enhance the deposition of platelets, release of certain chemical agents such as the platelet-derived growth factor for smooth muscle cells, and the uptake of atherogenic lipoproteins by the endothelial cells located in such regions. It is also positive that since vascular endothelial cells are sensitive to flow and exhibit certain morphological changes corresponding to the direction and magnitude of the local shear stress, being round shaped in regions of low shear and elongated in regions of high shear, endothelial cells in different regions may have different metabolic functions. It is speculated that localization of atherosclerosis may have its origin in either or both of the above two mechanisms.

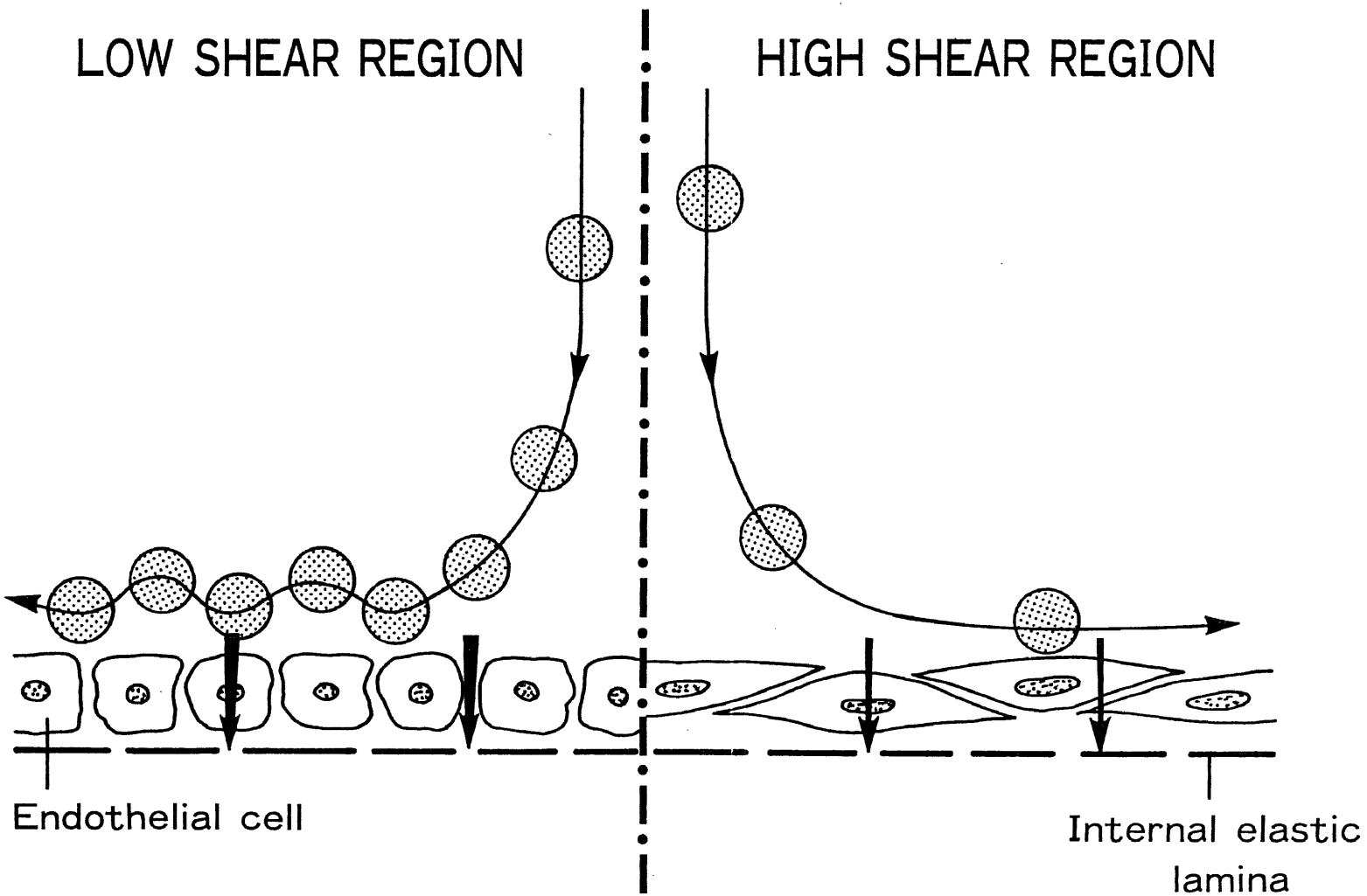
LOW SHEAR REGION
HIGH SHEAR REGION
Endothelial cell
Internal elastic lamina

cells located on the inner wall distal to the flow divider (where the shear stress is high) were found to be elongated in the direction of flow, while those cells located on the outer walls opposite to the flow divider (where secondary and recirculation flows may form and the shear stress is much lower) were not elongated but oriented in a random fashion.[169,170] It is possible that endothelial cells located in different regions and subjected to different levels of shear stress may have different biological and biochemical functions (shown in Figure 16).[171-177] It is necessary to further investigate the effects of shear stress on the morphology and metabolic function of endothelial cells, and on the permeability of the endothelium to atherogenic lipoproteins. Only after that, one may find a full explanation for the localization of atherosclerotic lesions in the human arterial tree.

Chapter V

CONCLUSIONS

We have described our latest findings on the exact sites of atherosclerosis and detailed flow patterns existing in such regions in human coronary arteries in relation to the localization of atherosclerosis in the human circulation. The results demonstrated convincingly that the flow separation and formation of secondary flows and standing recirculation zones, previously observed in various models of branching vessels, do occur also in natural blood vessels in both steady and pulsatile flow. Furthermore, it was confirmed repeatedly that preferred sites for the formation of atherosclerotic plaques and wall thickenings were localized not at flow dividers (high shear region) as observed previously by several investigators in experimental animals by feeding them diets containing high levels of cholesterol, but almost exclusively on the outer wall (hip) of one or both daughter vessels at major bifurcation and T-junctions and along the inner wall of curved segments where flow was either slow (low shear region) or disturbed with formation of secondary and recirculation flows. These results indicate that there is a strong correlation between the sites of flow disturbance and the preferred sites for the genesis and development of atherosclerosis in man.

ACKNOWLEDGMENTS

The author wishes to express his deepest appreciation to Dr. Takeshi Karino, Associate Professor of Medicine at McGill University for making this study possible in his laboratory at the Montreal General Hospital and for his supervision, help and encouragement throughout the entire course of this work.

The author is grateful to the National Heart, Lung and Blood Institute, N.I.H., U.S.A. for financial support in the form of an Operating Grant to Dr. T. Karino.

Thanks are also due to E. de Heuvel and M. Sgro for their technical assistance, Dr. W.P. Duguid and the staff of the Department of Pathology for their help in obtaining the human hearts at autopsy, and Dr. H.L. Goldsmith and Dr. C.A. Goresky, both Professors of the Department of Medicine at the Montreal General Hospital for their continuing interest and encouragement in this work.

Finally, the author takes special pleasure in thanking Dr. Motokazu Hori, Professor of Surgery and Dean of the School of Medicine, and Dr. Toshio Mitsui, Associate Professor of Surgery at University of Tsukuba for their excellent guidance, invaluable advice and encouragement throughout the entire course of my graduate studies leading to the submission of my Ph.D. thesis.

REFERENCES

1. Keys A, Kimura N, Kusukawa A, Bronte-Stewart B, Larsen N, Keys MH: Lessons from serum cholesterol studies in Japan, Hawaii and Los Angeles. Ann Intern Med 1958;48:83-94
2. Woolf N: Pathology of Atherosclerosis, London, Butterworths & Co Ltd, 1982
3. Geer JC, McGill HC Jr, Strong JP: The fine structure of human atherosclerotic lesions. Am J Pathol 1961;38:263-287
4. Haust MD: The morphogenesis and fate of potential and early atherosclerotic lesions in man. Hum Pathol 1971;2:1-29
5. Svindland A: The localization of sudanophilic and fibrous plaques in the main left coronary bifurcation. Atherosclerosis 1983;48:139-145
6. Schwartz CJ, Mitchell JRA: Observations on localization of arterial plaques. Circ Res 1962;11:63-73
7. Pearson TA, Solez K, Dillman JM, Heptinstall RH: Evidence for two populations of fatty streaks with different roles in the atherogenic process. Lancet 1980;II:496-498
8. Velican C, Velican D: The precursors of coronary atherosclerotic plaques in subjects up to 40 years old. Atherosclerosis 1980;37:33-46
9. Velican C: A dissecting view on the role of the fatty streak in the pathogenesis of human atherosclerosis: Culprit or bystander? Rev Roum Med Int 1981;19:321-337
10. Flaherty JT, Ferrans VJ, Pierce JE, Carew TE, Fry DL: Localizing factors in experimental atherosclerosis, in

Likoff W, Segal BL, Insull W Jr (eds): Atherosclerosis and Coronary Heart Disease, New York, Grune & Stratton, 1972, pp 40-84

11. Roach MR: The effects of bifurcations and stenoses on arterial disease, in Hwang NHC, Normann NA (eds): Cardiovascular Flow Dynamics and Measurements, Baltimore, University Park Press, 1977, pp 489-539
12. Aschoff L: Lectures in pathology, New York, Hoeber, 1924, pp 131-135
13. Anitschkow N: Experimental atherosclerosis in animals, in Cowdry EV (ed): Arteriosclerosis, New York, The Macmillan Company, 1933, pp 271-322
14. Caro CG, Fitz-Gerald JM, Schroter RC: Atheroma and arterial wall shear. Observation, correlation and proposal of a shear dependent mass transfer mechanism for atherogenesis. Proc Roy Soc Lond 1971;B177:109-159
15. Goldstein JL, Brown MS: Binding and degradation of low density lipoproteins by cultured human fibroblasts: Comparison of cells from a normal subject and from a patient with homozygous familial hypercholesterolemia. J Biol Chem 1974; 249:5153-5162
16. Brown MS, Faust JR, Goldstein JL: Role of the low density lipoprotein receptor in regulating the content of free and esterified cholesterol in human fibroblasts. J Clin Invest 1975;55:783-793
17. Brown MS, Brannan PG, Bohmfalk HA, et al: Use of mutant fibroblasts in the analysis of the regulation of cholesterol

metabolism in human cells. J Cell Physiol 1975;85:425-436

18. Goldstein JL, Brown MS: Atherosclerosis: The low-density lipoprotein receptor hypothesis. Metabolism 1977;26:1257-1275

19. Brown MS, Goldstein JL: A receptor-mediated pathway for cholesterol homeostasis. Science 1986;232:34-47

20. Duguid JB: Thrombosis as a factor in the pathogenesis of coronary atherosclerosis. J Path Bact 1946;58:207-212

21. Duguid JB: Thrombosis as a factor in the pathogenesis of aortic atherosclerosis. J Path Bact 1948;60:57-61

22. Rokitansky C: A Manual of Pathological Anatomy (translated, Day GE, 1952), vol.4, London, Sydenham Society, 1844, pp 261-272

23. Jørgensen L, Rowsell HC, Hovig T, Mustard JF: Resolution and organization of platelet-rich mural thrombi in carotid arteries of swine. Amer J Path 1967;51:681-719

24. Heggtveit HA: Atheromatous transformation of intracardiac mural thrombi. Amer J Path 1968;52:70a

25. Packham MA, Evans G, Glynn MF, Mustard JF: Localized protein accumulation in the wall of the aorta. Exp Molec Path 1967;7:214-232

26. Walton KW: Pathogenetic mechanisms in atherosclerosis. Am J Cardiol 1975;35:542-558

27. Geissinger HD, Mustard JF, Rowsell HC: The occurrence of micro-thrombi on the aortic endothelium of swine. Can Med Assoc J 1962;87:405-408

28. Campbell RSF: Early atherosclerosis in the pig: a histologi-

cal and histochemical study. J Atheroscler Res 1965;5:483-496

29. Virchow R: Phlogose ung Thrombose im Gefassystem: Gesammelte Abhandlungen zur Wissenschaftlichen Medizin, Frankfurt-am-Main, Meidinger Sohn and Company , 1856, pp 458-463

30. French JE: Atherosclerosis in relation to the structure and function of the arterial intima, with special reference to the endothelium. Int Rev Exp Pathol 1966;5:253-353

31. Ross R, Glomset JA: Atherosclerosis and the arterial smooth muscle cell. Science 1973;180:1332-1339

32. Ross R, Glomset JA: The pathogenesis of atherosclerosis. N Engl J Med 1976;295:369-377,420-425

33. Ross R, Harker L: Hyperlipidemia and atherosclerosis. Chronic hyperlipidemia initiates and maintains lesions by endothelial cell desquamation and lipid accumulation. Science 1976;193:1094-1100

34. Ross R, Glomset J, Kariya B, Harker L: A platelet-dependent serum factor that stimulates the proliferation of arterial smooth muscle cells in vitro. Proc Nat Acad Sci USA 1974;71:1207-1210

35. Ross R, Vogel A: The platelet-derived growth factor. Cell 1978;14:203-210

36. Björkerud S, Bondjers G: Arterial repair and atherosclerosis after mechanical injury. I. Permeability and light microscopic characteristics of endothelium in non-atherosclerotic and atherosclerotic lesions. Atherosclerosis 1971;13:355-363

37. Helin P, Lorenzen I, Garbarsch C, Matthiessen ME: Arterio-

sclerosis in rabbit aorta induced by mechanical dilatation. Biochemical and morphological studies. Atherosclerosis 1971; 13:319-331

38. Stemerman MB, Ross R: Experimental arteriosclerosis. I. Fibrous plaque formation in primates, an electron microscope study. J Exp Med 1972;136:769-789

39. Fry DL: Responses of the arterial wall to certain physical factors, in Porter R, Knight J (eds): CIBA Foundation Symposium, No.12 Atherogenesis: Initiating Factors, 1973, pp 93-120

40. Moore S: Thromboatherosclerosis in normolipemic rabbits. A result of continued endothelial damage. Lab Invest 1973;29: 478-487

41. Fishman JA, Ryan GB, Karnovsky MJ: Endothelial regeneration in the rat carotid artery and the significance of endothelial denudation in the pathogenesis of myointimal thickening. Lab Invest 1975;32:339-351

42. Minick CR, Murphy GE, Campbell WG Jr: Experimental induction of athero-arteriosclerosis by the synergy of allergic injury to arteries and lipid-rich diet. I. Effect of repeated injections of horse serum in rabbits fed a dietary cholesterol supplement. J Exp Med 1966;124:635-652

43. Minick CR, Murphy GE: Experimental induction of atherosclerosis by the synergy of allergic injury to arteries and lipid-rich diet. II. Effect of repeatedly injected foreign protein in rabbits fed a lipid-rich, cholesterol-pool diet. Am J Pathol 1973;73:265-300

44. Hardin NJ, Minick CR, Murphy GE: Experimental induction of athero-arteriosclerosis by the synergy of allergic injury to arteries and lipid-rich diet. III. The role of earlier acquired fibromuscular intimal thickening in the pathogenesis of later developing atherosclerosis. Am J Pathol 1973;73:301-327

45. Alonso DR, Starek PK, Minick CR: Studies on the pathogenesis of athero-arteriosclerosis induced rabbit cardiac allografts by the synergy of graft rejection and hypercholesterolemia. Am J Pathol 1977;87:415-442

46. Minick CR, Alonso DR, Rankin L: Role of immunologic arterial injury in atherogenesis. Thrombos Haemostas (Stuttg) 1978; 39:304-311

47. Harker LA, Slichter SJ, Scott CR, Ross R: Homocystinemia. Vascular injury and arterial thrombosis. N Engl J Med 1974; 291:537-543

48. Harker LA, Ross R, Slichter SJ, Scott CR: Homocystine-induced arteriosclerosis. The role of endothelial cell injury and platelet response in its genesis. J Clin Invest 1976;58:731-741

49. Reidy MA, Bowyer DE: Distortion of endothelial repair. The effect of hypercholesterolaemia on regeneration of aortic endothelium following injury by endotoxin. A scanning electron microscope study. Atherosclerosis 1978;29:459-466

50. Fabricant CG, Fabricant J, Litrenta MM, Minick CR: Virus-induced atherosclerosis. J Exp Med 1978;148:335-340

51. De Bruijn WC, Van Mourik W, Bosveld IJ: Cell border

demarcation in the scanning electron microscope by silver stains. J Cell Sci 1974;16:221-239

52. Gimbrone MA Jr: Endothelial dysfunction and the pathogenesis of atherosclerosis, in Gotto AM, Smith LC, Allen B (eds): Atherosclerosis, New York, Springer-Verlag, 1974, pp 415-425

53. Weber G, Fabbrini P, Resi L: Scanning and transmission electron microscopy observations on the surface lining of aortic intimal plaques in rabbits on a hypercholesterolic diet. Virchows Arch A Path Anat and Histol 1974;364:325-331

54. Nelson E, Gertz SD, Forbes MS, et al.: Endothelial lesions in the aorta of egg yolk-fed miniature swine: A study by scanning and transmission electron microscopy. Exp Mol Pathol 1976;25:208-220

55. Mustard JF, Rowsell HC, Murphy EA, Downie HG: Intimal thrombosis in atherosclerosis, in Jones RJ (ed): Evolution of the Atherosclerotic Plaque, Chicago, The University of Chicago Press, 1963, pp 183-203

56. Texon M: The role of vascular dynamics in the development of atherosclerosis, in Sandler M, Bourne GH (eds): Atherosclerosis and Its Origin, New York, Academic Press, 1963, pp 167-195

57. Eggen DA, Strong JP, McGill HC Jr: Coronary calcification. Relationship to clinically significant coronary lesions and race, sex, and topographic distribution. Circulation 1965; 32:948-955

58. Dymecki J, Kozlowski P: On the correlation between the shape of the carotid siphon and the localization of atheromatous

plaques. Pol Med J 1968;7:238-243

59. Montenegro MR, Eggen DA, Topography of atherosclerosis in the coronary arteries. Lab Invest 1968;18:586-593

60. Caro CG, Fitz-Gerald JM, Schroter RC: Arterial wall shear and distribution of early atheroma in man. Nature 1969;223: 1159-1161

61. Lallemand RC, Brown KGE, Boulter PS: Vessel dimensions in premature atheromatous disease of aortic bifurcation. Br Med J 1972;2:255-257

62. Meyer WW, Noll M: Gross patterns of early lipid deposits in the carotid artery and their relation to the preformed arterial structures. Artery 1974;1:31-45

63. Nerem RM, Cornhill JF: The role of fluid mechanics in atherogenesis. ASME J Biomech Eng 1980;102:181-189

64. Schettler G, Nerem RM, Schmid-Schönbein H, Mörl H, Diehm C (eds): Fluid Dynamics as a Localizing Factor for Atherosclerosis, Heidelberg, Springer-Verlag, 1983

65. Strandness DE Jr, Didisheim P, Clowes AW, Watson JT (eds): Vascular Diseases. Current Research and Clinical Applications, Orlando, Grune & Stratton, 1987

66. Yoshida Y, Yamaguchi T, Caro CG, Glagov S, Nerem RM (eds): Role of Blood Flow in Atherogenesis, Tokyo, Springer-Verlag, 1988

67. Bergel DH, Schultz DL: Arterial elasticity and fluid dynamics, in Butler JAV, Noble D (eds): Progress in Biophysics and Molecular Biology, vol. 22, New York, Pergamon Press, 1971, pp 1-36

68. Lighthill MJ: Physiological fluid dynamics: A survey. J Fluid Mech 1972;52:475-497

69. Willis GC: Localizing factors in atherosclerosis. Canad Med Assoc J 1954;70:1-9

70. Oka S, Azuma T: Physical theory of tension in thick-walled blood vessels in equilibrium. Biorheology 1970;7:109-117

71. Texon M, Imparato AM, Load JW Jr: The hemodynamic concept of atherosclerosis. The experimental production of hemodynamic arterial disease. Arch Surg 1960;80:47-53

72. Lee JS, Fung YC: Flow in nonuniform small blood vessels. Microvasc Res 1971;3:272-287

73. Gessner FB: Hemodynamic theories of atherogenesis. Circ Res 1973;33:259-266

74. Wesolowski SA, Fries CC, Sabini AM, Sawyer PN: The significance of turbulence in hemic systems and in the distribution of the atherosclerotic lesion. Surgery 1965;57:155-162

75. Wesolowski SA, Fries CC, Sabini AM, Sawyer PN: Turbulence, intimal injury, and atherosclerosis, in Sawyer PN (ed): Biophysical Mechanisms in Vascular Homeostasis and Intravascular Thrombosis, New York, Meredith Publishing Company, 1965, pp 147-157

76. Fry DL: Acute vascular endothelial changes associated with increased blood velocity gradients. Circ Rec 1968;22:165-197

77. Fry DL: Certain histological and chemical responses of the vascular interface to acutely induced mechanical stress in the aorta of the dog. Circ Res 1969;24:93-108

78. Ling SC, Atabek HB, Fry DL, Patel DJ, Janicki JS: Appli-

cation of heated-film velocity and shear probes to hemodynamic studies. Circ Res 1968;23:789-801

79. Ling SC, Atabek HB, Carmody JJ: Pulsatile flow in arteries, in Hetenyi M, Vincenti WE (eds): Proc 12th Intern Congr Appl Mech, Berlin, Springer-Verlag, 1969, pp 227-291

80. Caro CG: Mechanical factors in atherogenesis, in Hwang NHC, Normann NA (eds): Cardiovascular Flow Dynamics and Measurements, Baltimore, University Park Press, 1977, pp 473-487

81. Hung TK, Naff SA: A mathematical model of systolic blood flow through a bifurcation. Proc 8th Intern Conf Med Biol Engng, 1969, Paper no. 20-II

82. Lynn NS, Fox VG, Ross LW: Computation of fluid-dynamical contributions to atherosclerosis at arterial bifurcations. Biorheology 1972;9:61-66

83. Zamir M, Roach MR: Blood flow downstream of a two-dimensional bifurcation. J Theor Biol 1973;42:33-48

84. Friedman MH, O'Brien V, Ehrlich LW: Calculations of pulsatile flow through a branch. Circ Res 1975;36:277-285

85. O'Brien V, Ehrlich LW, Friedman MH: Unsteady flow in a branch. J Fluid Mech 1976;75:315-336

86. Schultz DL, Tunstall-Pedoe DS, Lee G DeJ, Gunning AL, Bellhouse BJ: Velocity distribution and transition in the arterial system, in Wolstenholme GEW, Knight J (eds): Circulatory and Respiratory Mass Transport (CIBA), Boston, Little, Brown And Company, 1969, pp 172-202

87. Reuben SR, Swadling JP, Lee G de J: Velocity profiles in the main pulmonary artery of dogs and man, measured with a thin-

film resistance anemometer. Circ Res 1970;27:995-1001

88. Nerem RM, Seed WA: An in vivo study of aortic flow disturbances. Cardiovasc Res 1972;6:1-14

89. Nerem RM, Rumberger JA Jr, Gross DR, Hamlin RL, Geiger GL: Hot-film anemometer velocity measurement of arterial blood flow in horses. Circ Res 1974;34:193-203

90. Stein PD, Sabbah HN: Turbulent blood flow in the ascending aorta of humans with normal and diseased aortic valves. Circ Res 1976;39:58-65

91. Stein PD, Sabbah HN, Anbe DT, Walburn FJ: Blood velocity in the abdominal aorta and common iliac artery of man. Biorheology 1979;16:249-255

92. Friedman MH, Hutchins GM, Bargeron CB, Deters OJ, Mark FF: Correlation between intimal thickness and fluid shear in human arteries. Atherosclerosis 1981;39:425-436

93. Spence JD, Perkins DG, Kline RL, Adams MA, Haust MD: Hemodynamic modification of aortic atherosclerosis. Effects of propranolol vs hydralazine in hypertensive hyperlipidemic rabbits. Atherosclerosis 1984; 50:325-333

94. Caro CG, Parker KH, Fish PJ, Lever MJ: Blood flow near the arterial wall and arterial disease. Clin Hemorheology 1985; 5:849-871

95. Caro CG, Fish PJ, Gross DE, Halls J, Lever MJ, Parker KH, Stacey-Clear A: Effect of isosorbide dinitrate on arterial haemodynamics in man. J Physiol 1985;365:93P

96. Langille BL, Reidy MA, Kline RL: Injury and repair of endothelium at sites of flow disturbances near abdominal aortic

coarctations in rabbits. Arteriosclerosis 1986;6:146-154

97. Gutstein WH, Schneck DJ: In vitro boundary layer studies of blood flow in branched tubes. J Atheroscler Res 1967;7:295-299

98. El Masry OA, Feuerstein IA, Round GF: Experimental evaluation of streamline patterns and separated flows in a series of branching vessels with implications for atherosclerosis and thrombosis. Circ Res 1978;43:608-618

99. Friedman MH, Bargeron CB, Hutchins GM, Mark FF, Deters OJ: Hemodynamic measurements in human arterial casts, and their correlation with histology and luminal area. ASME J Biomech Eng 1980;102:247-251

100. LoGerfo FW, Nowak MD, Quist WC, Crawshaw HM, Bharadvaj BK: Flow studies in a model carotid bifurcation. Arteriosclerosis 1981;1:235-241

101. Walburn FJ, Sabbah HN, Stein PD: Flow visualization in a mold of an atherosclerotic human abdominal aorta. ASME J Biomech Eng 1981;103:168-170

102. Walburn FJ, Stein PD: Velocity profiles in symmetrically branched tubes simulating the aortic bifurcation. J Biomech 1981;14:601-611

103. Roach MR, Cornhill JF, Fletcher J: A quantitative study of the development of sudanophilic lesions in the aorta of rabbits fed a low-cholesterol diet for up to six months. Atherosclerosis 1978;29:259-264

104. Kratky RG, Roach MR: Scanning electron microscopy of early atherosclerosis in rabbits using aortic casts. Scanning

Microsc 1988;2:465-470

105. Kjaernes M, Svindland A, Walløe L, Wille SØ: Localization of early atherosclerotic lesions in an arterial bifurcation in humans. Acta Path Microbiol Scand Sect A 1981;89:35-40

106. Fox B, James K, Morgan B, Seed A: Distribution of fatty and fibrous plaques in young human coronary arteries. Atherosclerosis 1982;41:337-347

107. Zarins CK, Giddens DP, Bharadvaj BK, Sottiurai VS, Mabon RF, Glagov S: Carotid bifurcation atherosclerosis. Quantitative correlation of plaque localization with flow velocity profiles and wall shear stress. Circ Res 1983;53:502-514

108. Grøttum P, Svindland A, Walløe L: Localization of atherosclerotic lesions in the bifurcation of the main left coronary artery. Atherosclerosis 1983;47:55-62

109. Sabbah HN, Khaja F, Brymer JF, Hawkins ET, Stein PD: Blood velocity in the right coronary artery: Relation to the distribution of atherosclerotic lesions. Am J Cardiol 1984; 53:1008-1012

110. Svindland A, Walløe L: Distribution pattern of sudanophilic plaques in the descending thoracic and proximal abdominal human aorta. Atherosclerosis 1985;57:219-224

111. Sabbah HN, Khaja F, Hawkins ET, Brymer JF, McFarland TM, van der Bel-Kahn J, Doerger PT, Stein PD: Relation of atherosclerosis to arterial wall shear in the left anterior descending coronary artery of man. Am Heart J 1986;112:453-458

112. Sakata N, Takebayashi S: Localization of atherosclerotic

lesions in the curving sites of human internal carotid arteries. Biorheology 1988;25:567-578

113. Zarins CK, Bomberger RA, Glagov S: Local effects of stenoses: Increased flow velocity inhibits atherogenesis. Circulation 1981;64(Suppl II):221-227

114. Frangos JA, Eskin SG, McIntyre LV, Ives CL: Flow effects on prostacyclin production by cultured human endothelial cells. Science 1985;227:1477-1479

115. Skarlatos SI, Hollis TM: Cultured bovine aortic endothelial cells show increased histamine metabolism when exposed to oscillatory shear stress. Atherosclerosis 1987;64:55-61

116. Sprague EA, Steinbach BL, Nerem RM, Schwartz CJ: Influence of a laminar steady-state fluid-imposed wall shear stress on the binding, internalization, and degradation of low-density lipoproteins by cultured arterial endothelium. Circulation 1987;76:648-656

117. Karino T, Goldsmith HL: Flow behaviour of blood cells and rigid spheres in an annular vortex. Phil Trans Roy Soc Lond 1977;B279:413-445

118. Karino T, Goldsmith HL: Adhesion of human platelets to collagen on the walls distal to a tubular expansion. Microvasc Res 1979;17:238-262

119. Karino T, Kwong HHM, Goldsmith HL: Particle flow behaviour in models of branching vessels: I. Vortices in 90° T-junctions. Biorheology 1979;16:231-248

120. Karino T, Goldsmith HL: Particle flow behavior in models of branching vessels. II. Effects of branching angle and

diameter ratio on flow patterns. Biorheology 1985;22:87-104

121. Stehbens WE: Flow in glass models of arterial bifurcations and berry aneurysms at low reynolds numbers. Q J Exp Physiol 1975;60:181-192

122. Fukushima T, Azuma T: The horseshoe vortex: A secondary flow generated in arteries with stenosis, bifurcation, and branchings. Biorheology 1982;19:143-154

123. Kratzer MAA, Kinder J: Streamline pattern and velocity components of flow in a model of a branching coronary vessel - Possible functional implication for the development of localized platelet deposition in vitro. Microvasc Res 1986; 31:250-265

124. Wells MK, Winter DC, Nelson AW, McCarthy TC: Blood velocity patterns in coronary arteries. ASME J Biomech Eng 1977;99: 26-32

125. Bharadvaj BK, Mabon RF, Giddens DP: Steady flow in a model of the human carotid bifurcation. Part II - Laser-Doppler anemometer measurements. J Biomech 1982;15:363-378

126. Liepsch D, Moravec S: Pulsatile flow of non-newtonian fluid in distensible models of human arteries. Biorheology 1984; 21:571-586

127. Kajiya F, Tomonaga G, Tsujioka K, Ogasawara Y, Nishihara H: Evaluation of local blood flow velocity in proximal and distal coronary arteries by laser Doppler method. ASME J Biomech Eng 1985;107:10-15

128. Reneman RS, van Merode T, Hick P, Hoeks APG: Flow velocity patterns in and distensibility of the carotid artery bulb in

subjects of various ages. Circulation 1985;71:500-509

129. Deters OJ, Bargeron CB, Mark FF, Friedman MH: Measurement of wall motion and wall shear in a compliant arterial cast. ASME J Biomech Eng 1986;108:355-358

130. Friedman MH, Deters OJ, Bargeron CB, Hutchins GM, Mark FF: Shear-dependent thickening of the human arterial intima. Atherosclerosis 1986;60:161-171

131. Roach MR, Scott S, Ferguson GG: The hemodynamic importance of the geometry of bifurcations in the circle of Willis (glass model studies). Stroke 1972;3:255-267

132. Walburn FJ, Stein PD: A comparison of steady and pulsatile flow in symmetrically branched tubes. ASME J Biomech Eng 1982;104:66-68

133. Fukushima T, Homma T, Azuma T, Harakawa K: Characteristics of secondary flow in steady and pulsatile flows through a symmetrical bifurcation. Biorheology 1987;24:3-12

134. Deters OJ, Mark FF, Bargeron CB, Friedman MH, Hutchins GM: Comparison of steady and pulsatile flow near the ventral and dorsal walls of casts of human aortic bifurcations. ASME J Biomech Eng 1984;106:79-82

135. Sabbah HN, Walburn FJ, Stein PD: Patterns of flow in the left coronary artery. ASME J Biomech Eng 1984;106:272-279

136. Mark FF, Bargeron CB, Deters OJ, Friedman MH: Nonquasi - steady character of pulsatile flow in human coronary arteries. ASME J Biomech Eng 1985;107:24-28

137. Karino T, Motomiya M: Flow visualization in isolated transparent natural blood vessels. Biorheology 1983;20:119-127

138. Karino T, Motomiya M: Flow through a venous valve and its implication for thrombus formation. Thromb Res 1984;36:245-257

139. Sohara Y, Karino T: Secondary flows in the dog aortic arch, in Harada M (ed): Fluid Control and Measurement, Oxford, Pergamon Press, 1985, pp 143-147

140. Motomiya M, Karino T: Flow patterns in the human carotid artery bifurcation. Stroke 1984;15:50-56

141. Guyton AC: Textbook of Medical Physiology (Sixth Edition), Philadelphia, W.B. Saunders Company, 1981, pp 298-299

142. Patel DJ, Greenfield JC Jr, Fry DL: In vivo pressure-length-radius relationship of certain blood vessels in man and dog, in Attinger EO (ed): Pulsatile Blood Flow, New York, McGraw-Hill Book Company, 1964, pp 293-305

143. Spiller P, Schmiel FK, Pölitz B, Block M, Fermor U, Hackbarth W, Jehle J, Körfer R, Pannek H: Measurement of systolic and diastolic flow rates in the coronary artery system by X-ray densitometry. Circulation 1983;68:337-347

144. Dole WP, Richards KL, Hartley CJ, Alexander GM, Campbell AB, Bishop VS: Diastolic coronary artery pressure-flow velocity relationship in conscious man. Cardiovasc Res 1984;18:548-554

145. Bharadvaj BK, Mabon RF, Giddens DP: Steady flow in a model of the human carotid bifurcation. Part I - Flow visualization. J Biomech 1982;15:349-362

146. Roach MR, Fletcher J: Alterations in distribution of sudanophilic lesions in rabbits after cessation of a

cholesterol-rich diet. Atherosclerosis 1979;32:1-10

147. Cornhill JF, Levesque MJ, Nerem RJ: Quantitative techniques for the study of the arterial wall, in Nerem RJ, Cornhill JF (eds): The Role of Fluid Mechanics in Atherogenesis, Ohio, Ohio State University, 1978, pp 7-1 - 7-4

148. Fox JA, Hugh AE: Localization of atheroma: A theory based on boundary layer separation. Brit Heart J 1966;28:388-399

149. Ferguson GG, Roach MR: Flow conditions at bifurcations as determined in glass models, with reference to the focal distribution of vascular lesions, in Bergel DH (ed): Cardiovascular Fluid Dynamics, vol. 2, New York, Academic Press, 1972, pp 141-156

150. Rodkiewicz CM: Localization of early atherosclerotic lesions in the aortic arch in the light of fluid flow. J Biomech 1975;8:149-156

151. White NK, Edwards JE, Dry TJ: The relationship of the degree of coronary atherosclerosis with age, in man. Circulation 1950;1:645-654

152. Young W, Gofman JW, Tandy R, Malamud N , Waters ESG: The quantitation of atherosclerosis. I. Relationship to artery size. Am J Cardiol 1960;6:288-293

153. Nerem RM, Seed WA: Coronary artery geometry and its fluid mechanical implications, in Schettler G, Nerem RM, Schmid-Schönbein H, Mörl H, Diehm C (eds): Fluid Dynamics as a Localizing Factor for Atherosclerosis, Heidelberg, Springer-Verlag, 1983, pp 51-59

154. Velican C, Velican D: Incidence, topography and light-

microscopic feature of coronary atherosclerotic plaques in adults 26-35 years old. Atherosclerosis 1980;35:111-122

155. Velican C, Velican D: Atherosclerotic involvement of coronary branch vessels. Atherosclerosis 1986;60:237-250

156. Ku DN, Giddens DP: Pulsatile flow in a model carotid bifurcation. Arteriosclerosis 1983;3:31-39

157. Ku DN, Giddens DP, Zarins CK, Glagov S: Pulsatile flow and atherosclerosis in the human carotid bifurcation. Positive correlation between plaque location and low and oscillating shear stress. Arteriosclerosis 1985;5:293-302

158. Karino T, Goldsmith HL: Role of blood cell-wall interactions in thrombogenesis and atherogenesis: A microrheological study. Biorheology 1984;21:587-601

159. Flaherty JT, Pierce JE, Ferrans VJ, Pater DJ, Tucker WK, Fry DL: Endothelial nuclear patterns in the canine arterial tree with particular reference to hemodynamic events. Circ Res 1972;30:23-33

160. Dewey CF Jr, Bussolari SR, Gimbrone MA Jr, Davies PF: The dynamic response of vascular endothelial cells to fluid shear stress. ASME J Biomech Eng 1981;103:177-185

161. Nerem RM, Levesque MJ, Cornhill JF: Vascular endothelial morphology as an indicator of the pattern of blood flow. ASME J Biomech Eng 1981;103:172-175

162. Dewey CF Jr: Effects of fluid flow on living vascular cells. ASME J Biomech Eng 1984;106:31-35

163. Eskin SG, Ives CL, McIntire LV, Navarro LT: Response of cultured endothelial cells to steady flow. Microvasc Res

1984;28:87-94

164. Levesque MJ, Nerem RM: The elongation and orientation of cultured endothelial cells in response to shear stress. ASME J Biomech Eng 1985;107:341-347

165. Levesque MJ, Liepsch D, Moravec S, Nerem RM: Correlation of endothelial cell shape and wall shear stress in a stenosed dog aorta. Arteriosclerosis 1986;6:220-229

166. Viggers RF, Wechezak AR, Sauvage LR: An apparatus to study the response of cultured endothelium to shear stress. ASME J Biomech Eng 1986;108:332-337

167. Koslow AR, Stromberg RR, Friedman LI, Lutz RJ, Hilbert SL, Schuster P: A flow system for the study of shear forces upon cultured endothelial cells. ASME J Biomech Eng 1986;108:338-341

168. Sato M, Levesque MJ, Nerem RM: Micropipette aspiration of cultured bovine aortic endothelial cells exposed to shear stress. Arteriosclerosis 1987;7:276-286

169. Reidy MA, Bowyer DE: Scanning electron microscopy of arteries. The morphology of aortic endothelium in haemodynamically stressed areas associated with branches. Atherosclerosis 1977;26:181-194

170. Reidy MA: Arterial endothelium around rabbit aortic ostia: A SEM study using vascular casts. Exp Mol Path 1979;30:327-336

171. Caplan BA, Schwartz CJ: Increased endothelial cell turnover in areas of in vivo Evans Blue uptake in the pig aorta. Atherosclerosis 1973;17:401-417

172. Vasile E, Simionescu M, Simionescu N: Visualization of the

binding, endocytosis, and transcytosis of low-density lipoprotein in the arterial endothelium in situ. J Cell Biol 1983;96:1677-1689

173. Davies PF, Dewey CF Jr, Bussolari SR, Gordon EJ, Gimbrone MA Jr: Influence of hemodynamic forces on vascular endothelial function - in vitro studies of shear stress and pinocytosis in bovine aortic cells. J Clin Invest 1984;73:1121-1129

174. Davies PF: Biology of disease - vascular cell interactions with special reference to the pathogenesis of atherosclerosis. Lab Invest 1986;55:5-24

175. Davies PF, Remuzzi A, Gordon EJ, Dewey CF Jr: Turbulent fluid shear induces vascular endothelial cell turnover in vitro. Proc Natl Acad Sci 1986;83:2114-2117

176. Lansman JB, Hallam TJ, Rink TJ: Single stretch-activated ion channels in vascular endothelial cells as mechanotransducers ? Nature 1987;325:811-813

177. Olesen SP, Clapham DE, Davies PF: Haemodynamic shear stress activates a K^+ current in vascular endothelial cells. Nature 1988;331:168-170

APPENDICES

A. Basic Fluid Mechanical Concepts

A.1 Reynolds Number

When we describe flow in the circulation, we face another difficult problem, that of comparing flow patterns in different regions of the circulation where vessel diameters and flow rates (or fluid velocities) are so different. To deal with this problem, it is necessary to apply the engineering or fluid mechanical concept of the Reynolds number.

The Reynolds number is a dimensionless number that is indicative of the ratio of inertial forces to viscous forces in the flow. For steady, developing incompressible flow in a constant-diameter, rigid tube, the Reynolds number is conventionally defined as $Re = dU_a \rho / \mu$, where U_a is the mean velocity averaged over the tube cross section, d is the internal diameter of the tube, ρ is the density of the fluid, and μ is the absolute viscosity of the fluid.

The Reynolds number of blood flow varies over a wide range. For the systemic circulation of a dog, the Reynolds number is about 1700 in the aorta, 130 in large arteries, 30 in main arterial branches, 0.02 in arterioles, 0.007 in venules, 12 in main venous branches, and 110 in large veins. In the human circulation, the Reynolds numbers are estimated to vary from about 10^{-3} in capillaries, to peak values as high as 10^4 in the aorta.

A.2 Shear Stress, Shear Rate and Viscosity

For viscous flow within a tube, the fluid motion near the wall is retarded, and a boundary layer develops. Within the boundary layer, adjacent laminas of fluid move at different speeds, and this movement induces a spatially varying shear stress (frictional force per unit surface area), $\tau = \mu\, du/dy$ [dynes/cm^2 = g cm/sec^2/cm^2], where u is the component of fluid velocity parallel to the wall and y is in a direction normal to the wall (shown in Figure A-1). The maximum shear stress occurs at the wall where the mean rate of strain is greatest. The velocity gradient, du/dy (sec^{-1}), is sometimes called shear rate. The constant of proportionality between shear rate and shear stress, μ, is called the "viscosity coefficient" or simply the "viscosity of the fluid"(g/cm sec, Poise or centiPoise), and it is a measure of the internal resistance of the fluid to flow.

Typical average values of τ in the major human arteries during basal conditions are 2-20 dynes/cm^2, with localized increases to 30-100 dynes/cm^2 near arterial branches and regions of sharp wall curvature.

A.3 Laminar, Disturbed and Turbulent Flows

For flow at low Reynolds numbers (Re<2300), the boundary layer remains "laminar", i.e., fluid particles move in orderly paths, because viscous forces are effective in damping out small, naturally occurring, disturbances in the flow. At higher Reynolds numbers, inertial forces become more important, small dis-

FIGURE A-1. Schematic diagram of the relationship between the motion of a viscous fluid and the vessel wall (A), showing the shear stress (τ) defined as the tangential force per unit area exerted in the direction of the flow. The velocity gradient, du/dy, is called shear rate. The constant of proportionality between shear rate and shear stress, μ, is called the viscosity coefficient or simply the viscosity of the fluid. Diagrammatic views of symmetric arterial branching (B), indicating the areas of high and low shear.

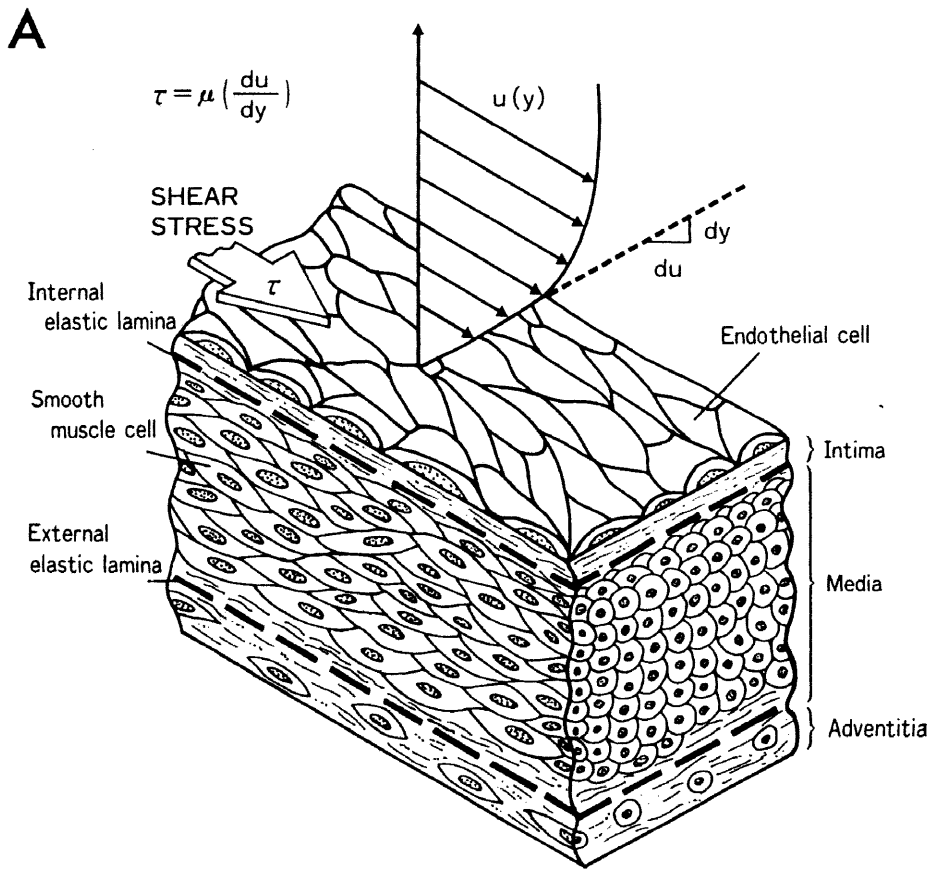
A
$\tau = \mu \left(\frac{du}{dy}\right)$
u (y)
SHEAR
STRESS
dy
du
τ
Internal
elastic lamina
Smooth
muscle cell
External
elastic lamina
Endothelial cell
Intima
Media
Adventitia

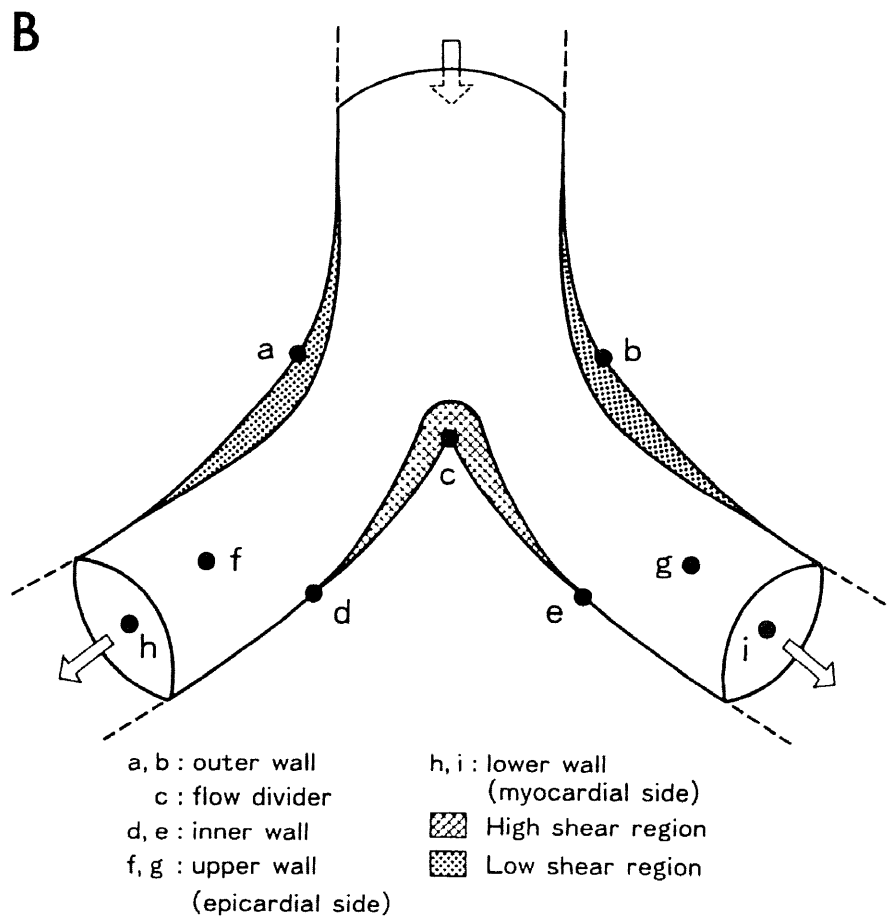
B
a
b
c
d
e
f
g
h
i
a, b : outer wall
c : flow divider
d, e : inner wall
f, g : upper wall
(epicardial side)
h, i : lower wall
(myocardial side)
High shear region
Low shear region

turbances tend to be amplified, and the flow within the boundary layer normally becomes "turbulent". Under these conditions, the instantaneous motion of fluid particles in the boundary layer is random in time and space, but the local flow is steady on a time-averaged basis. To describe a flow regime that is neither laminar nor turbulent, we have come to use the expression "disturbed flow". The term refers specifically to a flow regime where separation of streamlines and formation of standing vortices persists. Transition from laminar to disturbed flow, and from disturbed to turbulent flow is recognizable by the respective formation and total disappearance of macroscopic scale standing vortices.

The factors which must be considered in examining laminar-to-turbulent transitional behavior in a pulsatile flow are more complex. The complexity of the situation is compounded still further, of course, when flow is considered in the arterial system in which area change, wall distensibility, and branching effects influence the stability of the flow.

A.4 Boundary Layer Separation and Reattachment

To illustrate another phenomenon known as flow separation, consider the relatively simple case of steady, incompressible, laminar flow in a diverging tube. For moderate divergence angles the streamwise momentum of fluid in the near wall region may be insufficient to overcome the adverse pressure gradient induced by the expansion. Under these conditions, the flow will separate from the wall at a point where the velocity gradient is zero and

then reattach at some downstream location (shown in Figure A-2). At the separation point (A), the wall shear stress is zero, whereas immediately downstream from the reattachment point (stagnation point)(B), the wall shear stress can be relatively high. Between points A and B, a stable separation vortex may form in which the flow is locally reversed near the wall. If the flow is turbulent, separation can still occur, but then a stable separation vortex may no longer exist, and flow downstream from the separation point is generally unsteady.

For pulsatile flow, additional criteria for separation must be considered, because local flow reversal is possible in the absence of separation. The frequency of oscillation, the mean Reynolds number, and the dynamic (upstream) history of the boundary layer also influence flow separation in the arterial system, noting that flow separation is a distinct possibility at branching sites where local adverse pressure gradients may exist over the cardiac cycle.

FIGURE A-2. Schematic diagram of the streamwise momentum of fluid in the near wall region in a diverging tube in steady laminar flow. A sudden change in flow direction or sudden increase in vessel diameter creates a local adverse pressure gradient. This leads to the boundary layer separation or commonly called "flow separation". Under these conditions, the flow will separate from the wall at a point where the velocity gradient is zero and then reattach at some downstream location. At the separation point (A) the wall shear stress is zero ($du/dy=0$), whereas immediately downstream from the reattachment point (B), the wall shear stress can be relatively high ($du/dy>0$). Between points A and B, a stable separation vortex may form in which the flow is locally reversed near the wall.

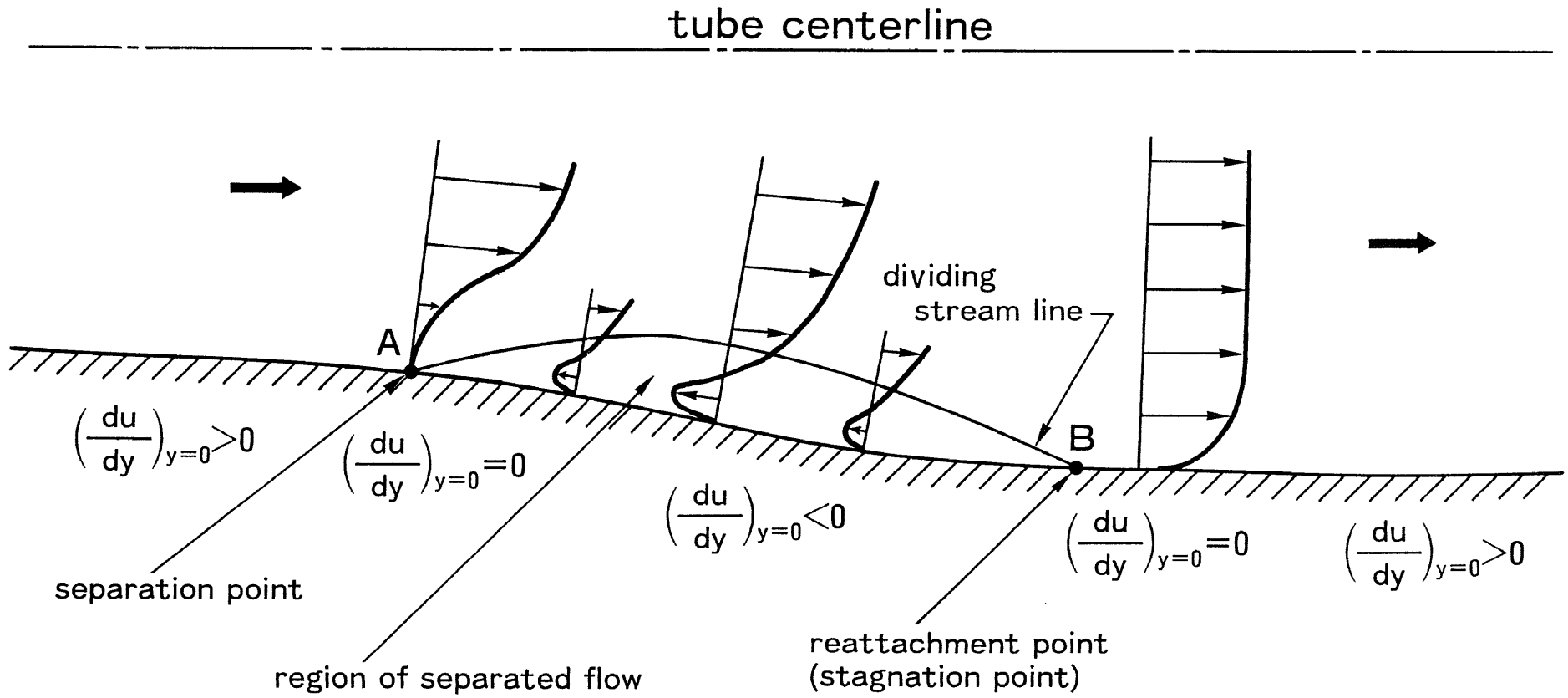
tube centerline
A
B
dividing
stream line
$\left(\frac{du}{dy}\right)_{y=0}>0$
$\left(\frac{du}{dy}\right)_{y=0}=0$
$\left(\frac{du}{dy}\right)_{y=0}<0$
$\left(\frac{du}{dy}\right)_{y=0}=0$
$\left(\frac{du}{dy}\right)_{y=0}>0$
separation point
region of separated flow
reattachment point
(stagnation point)

B. Detail of Various Apparatus Used in the Thesis Work

FIGURE B-1. Schematic diagram of experimental setup used for flow visualization and high speed cinemicrographic techniques using isolated transparent coronary arterial trees prepared from human post-mortem. This diagram also shows the connection between the transparent coronary arterial tree and the steady flow system and the pulse duplicating system used in this study.

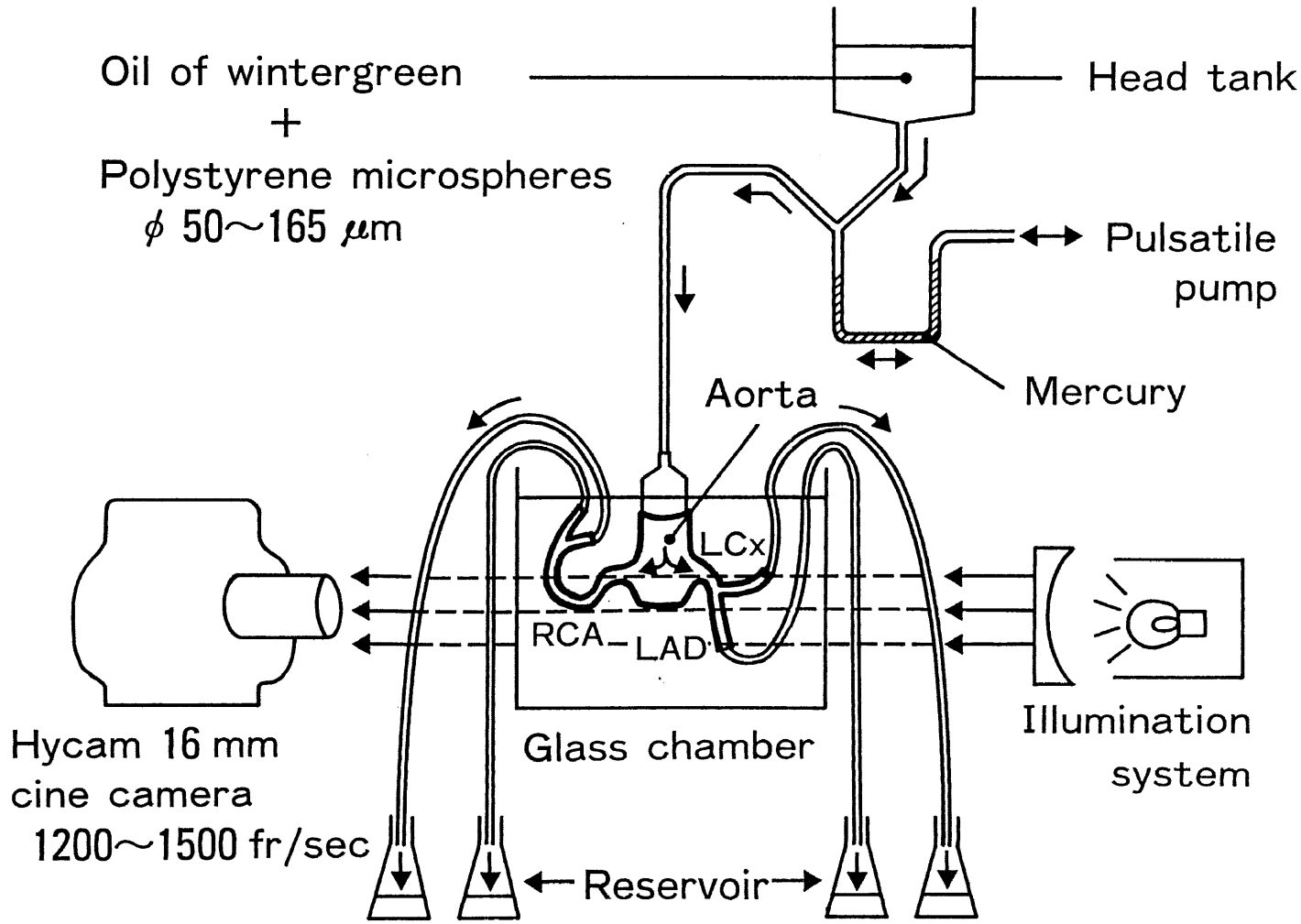
Oil of wintergreen
+
Polystyrene microspheres
φ 50~165 μm
Head tank
Pulsatile pump
Mercury
Aorta
LCx
RCA
LAD
Hycam 16 mm
cine camera
1200~1500 fr/sec
Glass chamber
Illumination system
Reservoir

FIGURE B-2. Photograph of the overall view of the apparatus. The Hycam 16 mm cine camera (A) with the zoom lens (B) is shown in the left side. The transparent glass chamber (C) is placed on the vertically movable horizontal stage (D) located in front of the vertically mounted stage of a microscope. The pair of 16 cm diameter plano-convex lenses (E) is aligned in series. The Reichert Binolux twin-lamp assembly consists of the low intensity light from a tungsten filament lamp (F) and high intensity light from a 200 W d.c. mercury arc lamp (G) with a filter to eliminate ultraviolet illumination (H).

A
B
C
D
E
F
G
H
I

FIGURE B-3. Overall view of the pulsatile flow system showing the reciprocating pump (A) with a microsyringe whose plunger is connected to a crank shaft and driven in simple harmonic motion by the flywheel rotated by a d.c. motor drive with an electronic control box (B). The oscillatory flow is superimposed on steady flow via a U-joint (C) to produce a pulsatile flow in the transparent human coronary arterial tree.

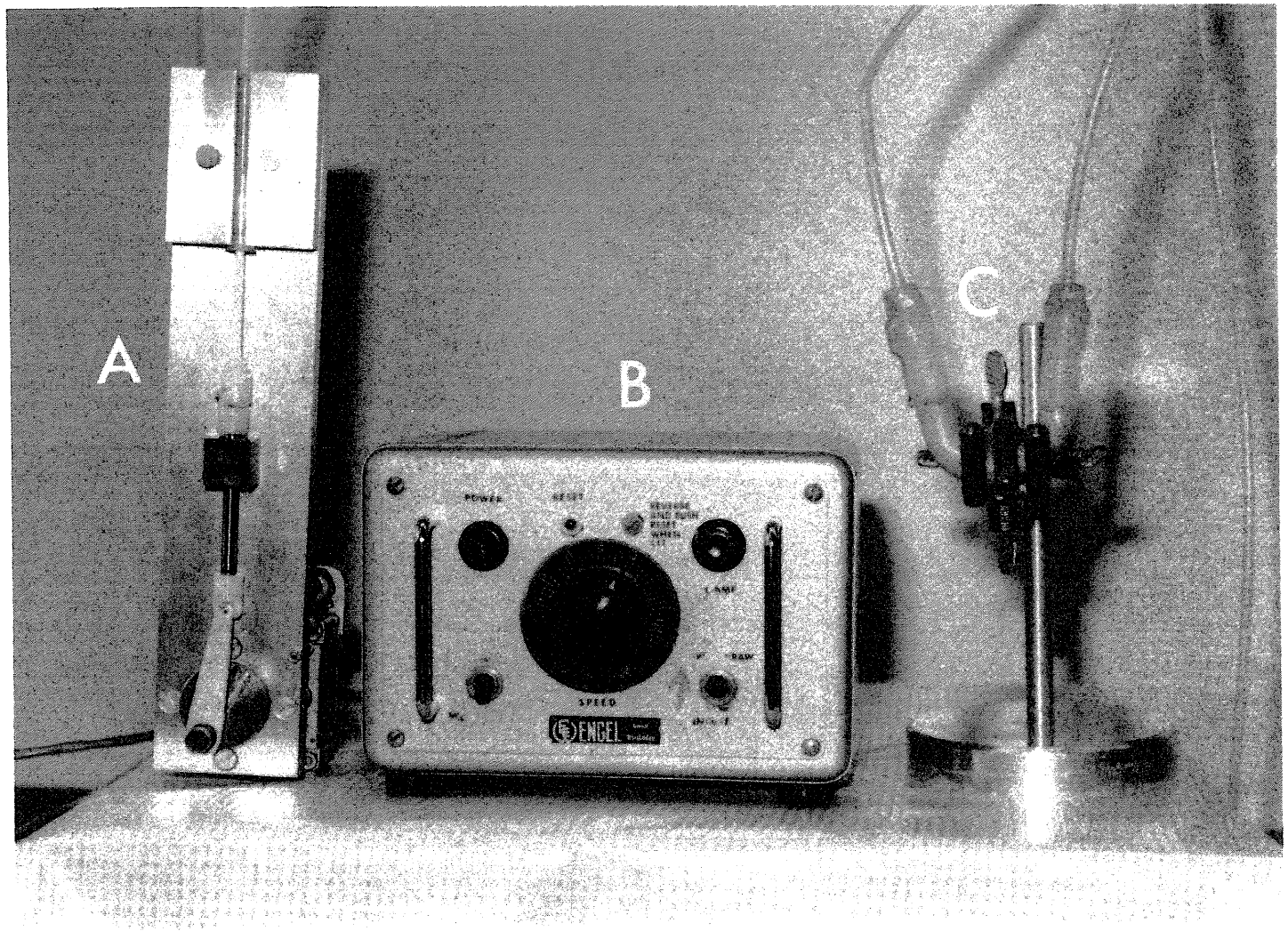
A
B
C
POWER
RESET
SPEED
ENGEL

FIGURE B-4. Photograph of the overall view of the analyzing system. The 16 mm cine film (A) is projected onto the drafting table (B) and the movements of individual tracer particles are analyzed frame by frame using the control box (C) with the aid of the stop-motion 16 mm movie analyzer (D).

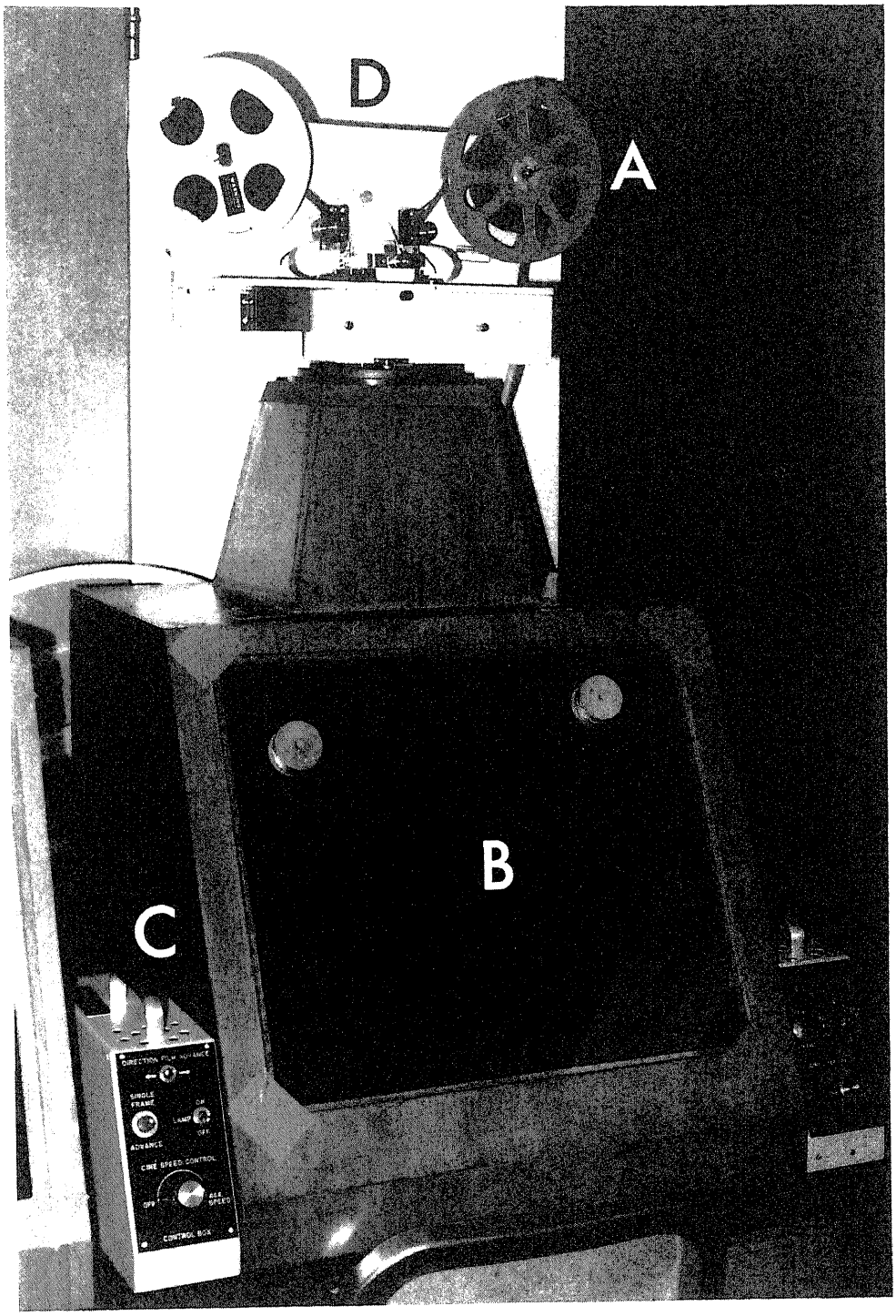
D
A
B
C
SINGLE FRAME
ADVANCE
CINE SPEED CONTROL
CONTROL BOX